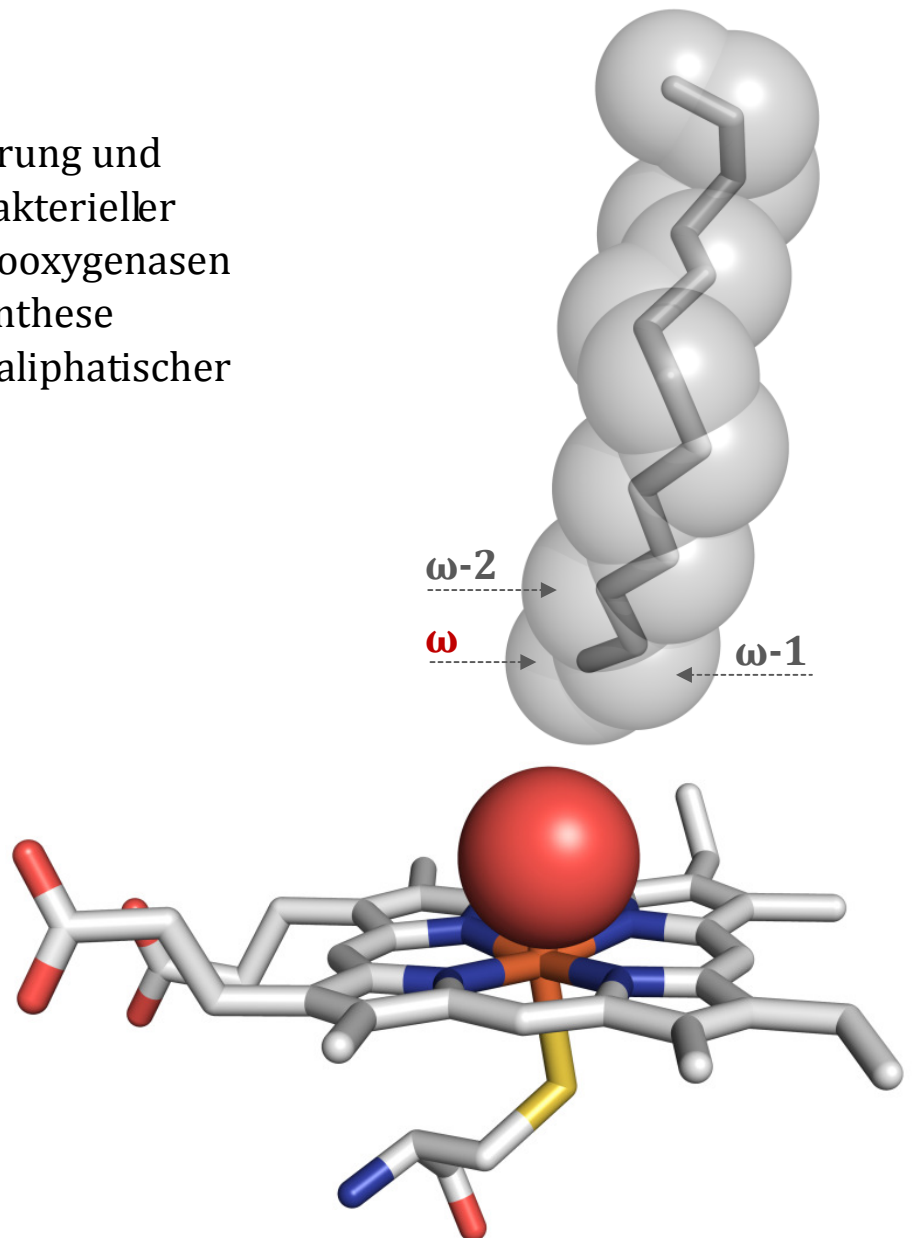


Substrate characterization and protein engineering of bacterial cytochrome P450 monooxygenases for the bio-based synthesis of omega-hydroxy aliphatic compounds

Substrat-Charakterisierung und Protein Engineering bakterieller Cytochrom-P450-Monooxygenasen für die bio-basierte Synthese omega-hydroxylierter aliphatischer Verbindungen



Sumire Honda Malca

Institut für Technische Biochemie – Universität Stuttgart

Substrate characterization and protein engineering of bacterial cytochrome P450 monooxygenases for the bio-based synthesis of omega-hydroxylated aliphatic compounds

Substrat-Charakterisierung und Protein Engineering bakterieller Cytochrom-P450-Monooxygenasen für die bio-basierte Synthese omega-hydroxylierter aliphatischer Verbindungen

an approved thesis presented to the
Faculty of Energy Technology, Process Engineering and
Biological Engineering of the University of Stuttgart
in fulfillment of the requirements for the
Degree of Doctor in Natural Sciences (Dr. rer. nat.)

submitted by

Sumire Honda Malca

from

Moquegua, Peru

Main examiner: Prof. Dr. Bernhard Hauer

Co-examiner: Prof. Dr. Georg Sprenger

Thesis defense date: 14.03.2013

Institute of Technical Biochemistry at the University of Stuttgart

2013

Cover

The terminal carbon atom position of *n*-tridecane in proximity to the oxygen-bound heme complex of a cytochrome P450 monooxygenase (modified from PDB ID 1DZ8). The image was generated by PyMOL.

Part of this work has already been published or submitted for publication

D. Scheps*, S. Honda Malca*, H. Hoffmann, B.M. Nestl and B. Hauer. "Regioselective omega-hydroxylation of medium-chain alkanes and primary alcohols by CYP153 enzymes from *Mycobacterium marinum* M. and *Polaromonas* sp. JS666." *Org Biomol Chem* 2011, 9 (19), 6727. *both authors contributed equally to this work.

S. Honda Malca, D. Scheps, L. Kühnel, E. Venegas-Venegas, A. Seifert, B.M. Nestl and B. Hauer. "Bacterial CYP153A monooxygenases for the synthesis of omega-hydroxylated fatty acids." *Chem Commun* 2012, 48 (42), 5115.

T. Vallon, M. Glemser, S. Honda Malca, D. Scheps, J. Schmid, M. Siemann-Herzberg, B. Hauer and R. Takors. "Production of 1-octanol from *n*-octane by *P. putida* KT2440 with heterologous P450 monooxygenase." *Chemie Ingenieur Technik*. Manuscript accepted.

Erklärung über die Eigenständigkeit der Dissertation

Ich versichere, dass ich die vorliegende Arbeit mit dem Titel „Substrat-Charakterisierung und Protein Engineering bakterieller Cytochrom-P450-Monooxygenasen für die bio-basierte Synthese omega-hydroxylierter aliphatischer Verbindungen“ selbständig verfasst und keine anderen als die angegebenen Quellen und Hilfsmittel benutzt habe; aus fremden Quellen entnommene Passagen und Gedanken sind als solche kenntlich gemacht. Des Weiteren bestätige ich ausdrücklich, dass die hier vorgelegte Dissertation nicht in gleicher oder ähnlicher Form bei einer anderen Institution zur Erlangung eines akademischen Grades eingereicht wurde.

Declaration of Authorship

I hereby declare that the present thesis entitled “Substrate characterization and protein engineering of bacterial cytochrome P450 monooxygenases for the bio-based synthesis of omega-hydroxylated aliphatic compounds” is the result of my own work, that all sources used or quoted have been indicated, and that I have not used any illegitimate means. I further declare that I have not submitted this thesis for a degree in some form or another.

Name: Sumire Honda Malca

Ort und Datum/Place and Date: Stuttgart, 16.01.2013

*Para mi madre,
por todo su cariño y dedicación*

Acknowledgments

This research project was performed from July 2009 to August 2012 at the Institute of Technical Biochemistry (ITB) of the University of Stuttgart, to obtain the Degree of Doctor in Natural Sciences. The work was carried out within the scope of the projects: “Systems Biology of *Pseudomonas* for Industrial Biocatalysis” and “Developing the Next Generation of Biocatalysts for Industrial Chemical Synthesis”, funded by the German Federal Ministry of Education and Research (BMBF) and the European Union 7th Framework Programme, respectively.

First, my sincerest gratitude goes to my advisor, Prof. Dr. Bernhard Hauer. I thank him for his supervision and support throughout the course of my Ph.D. project. I am also deeply grateful to Dr. Bettina Nestl for her sound guidance, encouragement and always helpful disposition during my research work. I am indebted to Prof. Dr. Vlada Urlacher, now in Düsseldorf, for introducing me to the world of P450 enzymes and for her assistance at the initial stage of the project.

I wish to thank Prof. Dr. Ing. Ralf Takors, Tobias Vallon and Matthias Glemser from the Institute of Biochemical Engineering at the University of Stuttgart, and Dr. Joachim Schmid from Insilico Biotechnology AG, for the shared work within the frame of the BMBF project. I also thank Dr. Alexander Seifert for his computational support in rational design and Dr. Per-Olof Syrén for fruitful discussions regarding enzyme kinetics.

For the very pleasant and cooperative teamwork, I owe special thanks to my colleague Daniel Scheps. I thank him for his help, for sharing his ideas and motivations while facing the challenges of working with CYP153A enzymes. I am very grateful to students Naemi Luithl, Lisa Kühnel, Ana Belen Alfaro Gómez and Carmen Elena Venegas Venegas for their support at different stages of the project.

I would like to thank all members of the ITB for their assistance and for making my lab days more amusing. For those great coffee breaks and other cheerful shared moments, I thank Luam, Clarisse, Lore, Anna, Eve, Susi, Miri, Ingrid, Jule, Jenny, Sabrina, Christine, Mina, Meli, Mihaela, Silke, Thorsten, Andy, Sven, Tobi, Björn, Chris K., Marko, Konrad, Sebastian, Stevie, Dennis, Chris G. and Bernd.

Finally, I would like to express my eternal gratitude to my family, especially to Violen and Melvin, for their love, their support and for being there for me.

Table of contents

Acknowledgments	7
Table of contents	9
Abbreviations	11
Abstract	13
Zusammenfassung	15
1 Introduction	17
1.1 Applications of ω -oxyfunctionalized aliphatic compounds.....	17
1.2 Synthesis of ω -oxyfunctionalized aliphatic compounds.....	19
1.2.1 Chemical catalysts	20
1.2.2 Biocatalysts	22
1.3 Bacterial whole cell bioconversions with oxygenases.....	31
1.3.1 <i>Pseudomonas</i> and <i>E. coli</i> as cell factories	31
1.3.2 Growing and resting cells as whole cell biocatalysts	33
1.4 Aim of the work.....	34
2 Experimental section	35
2.1 Genes, vectors and strains.....	35
2.2 Procedures	35
2.2.1 Substrate screening of CYP153A biocatalysts.....	35
2.2.2 Creation of a focused mutant library of CYP153A from <i>Marinobacter aquaeolei</i> .	35
2.2.3 Bacterial whole cells for the synthesis of ω -oxyfunctionalized aliphatic compounds.....	37
3 Results and Discussion	43
3.1 Substrate screening of CYP153A biocatalysts.....	43
3.1.1 Medium-chain linear alkanes and primary alcohols.....	43
3.1.2 Medium- and long-chain linear saturated and monounsaturated fatty acids	47
3.2 Creation of a focused mutant library of CYP153A from <i>Marinobacter aquaeolei</i>	51

3.3	Bacterial whole cells for the synthesis of ω -oxyfunctionalized aliphatic compounds	60
3.3.1	Biotransformations of <i>n</i> -octane by growing <i>P. putida</i> cells containing CYP153A gene clusters.....	60
3.3.2	Biotransformations of <i>n</i> -octane and fatty acids by resting <i>P. putida</i> and <i>E. coli</i> cells containing CYP153A fusion constructs	62
4	Conclusion and outlook	77
5	References	82
6	Supplementary material.....	99
6.1	Genes, vectors and strains.....	99
6.1.1	Genes.....	99
6.1.2	Vectors.....	102
6.1.3	Strains.....	105
6.2	Multiple protein sequence alignments.....	108
6.3	Supplementary tables.....	110
6.4	Supplementary figures.....	112
	Manuscript	115
	Curriculum vitae	147

Abbreviations

× g	gravitational acceleration
°C	degrees Celsius
μl	microliter
μm	micrometer
μM	micromolar
aa	amino acid
AlkB	alkane-1-monooxygenase from <i>Pseudomonas putida</i> Gpo1
AlkG	rubredoxin from <i>Pseudomonas putida</i> Gpo1
AlkT	rubredoxin reductase from <i>Pseudomonas putida</i> Gpo1
bp	base pair
CamA	putidaredoxin reductase from <i>Pseudomonas putida</i>
CamB	putidaredoxin from <i>Pseudomonas putida</i>
cdw	cell dry weight
CPR	cytochrome P450 reductase
cww	cell wet weight
CYP	cytochrome P450 monooxygenase
CYP153A16	CYP153A monooxygenase from <i>Mycobacterium marinum</i> M.
CYP153A <i>M. aq.</i>	CYP153A monooxygenase from <i>Marinobacter aquaeolei</i> VT8
CYP153A <i>P. sp.</i>	CYP153A monooxygenase from <i>Polaromonas sp.</i> JS666
DAD	diode array detector
DCA	dicarboxylic acid
DMSO	dimethyl sulfoxide
DNA	deoxyribonucleic acid
DSMZ	German Collection of Microorganisms and Cell Cultures
<i>E. coli</i>	<i>Escherichia coli</i>
FAD	flavin adenine dinucleotide
FdR	NAD(P)H-dependent ferredoxin oxidoreductase
Fdx	ferredoxin
FMN	flavin mononucleotide
g	gram
GC	gas chromatography
GC/FID	gas chromatography coupled to flame ionization detector
GC/MS	gas chromatography coupled to mass spectrometry
G6P	glucose-6-phosphate

G6PDH	glucose-6-phosphate dehydrogenase
h	hour
HPLC	high-performance liquid chromatography
IPTG	isopropyl- β -D-thiogalactopyranoside
kbp	kilobase pair
kDa	kilo Dalton
l	liter
LB	lysogeny (Luria-Bertani) broth
MaqFdR	ferredoxin reductase from <i>Marinobacter aquaeolei</i> VT8
MaqFdx	ferredoxin from <i>Marinobacter aquaeolei</i> VT8
MmFdR	ferredoxin reductase from <i>Mycobacterium marinum</i> M.
MmFdx	ferredoxin from <i>Mycobacterium marinum</i> M.
mg	milligram
min	minute
ml	milliliter
mM	millimolar
OCT	octane-degrading plasmid in <i>Pseudomonas putida</i> Gpo1
OD ₆₀₀	optical density measured at 600 nm
OHFA	hydroxylated fatty acid
<i>P. putida</i>	<i>Pseudomonas putida</i>
PCR	polymerase chain reaction
PMSF	phenylmethanesulfonyl fluoride
PspFdR	ferredoxin reductase from <i>Polaromonas</i> sp. JS666
PspFdx	ferredoxin from <i>Polaromonas</i> sp. JS666
RID	refractive index detector
ROS	reactive oxygen species
rpm	revolutions per minute
SDS-PAGE	sodium dodecyl sulfate polyacrylamide gel electrophoresis
TB	terrific broth
WT	wild type

Abstract

The selective oxyfunctionalization of alkanes and fatty acids is a challenging task in basic and applied chemistry. Biocatalysts belonging to the superfamily of cytochrome P450 monooxygenases (CYPs) can introduce oxygen into a wide variety of molecules in a very regio- and stereospecific manner, which can be used for the synthesis of fine and bulk chemicals. CYPs from the bacterial CYP153A subfamily have been described as alkane hydroxylases with high terminal regioselectivity. In the present work, CYP153A monooxygenases were screened for the synthesis of industrially relevant ω -hydroxylated aliphatic compounds, such as primary alcohols, α,ω -diols, ω -hydroxyfatty acids (ω -OHFAs) and α,ω -dicarboxylic acids (α,ω -DCAs). One enzyme candidate was tailored by rational design and applied in whole cell biotransformations with recombinant *E. coli* or *Pseudomonas* strains. The biocatalytic systems were further improved by utilizing a fusion enzyme construct for increased coupling efficiency.

CYP153A enzymes from *Polaromonas* sp. (CYP153A *P.* sp.), *Mycobacterium marinum* (CYP153A16) and *Marinobacter aquaeloei* (CYP153A *M. aq.*) were screened *in vitro* towards medium- to long-sized linear alkanes, alcohols and fatty acids using the redox partners of P450cam from *Pseudomonas putida*. CYP153A *P.* sp. was found to possess a predominant alkane ω -hydroxylase activity, while CYP153A16 and CYP153A *M. aq.* were identified as predominantly fatty acid ω -hydroxylases. CYP153A *M. aq.* offered higher flexibility for the synthesis of primary alcohols, α,ω -diols and ω -OHFAs of different size and saturation level. CYP153A *M. aq.* was thus selected as a model enzyme to create a small focused library of 19 variants aiming the terminal hydroxylation of C₆-C₇ primary alcohols and C₆-C₈ fatty acids *via* a shift in substrate range or a higher enzyme activity. Active site hotspots G307 and L354 were found to greatly influence enzyme activity or substrate specificity. Conversions of *n*-octane, 1-heptanol and nonanoic acid with variant G307A compared to the wild type enzyme were higher by 3- to 10-fold and equally ω -regioselective (>97 %). Further kinetic analyses demonstrated that variant G307A was 2- to 20-fold more catalytically efficient towards octanoic, nonanoic and tetradecanoic acids owing to a higher turnover number rather than an increased substrate affinity. Residue L354 was found to be determinant for the enzyme selectivity, with mutations L354I and L354F causing a 73 % and 17 % decrease in ω -regioselectivity in oxidation reactions towards nonanoic acid, respectively.

In order to increase the efficiency of redox biocatalysis, mutation G307A was incorporated into a fusion protein comprised by CYP153A *M. aq.* and the reductase domain (CPR) of P450 BM3 from *Bacillus megaterium*. The G307A variant within the fusion protein yielded 25 – 41 % higher

conversion levels towards octanoic, dodecanoic and oleic acids compared to the wild type fusion construct in whole cell biotransformations. The performance of non-engineered and non-solvent-adapted *E. coli* and *P. putida* strains was compared in shake flask biotransformations towards *n*-octane and dodecanoic acid. *E. coli* has been shown to be a suitable host for 1-octanol or 12-hydroxydodecanoic production. In the absence of an additional carbon and energy source, bioconversions by resting *E. coli* and *P. putida* cells, containing the engineered fusion construct, yielded 0.26 and 0.015 g l⁻¹ 1-octanol from 10 % (v/v) *n*-octane in 8 and 2 h, respectively. In a similar setup, resting *E. coli* and *P. putida* cells respectively produced 0.49 and 0.1 g l⁻¹ 12-hydroxydodecanoic acid from 1 g l⁻¹ dodecanoic acid in 8 h. Additional feeding with glucose and glycerol decreased fatty acid consumption as carbon or energy source, but did not contribute to increase the product yields. In contrast to *E. coli*, *P. putida* cells tended to aggregate, consumed the substrate or targeted products rapidly and produced larger amounts of overoxidized products. Final product yields in both *E. coli* and *P. putida* were affected by the decrease in product formation rates after 8 h. High hydrogen peroxide accumulation was identified as a limitation in the pseudomonads. *E. coli* cells produced high acetate levels which could contribute to the reduction of CYP activity and stability.

In summary, this work constitutes the first example of rational engineering of a CYP153A enzyme, which allowed the identification of key residues for activity and substrate specificity within the enzyme subfamily. CYP153A enzymes have also been applied for the first time in the ω -hydroxylation of fatty acids. Comparative *in vivo* studies with recombinant *E. coli* and *P. putida* cells provided information on the effects of host strains on product yields, eventually leading to the generation of an efficient bacterial whole cell biocatalyst for the synthesis of selected ω -hydroxylated aliphatic compounds.

Zusammenfassung

Die selektive Oxyfunktionalisierung von Alkanen und Fettsäuren ist eine herausfordernde Aufgabe sowohl in der chemischen Grundlagenforschung als auch in der angewandten Chemie. Biokatalysatoren aus der Superfamilie der Cytochrom-P450-Monooxygenase Enzyme (CYPs) können Sauerstoff regio- und stereospezifisch in eine Vielzahl von Molekülen einbauen, welche zur Synthese von Fein- und Bulk-Chemikalien verwendet werden können. CYPs aus der bakteriellen Unterfamilie CYP153A sind als Alkan-Hydroxylasen mit hoher terminaler Regioselektivität beschrieben worden. In der vorliegenden Arbeit wurden CYP153A Monooxygenasen durch Substrat-Screening für die Darstellung industriell relevanter ω -hydroxylierter, aliphatischer Verbindungen, wie primäre Alkohole, α,ω -Diole, ω -Hydroxyfettsäuren (ω -OHFAs) und α,ω -Dicarbonsäuren (α,ω -DCAs), getestet. Ein Enzymkandidat wurde durch rationales Design angepasst und für Ganzzellbiotransformationen mit rekombinanten *E. coli* oder *Pseudomonas* Stämmen verwendet. Die biokatalytischen Systeme wurden durch Verwendung eines Fusionskonstrukts für erhöhte Kopplungseffizienz verbessert.

CYP153A-Enzyme aus *Polaromonas* sp. (CYP153A *P. sp.*), *Mycobacterium marinum* (CYP153A16) und *Marinobacter aquaeleoi* (CYP153A *M. aq.*) wurden gegenüber mittel- und langkettigen linearen Alkanen, Alkoholen und Fettsäuren mit den Redoxpartnern von P450cam aus *Pseudomonas putida* in *in-vitro* Experimenten untersucht. CYP153A *P. sp.* wies überwiegend Alkan ω -Hydroxylase-Aktivität auf, wenn auch CYP153A16 und CYP153A *M. aq.* überwiegend als Fettsäure ω -Hydroxylasen identifiziert wurden. CYP153A *M. aq.* zeigte eine höhere Flexibilität für die Synthese von primären Alkoholen, α,ω -Diolen und ω -OHFAs mit variablen Kettenlängen und unterschiedlichen Sättigungsgraden. Aus diesem Grund wurde CYP153A *M. aq.* als Modell-Enzym für die Erstellung einer kleinen fokussierten Bibliothek von 19 Varianten ausgewählt. Ziel dieser Bibliothek war die terminale Hydroxylierung von C_6 - und C_7 -primären Alkoholen und C_6 - bis C_8 -Fettsäuren durch eine Verschiebung des Substratspektrums oder eine Erhöhung der Enzymaktivität. Die Aminosäuren G307 und L354 im aktiven Zentrum wurden als Hotspots mit einem starken Einfluß auf die Enzymaktivität bzw. die Substratspezifität ermittelt. Die Substratumsätze von *n*-Oktan, 1-Heptanol und Nonansäure waren 3- bis 10-fach höher mit der Variante G307A im Vergleich zu denen des Wildtyp-Enzyms bei gleichbleibender ω -Regioselektivität (>97 %). Weitere kinetische Analysen zeigten, dass die Variante G307A eine um den Faktor zwei bis 20 erhöhte katalytische Effizienz gegenüber Oktansäure, Nonansäure und Tetradekansäure besaß, was auf den höheren Umsatz (höhere Turnover Number) zurückzuführen ist. Die Aminosäure L354 wurde als essentiell für die Selektivität des Enzyms

nachgewiesen, da die Mutationen L354I und L354F einen Rückgang der ω -Regioselektivität um 73 % bzw. 17 % in Oxidationsreaktionen gegenüber Nonansäure verursachten.

Um die Effizienz der Redoxbiokatalyse zu erhöhen, wurde die Mutation G307A in ein Fusionsprotein, welches aus der Monooxygenasedomäne aus CYP153A *M. aq.* und der Reduktase-Domäne (CPR) von P450 BM3 aus *Bacillus megaterium* aufgebaut ist, eingeführt. Die Variante G307A im Fusionsprotein ergab 25 – 41 % höhere Substratumsätze von Oktansäure, Dodekansäure und Ölsäure im Vergleich zum Wildtyp-Fusionskonstrukt bei Ganzzellbiotransformationen. Die Leistungsfähigkeit von nicht-stammentwickelten und nicht-Lösungsmittel-adaptierten *E. coli* und *P. putida*-Zellen wurde in Biotransformationen von *n*-Oktan und Dodekansäure in Schüttelkolben verglichen. *E. coli* wurde als besser geeignet für die Darstellung von 1-Oktanol oder 12-Hydroxydodekansäure im Vergleich zu *P. putida* befunden. In Abwesenheit einer zusätzlichen Kohlenstoff- und Energiequelle produzierten ruhende *E. coli* und *P. putida*-Zellen, welche das erzeugte Fusionskonstrukt beherbergten, 0,26 bzw. 0,015 g l⁻¹ 1-Oktanol aus einer 10 % (v/v) *n*-Oktanstammlösung in 8 und 2 h Reaktionsdauer. In einem ähnlichen experimentellen Aufbau erzeugten ruhende *E. coli* und *P. putida*-Zellen in 8 h 0,49 bzw. 0,1 g l⁻¹ 12-Hydroxydodekansäure aus 1 g l⁻¹ Dodekansäure. Zusätzliche Fütterung mit Glukose und Glycerin erzielte einen geringeren Verbrauch der Fettsäuren, aber keine Erhöhung der Produktausbeuten. Im Gegensatz zu *E. coli* neigten *P. putida*-Zellen zu aggregieren. Des Weiteren konnte beobachtet werden, dass das Substrat und das Zielprodukt von den Zellen abgebaut wurden und größere Mengen an weiter oxidierten Produkten detektiert wurden. Die Ausbeute des Endprodukts in beiden *E. coli* und *P. putida* Ansätzen wurde nach 8 h Reaktionsdauer durch den Rückgang der Produktbildungsrate beeinträchtigt. Eine hohe Akkumulation vom Wasserstoffperoxid wurde als Limitierung in den Pseudomonaden identifiziert. In *E. coli* wurde eine hohe Acetatkonzentration detektiert, die zur Verringerung der Aktivität und Stabilität der CYPs beitragen könnte.

Zusammenfassend stellt diese Arbeit das erste Beispiel für das Engineering eines CYP153A-Enzyms durch rationales Design dar, welches die Identifizierung wichtiger Aminosäurereste für die Aktivität und die Substratspezifität der Enzym-Unterfamilie ermöglichte. CYP153A-Enzyme wurden ebenfalls zum ersten Mal in der ω -Hydroxylierung von Fettsäuren angewandt. Vergleichende *in-vivo*-Untersuchungen mit rekombinanten *E. coli* und *P. putida*-Zellen stellen Informationen über die Einwirkung von Wirtsstämmen auf Produktausbeuten bereit, was schließlich zu der Erzeugung eines effizienten bakteriellen Ganzzellbiokatalysators zur Synthese ausgewählter ω -hydroxylierter, aliphatischer Verbindungen führen kann.

1 Introduction

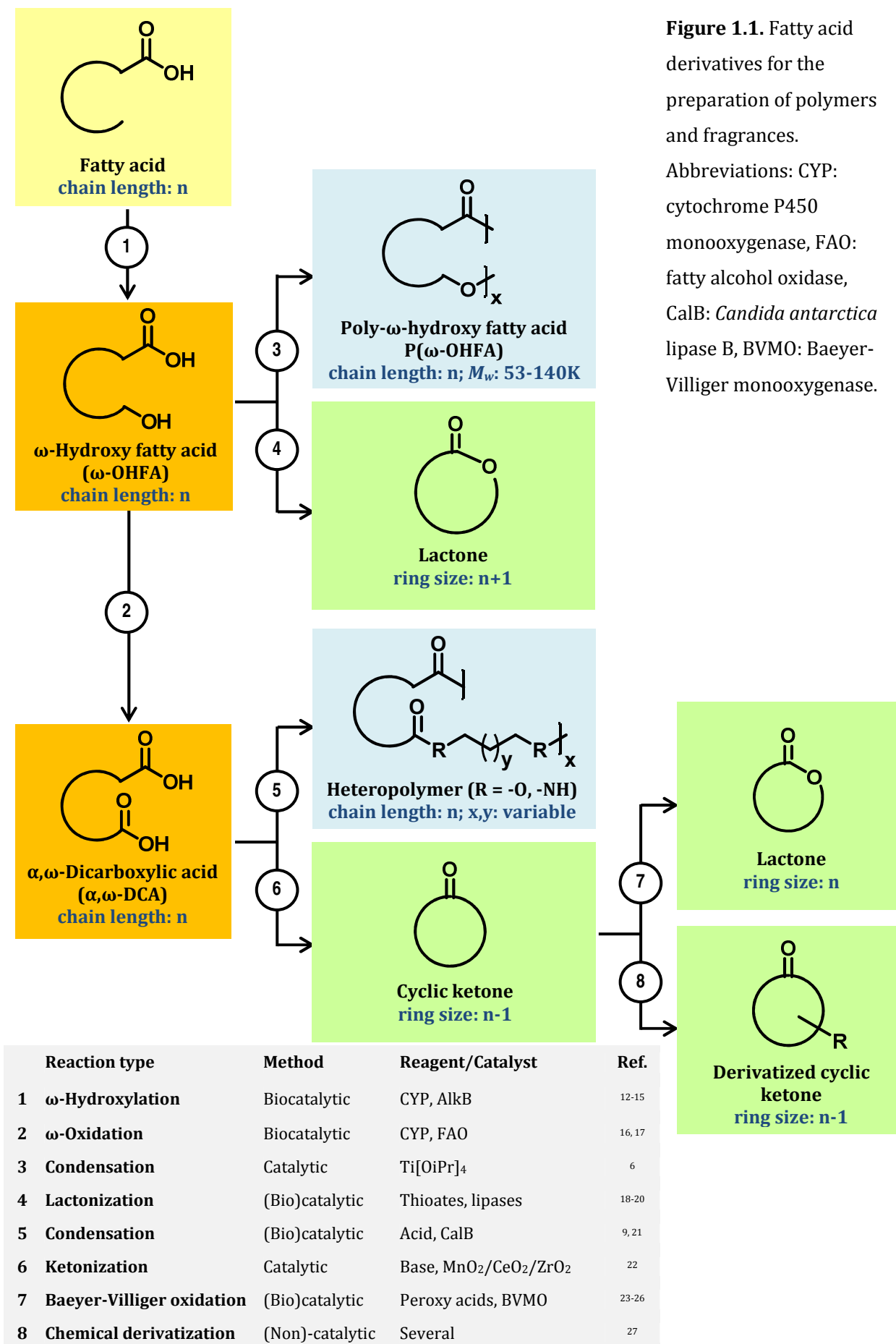
1.1 Applications of ω -oxyfunctionalized aliphatic compounds

ω -Hydroxylated hydrocarbons such as primary alcohols and α,ω -diols are of great industrial interest due to their use as fuels, versatile solvents, plasticizers, surfactants, cosmetic ingredients and precursors for polymer intermediates (table 1.1).¹ Terminally oxyfunctionalized fatty acids such as ω -hydroxyfatty acids (ω -OHFAs) and α,ω -dicarboxylic acids (α,ω -DCAs) are valuable chemicals for adhesives, lubricants, antiseptics, macrolide antibiotics and potential anticancer agents.²⁻⁵ They are also attractive for the fragrance industry and for several commodity and advanced plastic applications (figure 1.1; supplementary material table 6.3). ω -OHFAs serve as building blocks for the synthesis of poly(ω -hydroxyfatty acids), which are polyethylene-like polyhydroxyalkanoates exhibiting high durability, hydrolytic resistance and compatibility with other composite materials like polyamides and polyesters.⁶ In addition, unsaturated ω -OHFAs and α,ω -DCAs can be used to synthesize network copolyesters as the double bond sites enable their linkage to different types of monomers. These sites can also be decorated with flame-retardant moieties for industrial coatings or with bioactive functionalities for their application as components of bioresorbable materials, tissue engineering scaffolds and drug delivery vehicles.^{3, 7-11}

Table 1.1. Industrial applications of medium-chain primary alcohols and α,ω -diols^{1, a}

Product	Industrial use
1-alcohols	
C ₆	Hexylglycol, UV-absorber, solvent in the production of trimethylquinone
C ₈	Octylamine, plasticizer, catalyst
C ₆ -C ₁₀	Plasticizers, surfactants, solvents, coalescent aids
C ₁₂ -C ₁₇	Lubricant oils, alcohol ethoxylates and alcohol ethoxysulfates
α,ω-diols	
C ₄ -C ₁₂	Coatings, adhesives, plasticizers, polyesters, polyamides, polyurethanes, poly(diols co-citrates)

^aProduct information sheets from Shell Chemicals and BASF SE.



1.2 Synthesis of ω -oxyfunctionalized aliphatic compounds

Saturated hydrocarbons are a large constituent of petroleum and natural gas, but there are currently few processes to directly convert these into more valuable functionalized products. In fact, most alcohols, aldehydes and fatty acids are produced from unsaturated hydrocarbons, commonly referred to as olefins, rather than alkanes because of the low reactivity of these compounds. Primary alcohols ranging from C_{11} – C_{15} are obtained from olefins by means of the Shell Hydroformylation (SHF) technology since the late 1970s. This platform exploits the homogeneously catalyzed hydroformylation or “oxo” reaction.²⁸ The SHF technology can be basically described as the phosphine-modified cobalt-catalyzed addition of carbon monoxide and hydrogen to olefins to form aldehydes and alcohols under low pressure conditions. The concept of ligand modification has been further developed to allow the hydrogenation of aldehyde intermediates to alcohols in one step and to control reaction selectivity via steric impacts.²⁹⁻³²

Non-edible vegetable oils are also an important source of fatty acids and derivatives. Compared to petrochemical feedstocks, they possess important advantages such as renewability and relatively stable prices. Medium- to long-chain ω -OHFAs can be synthesized by cross-metathesis of unsaturated fatty acid esters, followed by hydroformylation and hydrogenation of the carbonyl group.³³⁻³⁵ They can also be obtained by partial reduction of α,ω -DCAs.³⁶ The diacids can be prepared by the catalytic ring-opening of lactones and cyclic ketones.³⁷⁻³⁹

The selective terminal functionalization of alkanes is a reaction that poses a greater challenge than olefin-based processes. Although the thermodynamically unfavorable C_1 atom can be induced to react by exposure to radicals or metal centers, weaker C-H bonds will be oxidized preferentially without an adequate selectivity control.⁴⁰ Another issue is that, even if site-specific activation is achieved by the use of a tailored catalyst, its activity on partial oxidation products is difficult to regulate. This is problematic when the ω -alcohol is the desired final product, because the oxygenated molecule is more reactive than the starting material and thus, more prone to undergo overoxidation to the aldehyde or carboxylic acid. Several methods for the C-H oxygenation of saturated hydrocarbons have been developed, some of them with moderate success in the control of activity and product selectivity. In this section, the properties, advantages and drawbacks of the most relevant chemical and biological catalysts described in the literature are presented.

1.2.1 Chemical catalysts

Chemical synthetic approaches for selective alkane functionalization are based on heterogeneous, biomimetic and organometallic catalysis.^{41, 42} It has been proposed that C-H activations begin with the formation of an intermediate alkane sigma-complex, in which a metal center interacts with the electron pair forming the C-H σ -bond.⁴³ Following the formation of this intermediate, the coordinated C-H bond is cleaved to yield the product. The C-H cleavage step causes the main difference among the approaches.⁴⁰

Heterogeneous and biomimetic catalysis rely on the same mechanism, the homolytic cleavage of the C-H bond by an H-atom abstracting species. However, there is a problem with homolytic cleavage: homolysis rates of C-H bonds are inversely proportional with the strength of the bonds, which implies a constraint for selectivity and activity. One of the major difficulties is to make the reaction stop at the desired product because the product has at least one C-H bond weaker than the starting material.⁴¹ In heterogeneous catalysis by metal oxides, the effect of bond strength on the reaction rate is reduced by applying elevated temperatures. It is also important to make the metal-oxygen (M-O) bond of the catalyst be of intermediate strength. A too strong M-O bond leads to low reactivity; a weak one, to overoxidation.⁴⁴ In biomimetic catalysis, reactions can be run at milder conditions. Selectivity is addressed by using shape-selective scaffolds that resemble those of metalloenzymes.^{40, 41}

In organometallic activation C-H cleavage occurs by different mechanisms, e.g., nucleophilic attack by water on the metal-alkane complex (Shilov chemistry). As C-H homolysis is not involved, thermodynamic factors are minimized allowing a better control of the reaction selectivity. Primary positions become easier sites to attack and oxygenated products might not be further oxidized because they are not necessarily more thermodynamically favoured than their precursors. Nevertheless, the vast majority of organometallic complexes are highly sensitive to oxygen and other oxidants and therefore not stable under catalytic oxidation conditions.⁴⁰

Information on various metal catalysts (e.g., mononuclear metal cores, metalloporphyrins and platinum-chloride complexes) which enter the above-mentioned classification can be found in the literature.⁴⁵⁻⁵⁴ Herein we illustrate three examples for the oxidation of *n*-alkanes by shape-selective biomimetic catalysts because they are considered to be milder than other catalysts (figure 1.2). They contain non-toxic high-oxidation state transition metal ions (e.g., Mn^{III}, Fe^{III} and Co^{III}) and operate between 25 and 60°C. However, as explained before, controlled activity

and selectivity have not been completely solved and they generally result in the mixture of at least two regioisomeric alcohols and/or their overoxidized derivatives.

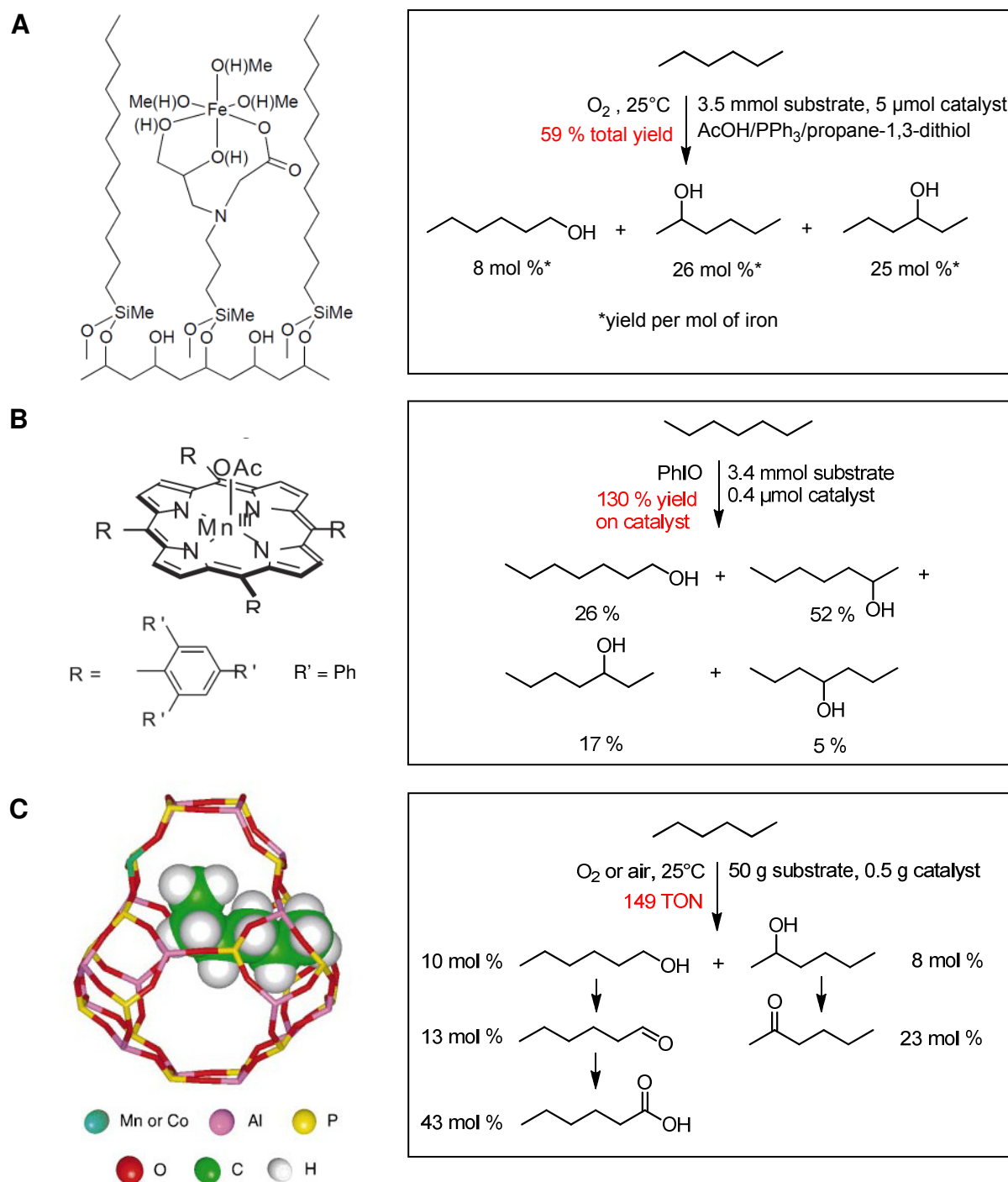


Figure 1.2. Shape-selective chemical catalysts for the oxyfunctionalization of *n*-alkanes. (A) Biomimetic non-heme iron complex: Oxidation of *n*-hexane by an immobilized mononuclear iron carboxylate complex.⁵⁰ (B) Biomimetic metalloporphyrin complex: Oxidation of *n*-heptane by the Mn^{III} acetate complex of bis-pocket porphyrin $[\text{Mn}(\text{TTPPP})(\text{OAc})]$.^{47, 48} (C) Heterogeneous microporous catalyst: Oxidation of *n*-hexane by the molecular sieve MnAlPO-18.⁵²

1.2.2 Biocatalysts

Chemically-based approaches for the selective oxidation of hydrocarbons are not economical as they rely on expensive transition metals and complex ligand designs for the control of selectivity.⁴⁰ They are not sustainable either because they often require harsh reaction conditions and high energy-demanding processes. Similarly to chemical biomimetic catalysts, biological catalysts carry out homolytic C-H cleavage under physiological temperatures and pressures. Biocatalysts, however, offer higher C₁ selectivity and lower byproduct formation than biomimetic catalysts.⁴¹

For their biotechnological potential, several ω -oxidizing microorganisms and their enzymes have been studied intensively during the last two decades. Such enzymes are oxygenases whose substrate ranges depend on the chain length of the hydrocarbon.^{46, 55-57} Short-chain alkanes (C₁-C₄) are hydroxylated by binuclear metallic monooxygenases of different bacterial origin. Medium-chain alkanes (C₅-C₁₆) are oxidized by non-heme diiron monooxygenases or alternatively by cytochrome P450 monooxygenases (CYP or P450s). Longer alkanes (\geq C₁₆) can be oxidized by yeast CYP enzymes, flavin-containing alkane monooxygenases, dioxygenases and other oxygenases. Several of these biocatalysts are presented in table 1.2.

Table 1.2. Examples of native and engineered microbial alkane and fatty acid ω -hydroxylases

Enzyme	Strain(s)	Enzyme characteristics			Ref.
		Components	Substrate spectrum	Remarks	
Binuclear metallic (di)iron or di(copper) alkane monooxygenases					
Methane monooxygenases					
sMMO (soluble)	<i>Methylococcus capsulatus</i> (Bath)	(1) Diiron hydroxylase (2) NADH-dependent, [2Fe-2S]- and FAD-containing reductase (3) Regulatory protein	C ₁ -C ₇ (halogenated)-alkanes, alkenes, cycloalkanes, aromatic compounds	Regioselectivity depends on the chain length of the substrate (27 % ω -OH from C ₅ alkane; 63 % ω -OH from C ₆ alkane)	58-60
pMMO (particulate)	<i>Methylococcus capsulatus</i> (Bath), <i>Methylosinus trichosporium</i> OB3b, <i>Methylocystis</i> sp.	(1) Dicopper-or copper/iron hydroxylase (2) Reductase (3) Regulatory protein			61-63
Propane monooxygenases					
PMO	<i>Arthrobacter</i> strain B3aP <i>Gordonia</i> sp. TY-5, <i>Mycobacterium</i> sp. TY-6, <i>Pseudonocardia</i> sp. TY-7	Putative components: (1) Diiron hydroxylase (2) Reductase (3) Coupling protein	C ₁ -C ₃ alkanes C ₃ -C ₆ alkanes	Products include 1-alcohols, 2-alcohols, aldehydes and acids	64 65, 66

Table 1.2. (continued)

Enzyme	Strain(s)	Enzyme characteristics			Ref.
		Components	Substrate spectrum	Remarks	
Binuclear metallic (di)iron or di(copper) alkane monooxygenases					
Butane monooxygenases					
sBMO (soluble)	<i>Thauera butanivorans</i> sp. ("Pseudomonas butanovora")	(1) Iron-containing hydroxylase (2) NADH-dependent flavo-FeS reductase (3) Small regulatory protein	C ₂ -C ₉ alkanes (especially C ₃ -C ₅), C ₂ -C ₄ 1-alcohols, aromatic, halogenated compounds	85 % ω -regio-selectivity towards C ₄ alkane. Ketone formation is prevented by addition of 1-propanol or 1-pentanol	67-72
	<i>Nocardioides</i> CF8	Putative copper-containing BMO (similar to pMMO)	C ₃ -C ₄ alkanes		73
Integral-membrane non heme-iron alkane monooxygenases					
AlkB	<i>Pseudomonas putida</i> GPo1 ("Pseudomonas oleovorans")	(1) Integral-membrane alkane hydroxylase (AlkB) (2) Rubredoxin reductase (AlkT) (3) Rubredoxin (AlkG)	C ₅ -C ₁₆ alkanes (especially C ₃ -C ₁₂), cycloalkanes, <i>N</i> -benzylpyrrolidine, C ₅ -C ₁₂ fatty acid methyl esters	\geq 95 % ω -regio-selectivity	15, 74-76
		(1) AlkB-BMO2 (V129M/L132V/I233V) mutant (2) AlkT; (3) AlkG	C ₃ -C ₈ alkanes	150 % higher productivity than wild type AlkB	77
AlkB-like	<i>Mycobacterium vaccae</i> JOB5	Putative diiron cluster	C ₂ -C ₁₆ alkanes, alcohols, chlorobutanol and fatty acids	Similar to sMMO and AlkB	78, 79
	<i>Dietzia</i> sp.	Native fusion protein: (1) AlkB domain (2) Rubredoxin domain	C ₈ -C ₄₀ alkanes (especially C ₁₈ -C ₃₂)	Not fully characterized yet	80
Heme-iron monooxygenases					
Cytochrome P450 monooxygenases (P450s or CYPs)					
CYP52	<i>Candida tropicalis</i> , <i>Candida maltosa</i> , <i>Candida apicola</i> , <i>Yarrowia lipolytica</i>	(1) Membrane-bound CYP52 (2) Membrane-bound NADPH-dependent reductase	>C ₁₂ alkanes and fatty acids	1-alcohols, ω -OHFAs and α,ω -DCAs as products	12, 14, 17, 81
	CYP153	<i>Acinetobacter</i> sp. EB104, OC4, <i>Alcanivorax borkumensis</i> SK2, <i>Mycobacterium</i> sp. HXN-1500 and several others	(1) CYP153 (2) NAD(P)H-dependent ferredoxin reductase (3) [2Fe-2S] ferredoxin	C ₄ -C ₁₆ alkanes, alkenes, cycloalkenes, 1-alcohols, L-limonene, <i>N</i> -benzylpyrrolidine	\geq 95 % ω -regioselectivity
<i>Mycobacterium</i> sp. HXN-1500		(1) CYP153A6-BM01 (A97V) mutant (2) Ferredoxin reductase (3) Ferredoxin	C ₃ -C ₈ alkanes	75 % higher activity than wild type CYP153A6; 89 % ω -selectivity towards C ₄ alkane	77

Table 1.2. (continued)

Enzyme	Strain(s)	Enzyme characteristics			Ref.
		Components	Substrate spectrum	Remarks	
Heme-iron monooxygenases					
Cytochrome P450 monooxygenase (P450s or CYPs)					
CYP153	<i>Acinetobacter</i> sp. OC4, <i>Alcanivorax borkumensis</i> SK2	Chimeric fusion protein: (1) CYP153 (2) FMN/[2Fe-2S]-reductase domain of P450RhF	C ₆ -C ₁₄ alkanes, alkenes 1-alcohols, cycloalkanols	Production of 1-alcohols and α,ω -diols from C ₅ -C ₁₂ alkanes	89-92
CYP124	<i>Mycobacterium tuberculosis</i>	(1) CYP124 (2) Ferredoxin reductase (3) Ferredoxin	C ₁₂ -C ₁₆ methyl-branched fatty acids	Low activity and low ω -regioselectivity towards linear fatty acids	93
CYP101 mutant	<i>Pseudomonas putida</i>	(1) CYP101 (9 point mutations) (2) Ferredoxin reductase (3) Ferredoxin	C ₂ -C ₃ alkanes	Low ω -regioselectivity towards C ₃ alkane	94
CYP102A mutants/ reaction tuning	<i>Bacillus megaterium</i> , <i>Bacillus subtilis</i>	Natural fusion protein: (1) Mutated heme domain: CYP102A1 (77-9H) CYP102A3 (S189Q/A330V) (2) FAD/FMN-reductase domain	C ₈ -C ₁₂ alkanes	50% ω -regioselectivity towards C ₈ alkane	95-97
	<i>Bacillus megaterium</i>	(1) Native CYP102A1 heme domain (2) FAD/FMN-reductase domain	C ₁ alkane	Tuning of activity by addition of perfluorocarboxylic acids	98, 99
Putative CYPs	<i>Corynebacterium</i> sp. strain 7E1C, <i>Anabaena</i> 7120	(1) Putative CYP (2) NAD(P)H-dependent flavoprotein	alkanes, fatty acids	C ₈ alkane yielded 76 % 1-octanol and 24 % octanoate in <i>Corynebacterium</i> . CYP110 is a hypothetical fatty acid ω -hydroxylase in <i>Anabaena</i>	100-103
Long-chain alkane oxygenases					
CHA0	<i>Pseudomonas fluorescens</i> CHA0	Inferred alkane oxygenase	C ₁₈ -C ₂₈ alkanes	Discovered in complementation studies	104
AlkM	<i>Acinetobacter</i> sp. M-1	(1) Integral-membrane copper dioxygenase (2) Rubredoxin (3) Rubredoxin reductase	C ₁₀ -C ₄₄ alkanes and alkenes	Strongly inhibited by Fe ²⁺ and Zn ²⁺	105, 106
LadA	<i>Geobacillus thermodenitrificans</i> NG80-2	Soluble FMNH ₂ or NADPH-dependent metal-free flavoprotein monooxygenase	C ₁₅ -C ₃₆ alkanes	Thermostable	107, 108
		LadA (F146N/N376I) mutant	C ₁₆ alkane	3.4-fold higher activity than wild type LadA	109

As indicated in table 1.2, all biocatalysts are multicomponent proteins. This makes their functional expression difficult. Some of them (e.g. binuclear metallic enzymes) are even quite unstable and subject to strong product inhibition.¹¹⁰ Given their substrate range and stability, AlkB and CYP monooxygenases are more relevant to the scope of this work. AlkB enzymes have relatively high turnover rates, but their membrane-integrated nature limits their application in *in vitro* studies.¹¹¹ In the following section we describe the CYP superfamily, focusing on the membrane-bound CYP52 and soluble CYP153 enzymes. Other microbial CYPs are much less documented, have poor performance or ω -regioselectivity towards aliphatic compounds.

1.2.2.1 Cytochrome P450 monooxygenases

CYP enzymes (EC 1.14.x.x) catalyze the cleavage of molecular oxygen by the incorporation of one atom of molecular oxygen into a substrate molecule while reducing the second one to water.¹¹² The proposed reaction mechanism catalyzed by CYPs is shown in figure 1.3.

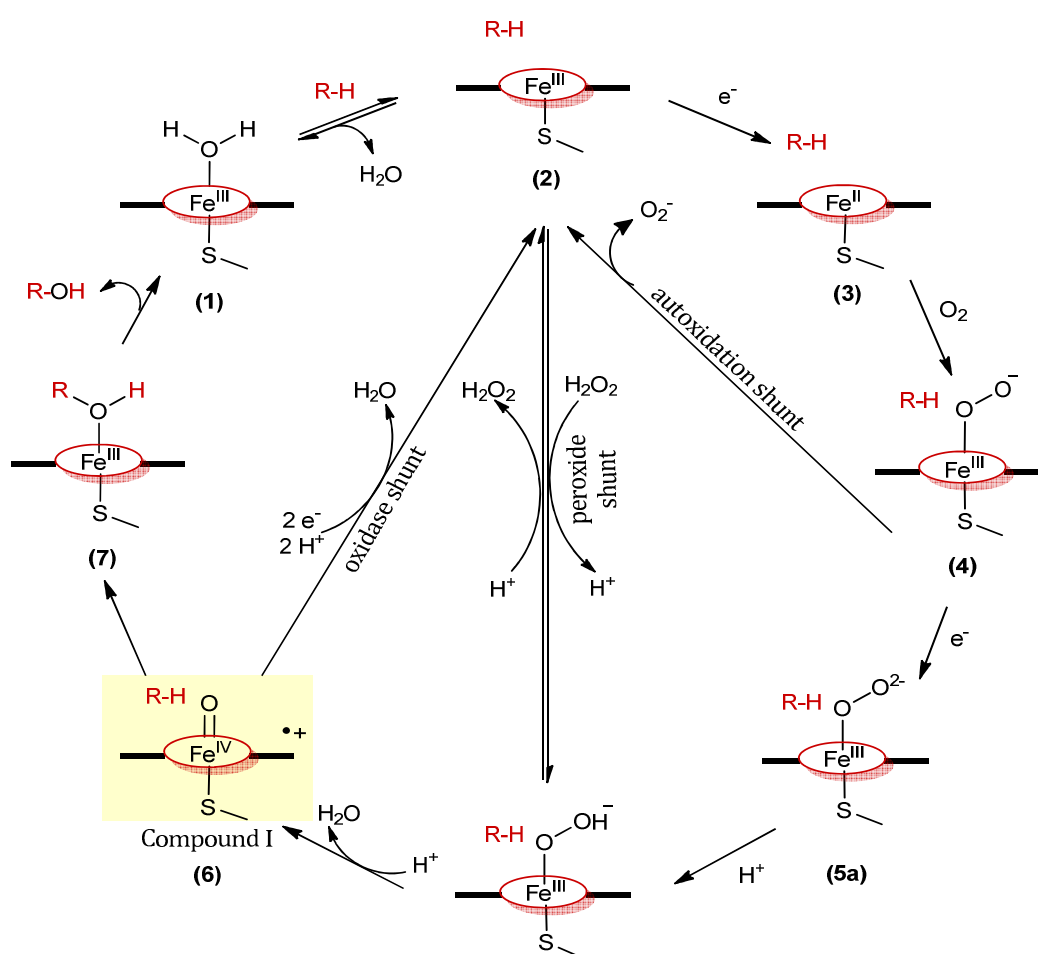


Figure 1.3. Proposed catalytic cycle of cytochrome P450 monooxygenases in hydroxylation reactions. The catalytically active iron-oxo ferryl species (Compound I) is highlighted in yellow. Graphic adapted from Denisov *et al.*¹¹³

The substrate first displaces a water molecule (1) and binds Fe^{III} (2), which is then reduced to Fe^{II} (3) by a one-electron transfer. Fe^{II} binds dioxygen to form an oxy-ferrous intermediate (4). A second one-electron reduction generates a negatively charged iron-peroxo complex (5a), which is protonated to yield an iron-hydroperoxo intermediate (5b). The O-O bond of this intermediate is cleaved, resulting in the release of one water molecule and the formation of the iron-oxo ferryl species, known as compound I (6). The activated oxygen atom of compound I oxidizes the substrate (7). The product is finally displaced by a water molecule. In addition to these steps, there are three side reactions: (i) the autoxidation shunt, in which the oxy-ferrous intermediate (4) is oxidized with production of a superoxide anion, (ii) the peroxide shunt, where the coordinated peroxide or hydroperoxide anion (5a,b) dissociates from the iron, resulting in hydrogen peroxide formation, and (iii) the oxidase shunt, wherein the activated oxygen from compound I (6) is reduced to water instead of resulting in oxidation of the substrate. These three processes are often referred to as uncoupling.¹¹³

The vast majority of CYPs are active only after interacting with one or more redox proteins from which they obtain their reducing equivalents. The electron transfer chain usually begins with the delivery of two electrons from NAD(P)H to the redox protein(s) and then to the heme iron catalytic site. Depending on the topologies of the heme and the reductase components, CYPs have been grouped in up to 10 classes.¹¹⁴ However, the most widespread topology classification includes only 4 classes (figure 1.4).^{115, 116}

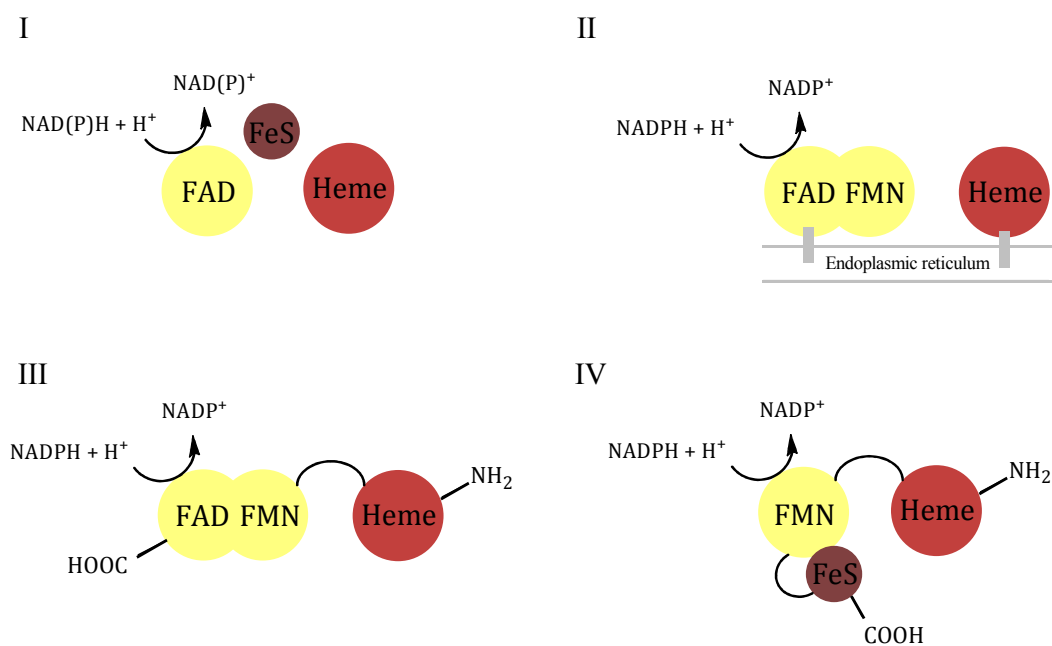


Figure 1.4. Topologies of CYP enzymes. FAD, flavin adenine dinucleotide; FeS, iron-sulfur ferredoxin, FMN, flavin mononucleotide. Examples of each class are: (I) P450cam (CYP101) from *Pseudomonas putida*, (II) Human CYP3A4, (III) P450 BM3 (CYP102A1) from *Bacillus megaterium*, (IV) P450 RhF from *Rhodococcus* sp. Graphic adapted from O'Reilly *et al.*¹¹⁵

CYP enzymes have been widely studied for synthetic applications due to their high chemo-, regio- or stereoselectivity and broad substrate spectrum. However, their cofactor dependence, low turnover number and low stability have limited their use in industrial processes.¹¹⁷⁻¹¹⁹ Current applications of CYPs are restricted to microbial fermentation processes to produce high value-added pharmaceuticals and fine chemicals that are difficult to obtain by chemical syntheses. The conversion of progesterone to cortisone by *Rhizopus* sp., established in the 1950s by Pharmacia and Upjohn (now Pfizer), is the first industrial application of a CYP.^{120, 121} The 11 β -hydroxylation of Reichstein S to hydrocortisone by *Curvularia* sp.¹²² is a process run at 100 tons/year at Schering.¹²³ Pravastatin, a drug that reduces cholesterol levels in blood, is produced by the microbial hydroxylation of compactin at Sankyo Pharma and Bristol-Myers Squibb, with an annual market value of US\$ 3.6 billion.¹²³ The fungal strain *Beauveria bassiana* Lu 700, which hydroxylates 2-phenoxypropionic acid to 2-(4'-hydroxyphenoxy)propionic acid is used for the synthesis of a number of agrochemicals at BASF.¹²⁴ This strain is also able to selectively hydroxylate other aromatic carboxylic acids.¹²⁵ Several other examples of the industrial applications of CYPs have been reviewed in the literature.^{119, 123, 126}

1.2.2.1.1 Fungal CYP52 monooxygenases

Selective terminal oxidation reactions occur naturally in mammals, plants and in certain fungi and bacteria.¹²⁷ Fungal CYP52 enzymes are membrane-bound microsomal monooxygenases that belong to class II CYPs, comprised by the CYP protein and an accompanying NADPH-dependent FAD/FMN-containing cytochrome P450 reductase (NCP). CYP52 monooxygenases – as well as NCPs – are encoded in one organism by different gene isoforms. The isoenzymes have diversified in their inducibility and substrate specificity. CYP52 genes have been found in filamentous fungi, including *Aspergillus*, and in yeasts of the genera *Candida*, *Yarrowia* and *Pichia*, to name a few.¹²⁸ The most studied CYP52 enzymes belong to *Candida maltosa*, *Candida tropicalis* and *Yarrowia lipolytica*, where they have been found to be responsible for the ω -hydroxylation of alkanes, fatty acids and alkylbenzenes.^{129, 130}

C. maltosa contains at least 8 CYP52 gene isoforms.^{131, 132} From them, CYP52A3 and CYP52A4, have been fully characterized.¹⁴ CYP52A3 converts its preferred substrate hexadecane to 1-hexadecanol as major product, but it also produces the corresponding aldehyde, acid, ω -OHFA and α,ω -DCA.¹⁷ CYP52A4 prefers dodecanoic acid as substrate, yielding the corresponding ω -OHFA. *C. tropicalis* possesses at least 18 CYP52 gene isoforms.¹² Two of them, CYP52A13 and CYP52A17, are known to act preferentially on oleic and tetradecanoic acid, respectively. Both enzymes yield the corresponding ω -OHFAs and α,ω -DCAs, with CYP52A17 displaying higher

diacid formation.⁸¹ *Y. lipolytica* has also been explored for its potential in alkane ω -oxidation.¹³ This microorganism counts with 12 gene isoforms. CYP52F1, for instance, acts on decane and dodecane. CYP52F2 oxidizes molecules larger than dodecane. Other three isoenzymes have ω -hydroxylation activities towards dodecanoic acid.¹³³⁻¹³⁵

Yeast CYP52 enzymes currently constitute the basis of the bio-based production of terminally oxidized fatty acids from alkanes or fatty acids. In all cases, metabolic engineering is required to prevent substrate and product depletion. One example is the accumulation of 20 g l⁻¹ α,ω -DCA from 23 g l⁻¹ dodecane after 50 h in a *Y. lipolytica* strain wherein four peroxisomal acyl-CoA oxidases (POX genes) were deleted.¹³⁶ The latest achievement consists of the production of 174 g l⁻¹ ω -OHFA and 6 g l⁻¹ α,ω -DCA from 200 g l⁻¹ methyl tetradecanoate after 6 days using an improved *C. tropicalis* strain. The host was engineered to overexpress a genome-integrated codon-optimized version of CYP52A17 under the control of the fatty acid-inducible isocitrate lyase (*ICL*) promoter. Since the target product was the ω -OHFA compound, a total of 16 genes (the native CYP52A17, 4 other CYP52 isoenzymes, 4 fatty acid alcohol oxidases and 7 alcohol dehydrogenases) ought to be deleted in order to prevent unspecific substrate oxidation and minimize ω -OHFA overoxidation.⁴ A recently constructed *Y. lipolytica* mutant lacking all its constitutive CYP52 gene isoforms is also a promising host for specific CYP52 characterization studies and biotechnological applications.¹³⁷

1.2.2.1.2 Bacterial CYP153 monooxygenases

CYP153 enzymes are class I CYPs that operate as three-component systems, comprised by the CYP itself, an iron-sulfur ferredoxin and a FAD-containing ferredoxin reductase, which are necessary for the transfer of electrons from NADH to the CYP active site (figure 1.5).^{86, 138} Enzymes of the CYP153A subfamily are regarded as promising biocatalysts due to their functional expression in soluble form as well as their high regioselectivity for the ω -position of alkanes and other compounds.⁸⁷ Previous to this work, CYP153 enzymes are not mentioned in the literature as fatty acid ω -hydroxylases.

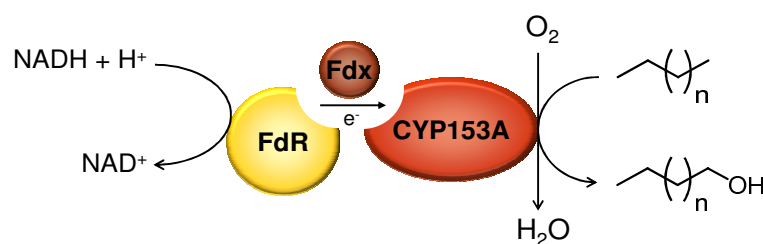


Figure 1.5. Schematic representation of a soluble CYP153A enzyme system catalyzing a typical *n*-alkane oxidation reaction. FdR, FAD-containing ferredoxin reductase; Fdx, ferredoxin.

CYP153 enzymes are found in α -, β - and γ -Proteobacteria (Gram-negatives) and Actinomycetales (high G+C Gram-positives) from oil-contaminated soil and marine environments.^{104, 139} CYP153A1 from *Acinetobacter* sp. EB104 was the first cloned and molecularly characterized CYP153.⁸⁶ In the early 2000s, Witholt and van Beilen collected a total of 137 alkane-degrading strains from natural and artificial environments, which were used as sources of CYP153A enzymes.¹⁴⁰ Fifteen of them, including *Mycobacterium* sp. HXN-1500, were isolated from a trickling-bed bioreactor by Engesser's group at the University of Stuttgart.¹⁴¹ Due to its higher turnover rates towards *n*-alkanes compared to other CYP153A enzymes, CYP153A6 from *Mycobacterium* sp. HXN-1500 has been further characterized, engineered and applied in whole cell biotransformations.^{77, 83, 84, 88, 142} CYP153A6 converts C₆ to C₁₁ to primary alcohols with a maximal turnover of 70 min⁻¹ and ≥ 95 % ω -regiospecificity.⁸³ Not only does this enzyme possess higher hydroxylation activity towards *n*-octane, but it is also able to catalyze the terminal oxidation of 1-octene and cyclohexene to the corresponding alcohols and epoxides, of styrene to styrene epoxide, *p*-cymene to *p*-isopropylbenzyl alcohol and of L-limonene to the anticancer agent perillyl alcohol (figure 1.6).^{83, 84} Two-phase bioconversions of L-limonene to perillyl alcohol by CYP153A6 and natural redox partners in *Pseudomonas putida* have resulted in a production yield of 6.8 g l⁻¹ in the organic phase after 75 h.⁸⁸ Lately, bioconversions of *n*-octane by CYP153A6 expressed with its natural redox partners in *E. coli* resulted in the production of 8.7 g l⁻¹ 1-octanol after 48 h using 20 % (v/v) substrate and 11 g_{cdw} l⁻¹ resting cells.¹⁴²

Misawa and collaborators have also made great contributions in the field by analyzing CYP153A13a (P450balk) from *Alcanivorax borkumensis* SK2 and 16 other new CYP153A genes isolated from polluted soil and groundwater.⁸⁵ The same group later found that CYP153 from *Acinetobacter* sp. OC4 (P450aci) had the ability to oxidize C₆-C₁₂ primary alcohols to α,ω -diols. Biotransformations of *n*-octane with 200 g_{cww} l⁻¹ *E. coli* cells containing P450aci and its natural redox partners yielded 2.3 g l⁻¹ 1-octanol and 0.7 g l⁻¹ 1,8-octanediol after 24 h.⁹⁰ P450aci and CYP153A13a were later co-expressed with the redox partners of P450cam – namely putidaredoxin reductase (CamA) and putidaredoxin (CamB) – or expressed as a fusion protein with the reductase domain of P450RhF (RhFred). Besides converting *n*-octane to the corresponding 1-alcohol and α,ω -diol, they hydroxylated cyclohexane to cyclohexanol and ω -oxidized the aliphatic chain of *n*-butyl-substituted aromatic and heterocyclic compounds (figure 1.6).⁹¹ More strikingly, CYP153A13a-RhFred has been found to hydroxylate the *p*-position of halogenated or acetyl-substituted phenolic compounds.¹⁴³ Other studies on CYP153A13a-RhFred include substrate binding, coupling efficiency and bioconversion towards *n*-alkanes.⁸⁹

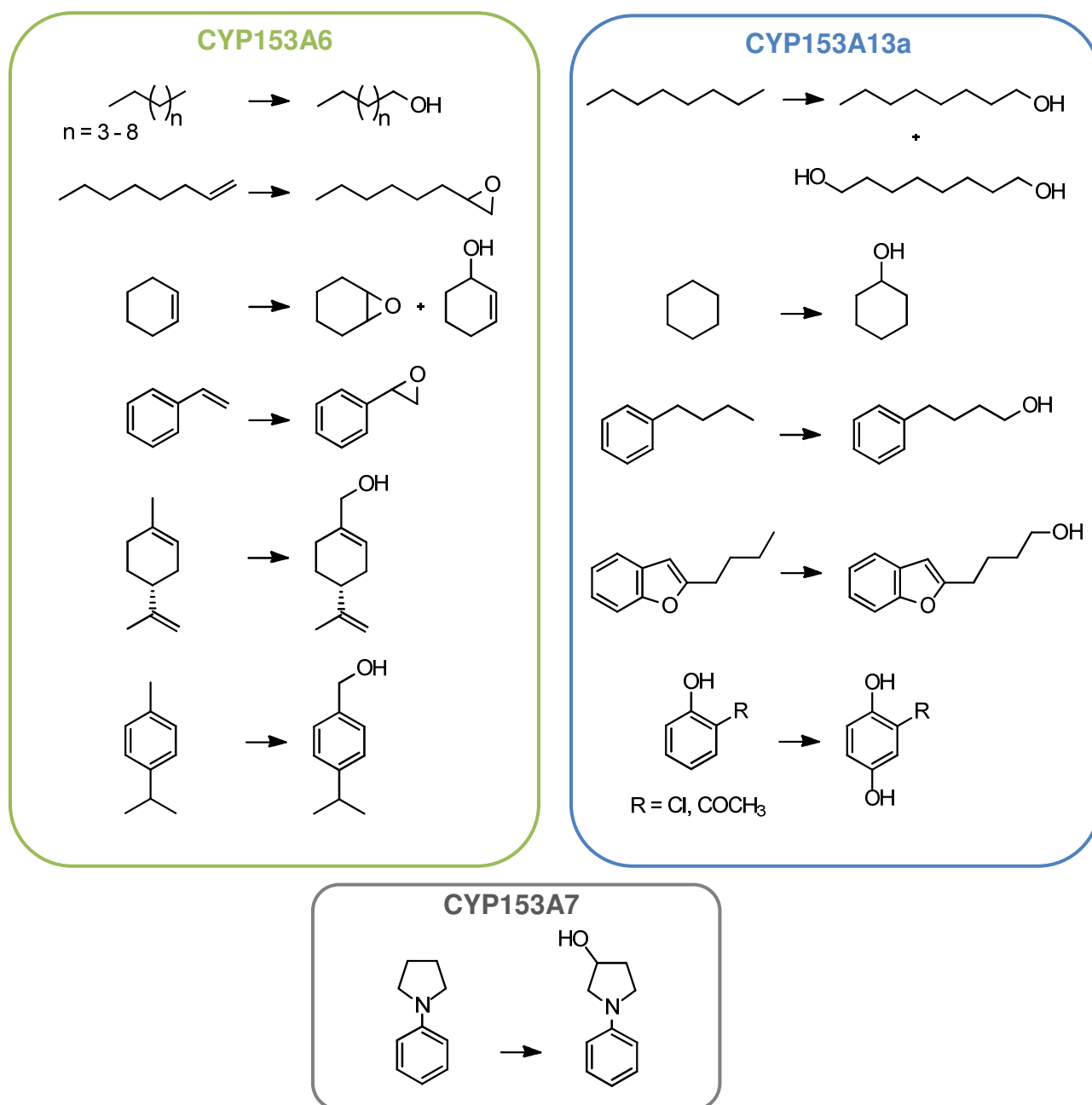


Figure 1.6. Substrate spectra of well-characterized CYP153A enzymes. CYP153A6 from *Mycobacterium* sp. HXN-1500, CYP153A13a from *Alcanivorax borkumensis* SK2 and CYP153A7 from *Sphingopyxis macrogoltabida*.

Prior to this work, rational design studies on CYP153A enzymes have not been reported in the literature. Structural insights have been provided by a substrate-docked homology model of CYP153A6, which allows the visualization of 11 active site residues.⁸³ This model suggested that the active site of CYP153A6 is predominantly hydrophobic in nature. Recently, the crystal structure of a CYP153A enzyme was published for the first time. It belongs to CYP153A7 (P450pyr) from *Sphingopyxis macrogoltabida* (PDB ID 3RWL),¹⁴⁴ a catalyst useful for the selective hydroxylation of *N*-substituted azetidines and piperidines (figure 1.6).¹⁴⁵ However, the

final structure lacks 9 residues located in a loop on the top of the cavity leading to the active site. This region was not visible in the electron density maps, a phenomenon that has also been described for the substrate-free state (“open state”) of P450cam.¹⁴⁶

Directed evolution on CYP153A enzymes has been carried out in Arnold’s laboratory. CYP153A6 was randomly mutated *in vivo* to shift its substrate range towards shorter gaseous alkanes. Mutator strains were used to generate a library of 10⁸ plasmid variants encoding CYP153A6. The plasmids were incorporated in adapted *P. putida* Gpo12(pGEc47ΔB) cells, which lack the alkane-degrading OCT plasmid and are thus unable to grow on alkanes without gene complementation. Evolved variants were selected by enhanced cell growth on the target alkanes as the sole carbon source. The effects of plasmid mutations and host adaptation were excluded by recloning the promising variants into a wild type vector and transferring them into a wild type strain. A single point mutation (A97V) was observed to be responsible for the 75 % increase in activity towards *n*-butane compared to the wild type enzyme in whole cell bioconversions using *E. coli*. However, the effect of the mutation – located in a loop region outside the active site – was not clearly understood.⁷⁷

1.3 Bacterial whole cell bioconversions with oxygenases

In biocatalytic reactions with oxygenases whole cells are preferred over isolated enzymes primarily because cells are capable of regenerating NAD(P)H. Cells may also confer higher oxygenase stability by providing a protected compartment (soluble enzymes) or a better organization of its components (membrane-bound enzymes). Additionally, cells contain the necessary machinery to scavenge reactive oxygen species originating from uncoupling, which could inactivate the enzyme. Despite these advantages, important issues such as substrate/product toxicity, low substrate uptake, byproduct formation, limited oxygen transfer and reduced cofactor availability should be overcome.¹⁴⁷⁻¹⁴⁹

1.3.1 *Pseudomonas* and *E. coli* as cell factories

The selection of the ideal host strain relies on high cell growth rates in simple media and access to knowledge and tools for its genetic manipulation. Other strain-related factors directly influencing the efficiency of a biocatalytic process include tolerance towards the substrate/product(s), stable recombinant protein expression, high NAD(P)H regeneration rate, low byproduct formation and the possibility of reuse for multiple reaction cycles.¹⁵⁰ In this

sense, *Pseudomonas* strains possess desirable features such as: 1) simple nutrient demand, 2) robustness to tolerate and modify several toxic aliphatic, aromatic and heterocyclic compounds, 3) efficient cofactor supply, and 4) inherent self-immobilization ability which facilitates the formation of stable and catalytically active biofilms.¹⁵¹⁻¹⁵⁴

Pseudomonas putida and related strains are nowadays used in diverse industrial applications, including the synthesis of bio-based materials, *de novo* synthesis and biotransformation of fine chemicals and pharmaceuticals.¹⁵³ Most of these processes exploit the unique xenobiotic-degrading enzymatic machinery of pseudomonads and are thus based on metabolically-engineered overproducing strains. The application of *Pseudomonas* strains in recombinant oxygenase-based biotransformations is still on the research level. In general, *Pseudomonas* strains seem more advantageous than *E. coli* because they have a network of glucose metabolism with multiple reduction and oxidation steps leading to a more efficient generation of redox power.¹⁵⁵ In terms of solvent tolerance, *Pseudomonas putida* strains are able to grow in the presence of high organic solvent concentrations (e.g. 6 % (v/v) 1-butanol).¹⁵⁶ However, solvent-tolerant strains also need more energy and cofactor to sustain defense mechanisms when exposed to toxic compounds.¹⁵⁷⁻¹⁵⁹ Considering that the carbon source is one of the highest operation costs in a bioprocess, the use of a *Pseudomonas* biocatalyst is economically justified if it exhibits not only a significantly higher solvent tolerance compared to other industrial production organisms (e.g., *E. coli*), but a similar product yield on carbon source as well.¹⁶⁰ Oxygen transfer is also a critical factor during reactions with the strictly aerobic pseudomonads; therefore, the process design should allow sufficient aeration to support both cell growth/maintenance and redox catalysis. Additional issues that should be addressed for industrial applications have been discussed elsewhere.¹⁶¹

In a recent study on the synthesis of (*S*)-styrene oxide from styrene in a biphasic system, recombinant *E. coli* (containing styrene monooxygenase/reductase) and *Pseudomonas* sp. strain VLB120ΔC were compared.¹⁶⁰ This pseudomonad is a solvent-tolerant strain expressing styrene monooxygenase and reductase constitutively but lacking styrene oxide isomerase, which mediates the conversion of the target product styrene oxide to phenylacetaldehyde. Biotransformations in *E. coli* resulted in higher specific activities, product yields on glucose and volumetric productivities than the investigated *Pseudomonas* strain. Nevertheless, the pseudomonad provided the advantages of tolerance towards higher product titers and higher process durability. In contrast to *E. coli*, the pseudomonad did not accumulate the byproduct 2-phenylethanol because it was able to degrade it.¹⁶⁰ Moreover, *Pseudomonas* sp. produced ten times less acetate than *E. coli* (0.3 vs. 3.6 g l⁻¹). Acetate formation is known to reduce the cofactor

regeneration yield per glucose consumed and to negatively influence the proton gradient across the cytoplasmic membrane.^{162, 163}

A step forward in the application of pseudomonads in redox biocatalysis consists of the establishment of biofilm-forming and engineered *Pseudomonas* strains for efficient styrene oxide production in novel continuous reactors. The bioprocess resulted in high volumetric productivities as well as improved tolerance and robustness comparable to those of planktonic cultures.¹⁶⁴⁻¹⁶⁶

1.3.2 Growing and resting cells as whole cell biocatalysts

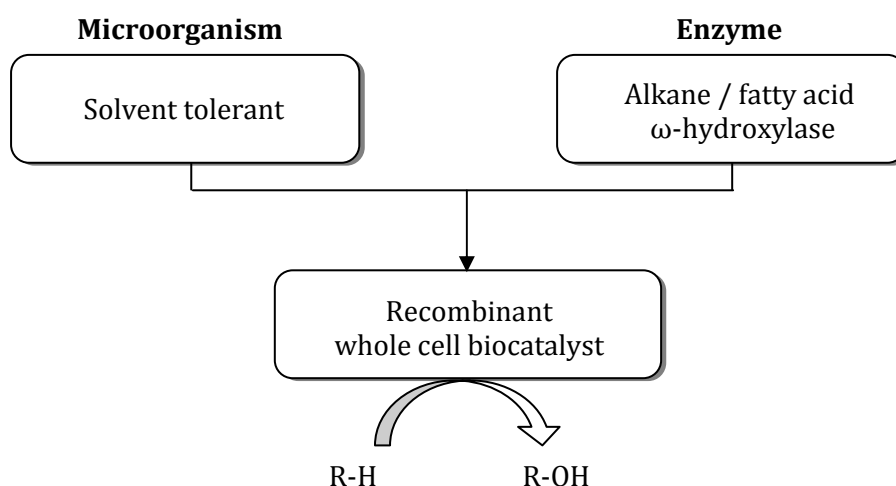
One key question in whole cell biocatalysis is whether to use growing or resting cells. Growing cells are capable of constant oxygenase synthesis and they should have a more active metabolism for cofactor regeneration. However, most of the available energy and cofactor are used for biomass formation rather than for redox biocatalysis. These cells also have low durability and low tolerance to substrate/product toxicity. Metabolically active resting cells have lower carbon and energy demands than growing cells, thus the cofactor formed during central carbon catabolism can be exploited more efficiently for biocatalysis rather than for cell growth. This results in higher specific activities and product yields on energy source. In addition, resting cells display a higher biomass durability which might enable their reuse, provided high oxygenase activities are retained over time.¹⁶⁷⁻¹⁷⁰

Most limitations observed in whole biotransformations with resting cells depend on factors intrinsically associated to the biocatalyst (e.g., enzyme stability, enzyme kinetics, uncoupling) rather than on the metabolic capacity of the host strain.¹⁶⁷ For example, in the oxygenase-mediated epoxidation of styrene in biphasic medium, maximal specific activities with resting *E. coli* cells doubled those of growing cells in a similar setup.¹⁷¹ Toxicity was not a problem and the enzyme was not deactivated, but product formation rates decreased steadily mainly due to product inhibition.¹⁶⁷ In another study with *E. coli* containing a recombinant Baeyer-Villiger monooxygenase, space-time yields of non-growing cells were 20 times higher than those of growing cells. Here the duration and rate of the oxidation reaction were limited by the intracellular stability of the oxygenase and the rate of substrate transport across the cell membrane.¹⁶⁹ Therefore, strategies to minimize product inhibitory effects on the biocatalyst include the application of two-liquid phase systems and *in situ* product removal techniques. The use of solvent tolerant strains can also contribute to avoid inhibition by efficient transport of the product out of the cell.¹⁷²

1.4 Aim of the work

Within the frame of the “Systems Biology of *Pseudomonas* for Industrial Biocatalysis”ⁱ and “Developing the Next Generation of Biocatalysts for Industrial Chemical Synthesis”ⁱⁱ projects, the aim of this work was to develop a stable recombinant bacterial system harboring a regioselective alkane hydroxylase to catalyze the omega-oxygenation of industrially-relevant aliphatic compounds, including alkanes, primary alcohols and fatty acids (scheme 1). For this purpose, the following tasks were established:

- Identification of appropriate bacterial cytochrome P450 monooxygenases or non-heme monooxygenases *via* substrate screening or database-driven search.
- Tailoring of the biocatalyst by rational design or directed evolution to suit the target substrates and functional expression of the best candidates in solvent-tolerant *Pseudomonas* and *E. coli* strains.
- Improvement of the designed biocatalytic system by optimization of electron coupling efficiency in solvent-tolerant *Pseudomonas* or *E. coli* strains using a protein engineering or systems biology approach.



Scheme 1

ⁱ German Federal Ministry of Education and Research (BMBF)

ⁱⁱ European Union’s 7th Framework Programme FP7/2007-2013, Grant Agreement No. 266025

2 Experimental section

2.1 Genes, vectors and strains

Genes, vector constructs and strains are detailed in supplementary material section 6.1.

2.2 Procedures

2.2.1 Substrate screening of CYP153A biocatalysts

Materials and methods for the screening of CYP153A enzymes towards linear alkanes,¹⁷³ primary alcohols¹⁷³ and fatty acids¹⁷⁴ are described in the corresponding references.

2.2.2 Creation of a focused mutant library of CYP153A from *Marinobacter aquaeolei*

2.2.2.1 Site-directed mutagenesis

Plasmid pET28a(+) harboring His₆-tagged CYP153A *M. aq.* was mutated using the QuikChange standard protocol. Nineteen variants were created by PCR amplification with the oligonucleotides indicated in table 2.1. Competent *E. coli* DH5 α cells were transformed with the *DpnI*-treated PCR mixtures. Isolated plasmids with the desired mutations were verified by sequencing (GATC-Biotech, Köln, Germany) and used to transform *E. coli* BL21(DE3) cells.

Table 2.1. Primers for site-directed mutagenesis

Variant	Primer	Sequence (5' → 3')
M143R	F	CTG TCG GTG GAA CGT TTC ATA GCG ATG GAT CC
	R	GGA TCC ATC GCT ATG AAA CGT TCC ACC GAC AG
I145M	F	CG GTG GAA ATG TTC ATG GCG ATG GAT CCG CC
	R	GG CGG ATC CAT CGC CAT GAA CAT TTC CAC CG
I145F	F	CG GTG GAA ATG TTC TTT GCG ATG GAT CCG CC
	R	GG CGG ATC CAT CGC AAA GAA CAT TTC CAC CG

F = Forward primer; R = Reverse primer (complementary sequence); mutated codons (bold)

Table 2.1. (continued)

Variant	Primer	Sequence (5' → 3')
I145S/T	F	CG GTG GAA ATG TTC ASC GCG ATG GAT CCG CC
	R	GG CGG ATC CAT CGC GST GAA CAT TTC CAC CG
T302M	F	T ATC GGT AAT TTG RTG CTG CTC ATA GTC GGC G
	R	C GCC GAC TAT GAG CAG CAY CAA ATT ACC GAT A
T302V	F	G GAG TTT ATC GGT AAT TTG GTG CTG CTC ATA GTC GGC GGC AAC GAT ACG AC
	R	GTC GTA TCG TTG CCG CCG ACT ATG AGC AGC ACC AAA TTA CCG ATA AAC TCC
L303T	F	T ATC GGT AAT TTG ACG ACC CTC ATA GTC GGC G
	R	C GCC GAC TAT GAG GGT CGT CAA ATT ACC GAT A
V306T	F	TG ACG CTG CTC ATA ACC GGC GGC AAC GAT ACG
	R	CGT ATC GTT GCC GCC GGT TAT GAG CAG CGT CA
G307A/V	F	C GGT AAT TTG ACG CTG CTC ATA GTC GYG GGC AAC GAT ACG ACG CGC
	R	GCG CGT CGT ATC GTT GCC CRC GAC TAT GAG CAG CGT CAA ATT ACC G
L354I/F	F	G GTG TCG GAA ATC ATC CGC TGG CAA ACG CCG WTT GCC TAT ATG CGC CGA ATC GCC GCC AAG CAG GAT GTC GAA CTG
	R	CAG TTC GAC ATC CTG CTT GGC GGC GAT TCG GCG CAT ATA GGC AAW CGG CGT TTG CCA GCG GAT GAT TTC CGA CAC C
M357F	F	CAA ACG CCG CTG GCC TAT TTT CGC CGA ATC GCC AAG CAG G
	R	CCT GCT T GG CGA TTC GGC GAA AAT AGG CCA GCG GCG TTT G
M357Y	F	G CCG CTG GCC TAT TWT CGC CGA ATC GCC AAG
	R	CTT GGC GAT TCG GCG AWA ATA GGC CAG CGG C
M357N	F	G CCG CTG GCC TAT AAC CGC CGA ATC GCC AAG
	R	CTT GGC GAT TCG GCG GTT ATA GGC CAG CGG C
F465L	F	GTG CAG TCC AAC CTG GTG CGG GGC TAT TC
	R	GA ATA GCC CCG CAC CAG GTT GGA CTG CAC
F465I	F	GTG CAG TCC AAC ATT GTG CGG GGC TAT TC
	R	GA ATA GCC CCG CAC AAT GTT GGA CTG C AC
F465Y	F	GTC GAA GAG CCC GAG CGG GTG CAG TCC AAC TAT GTG CGG GGC TAT TCC AGG TTG ATG GTC
	R	GAC CAT CAA CCT GGA ATA GCC CCG CAC ATA GTT GGA CTG CAC CCG CTC GGG CTC TTC GAC

F = Forward primer; R = Reverse primer (complementary sequence); mutated codons (bold)

2.2.2.2 Protein expression, purification and quantitation

Expression and purification of the His₆-tagged CYP153A *M. aq.* variants were carried out as described elsewhere.¹⁷³ Concentrations of the P450 enzymes were determined by the carbon monoxide (CO) differential spectral assay described by Omura and Sato.^{175, 176}

2.2.2.3 *In vitro* oxidation assays and kinetic analysis

All variants including wild type enzyme were screened in a preliminary assay using cell-free extracts resulting from disrupted cells resuspended in 50 mM potassium phosphate buffer pH 7.5 and protease inhibitor (0.1 mM PMSF). Reaction mixtures were run for 4 h at 30°C in a final volume of 0.5 ml containing 50 mM potassium phosphate buffer pH 7.5, 2 μ M P450 (as lysate), 10 μ M CamA, 20 μ M CamB, 1 mM substrate in ethanol (*n*-alkane and primary alcohols) or in DMSO (fatty acids), 1 mM NADH and the glucose-6-phosphate/glucose-6-phosphate dehydrogenase (G6P/G6PDH) system (1 mM MgCl₂, 5 mM G6P and 12 U ml⁻¹ G6PDH) for cofactor regeneration.¹⁷⁴ Reactions with poorly expressible variants were run with 0.2 μ M CYP. The results were contrasted with those obtained with 0.2 μ M wild type enzyme. Procedures concerning reaction setups with purified proteins for substrate conversions (wild type enzyme and variants G307A, L354I and L354F) and the determination of kinetic parameters (wild type enzyme and variant G307A) are detailed in the corresponding reference.¹⁷⁴ Sample treatment and GC/MS analysis of substrates and products are therein described as well.

2.2.3 Bacterial whole cells for the synthesis of ω -oxygenated aliphatic compounds

2.2.3.1 Biotransformations of *n*-octane by growing *P. putida* cells containing CYP153A gene clusters

2.2.3.1.1 Cloning of CYP153A gene clusters

Alkane hydroxylase gene clusters from *Mycobacterium marinum* M. (ATCC BAA-535), *Marinobacter aquaeolei* VT8 (DSM 11845) and *Polaromonas* sp. JS666 (ATCC BAA-500) were isolated from genomic DNA. Each cluster was comprised by the CYP153A monooxygenase and two neighbouring redox proteins annotated as putative electron partners of the corresponding CYP enzyme (table 2.2; supplementary material section 6.1.1). For their expression in *Pseudomonas*, plasmids derived from the L-rhamnose-inducible pJOE^{177, 178} and the *n*-alkane-inducible pCom¹⁷⁹ series were utilized.

Table 2.2. Alkane hydroxylase gene clusters and plasmid constructs

Strain	Gene cluster abbreviation	Gene cluster composition (5'→3') and size	Plasmids
<i>Mycobacterium marinum</i> M.	MmAlk	MmFdx→CYP153A16→MmFdR (2932 bp)	pJOE-MmAlk pCom10-MmAlk
<i>Marinobacter aquaeolei</i> VT8	MaqAlk	MaqFdx→CYP153A <i>M.aq.</i> → MaqFdR (3063 bp)	pJOE-MaqAlk pCom10-MaqAlk
<i>Polaromonas</i> sp. JS666	PspAlk	CYP153A <i>P. sp.</i> → PspFdR→PspFdx (2898 bp)	pJOE-PspAlk pCom10-PspAlk

Fdx, ferredoxin; FdR, ferredoxin reductase

Vectors were provided as pJOE4782.1¹⁸⁰ and pCom10-alkB-BMO2⁷⁷ constructs by J. Altenbuchner (University of Stuttgart) and F. H. Arnold (California Institute of Technology), respectively (supplementary material figure 6.1). Plasmid pJOE4782.1 originally contains genes encoding malE (maltose-binding protein) and eGFP (enhanced green fluorescent protein) between sites *NdeI* and *HindIII*. In a previous work at our institute, the *NdeI* site was mutated to introduce an *XbaI* site. The malE-eGFP region was excised with endonucleases *XbaI* and *BsrGI* (*BsrGI* cuts eGFP 3 bp before its stop codon) to insert the gene coding for P450 BM3.¹⁸¹ Here we removed the P450 BM3 gene insert to introduce the MmAlk gene cluster, while the original pJOE4782.1 was used to insert the MaqAlk and PspAlk operons. Plasmid pCom10-alkB-BMO2 did not contain an *NdeI* site; therefore, primer 5'-TAA AAA TTG GAG AAT TCA TAT GCT TGA GAA ACA CAG AGT TC-3' and its complementary sequence 5'-GAA CTC TGT GTT TCT CAA GCA TAT GAA TTC TCC AAT TTT A-3' were designed to insert the restriction site into the construct following the QuikChange site-directed mutagenesis protocol. The gene clusters were amplified using a standard PCR protocol with the primers indicated in table 2.3. The PCR-amplified gene clusters were digested and ligated with the corresponding linearized vectors.

Table 2.3. Primers for cloning the alkane ω -hydroxylase gene clusters

Primer name	Sequence (5' → 3')	Use
MmAlk_Xba_F	C TAG tct aga <u>GGA GAT</u> ATT GAA ATG GCA GTT GTC A	Cloning of MmarAlk into pJOE
MmAlk_BsrG_R	G TAC tgt aca TCA GTC CGA GCC GGC	
MmAlk_Eco_F	AA TTg aat tcA ATT CCA ATG GCA GTT GTC ACA TTT GTC	Cloning of MmarAlk into pCom10
MmAlk_Hind_R	A GCT aag ctt TCA GTC CGA GCC GG	
MaqAlk_Nde_F	TA cat atg GGC GGT CAC GAT GGG CC	Cloning of MaqAlk into pJOE and pCom10
MaqAlk_Hind_R	A GCT aag ctt TCA ACT CTG GAG CCT TCC GT	
PspAlk_Nde_F	GGT cat atg AGA TCA TTA ATG AGT GAA GCG ATT GTG GTA	Cloning of PspAlk into pJOE and pCom10
	AAC AAC C	
PspAlk_Hind_R	A GCT aag ctt TCA GTG CTG GCC GAG CGG	

Restriction site (lower-case letters); ribosome binding site (underlined); start/stop codon (bold)

The resulting constructs were verified by sequencing (GATC-Biotech, Köln, Germany). The pJOE vector constructs were sequenced with the forward primer 5'-GGC GCT TTT TAG ACT GGT CG-3', which hybridized with the L-rhamnose promoter, and with the reverse primer 5'-GAG CAA ACT GGC CTC AGG CA-3', which encodes a region of the pJOE vector. The pCom10 vector constructs were sequenced with the forward primer 5'-TGG GCG GCT TAA CTT TCT CAG TTA-3', which hybridized with the *PalkB* promoter region, and with the reverse primer 5'-TTA TCA GAC CGC TTC TGC GTT CT-3', which is complementary to a section of the pCom10 vector. The complete sequences were verified by additional sequencing with two primers matching specific regions of each cluster: 5'-CGA AGA ACC TGC GTG AGA TG-3' (811-830) and 5'-GAT CCT GTG GGA GGA GCT G-3' (1601-1620) for MmAlk; 5'-TAG TGG CAC CGA AAA ACC TGA AG-3' (811-833) and 5'-CAT CCG AAC GTG TGG AGA GTC-3' (1760-1790) for MaqAlk and; 5'-CGG ACG AAT ACC GCA AGC TG-3' (821-840) and 5'-ACG TCG GAC TCG AGA TCG C-3' (1731-1749) for PspAlk. Vector constructs were used to transform *Pseudomonas putida* KT2440 by electroporation.¹⁸²

2.2.3.1.2 Verification of functional expression of MmAlk in a pseudomonad

P. putida S12 cells were transformed with the pJOE-MmAlk construct and with religated empty pJOE (negative control) by electroporation. One colony of each recombinant strain was grown overnight in 5 ml LB_{Kan} medium at 30°C, 180 rpm. Two milliliters of the pre-culture were used to inoculate 400 ml TB_{Kan} medium. When an OD₆₀₀ of 0.6 was reached, cells were induced with 0.2 % L-rhamnose plus 0.5 mM 5-aminolevulinic acid and incubated at 25°C, 180 rpm for 20 h. Cells were harvested, suspended in 50 mM potassium phosphate buffer pH 7.5 with 100 µM PMSF and disrupted by sonication (3 x 2 min, 1.5 min intervals). P450 concentrations were determined in the cell-free extracts as described elsewhere.^{175, 176} Cell lysates (4 mg total protein ml⁻¹), 0.1 mM cytochrome *c* and 0.5 mM NADH were used for the cytochrome *c* reductase assay.¹⁸³ *n*-Octane oxidation reactions were performed in 50 mM potassium phosphate buffer pH 7.5 with 1 mM substrate, 1 mM NADH, the G6P/G6PDH cofactor regeneration system and cell lysate to a final concentration of 3 µM P450. Sample treatment and GC/MS analysis proceeded as previously described.¹⁷³

2.2.3.1.3 *n*-Octane oxidation by growing *P. putida* KT2440 cells

P. putida KT2440 transformants containing the pJOE constructs were grown in 200 ml TB_{Kan} medium, while those harboring pCom10 vectors were grown in 200 ml modified M12 mineral medium (MM-BVT_{Kan}). The medium consisted of 10X mineral salts solution (22 g l⁻¹ (NH₄)₂SO₄, 4

g l⁻¹ MgSO₄·7H₂O; 0.4 g l⁻¹ CaCl₂; 0.2 g l⁻¹ NaCl), 50X phosphate solution (100 g l⁻¹ KH₂PO₄) and 100X trace elements solution (0.2 g l⁻¹ ZnSO₄·7H₂O, 0.1 g l⁻¹ MnCl₂·4H₂O; 1.5 g l⁻¹ Na₃-citrate·2H₂O; 0.1 g l⁻¹ CuSO₄·5H₂O; 0.002 g l⁻¹ NiCl₂·6H₂O; 0.003 g l⁻¹ NaMoO₄·2H₂O; 0.03 g l⁻¹ H₃BO₃ and 1 g l⁻¹ FeSO₄·7H₂O). MM-BVT_{Kan} was supplemented with additional citrate (5 g l⁻¹) as carbon source to prevent repression of the *PalkB* promoter by glucose.¹⁸⁴ Cultures were left to grow at 30°C, 180 rpm, induced for recombinant protein expression at exponential growth phase (OD₆₀₀ = 0.6) and fed with 15 % (v/v) *n*-octane upon induction. In the case of pCom10-containing strains, the substrate acted as inducer as well. To prevent carbon and energy source depletion, 5 g l⁻¹ glucose and 5 g l⁻¹ citrate were added to TB_{Kan} and MM-BVT_{Kan}, respectively, 6 and 12 h after starting the cultures. Fifty milliliter culture samples were collected at different time points after induction/substrate addition for the measurement of optical cell densities (OD₆₀₀) and quantitative analysis of products by GC/FID. For the determination of 1-octanol concentrations, 0.5 ml culture samples were treated with 20 µl 37 % HCl and extracted twice with 0.5 ml ethyl acetate containing 0.2 mM 1-hexanol as internal standard. Samples were analyzed on a GC/FID (Shimadzu, Japan) equipped with an Agilent DB-5 column (30 m x 0.25 mm x 0.25 µm) with hydrogen as carrier gas (flow rate, 1.1 ml/min; linear velocity, 32 cm/s). The injector and detector temperatures were set at 250°C and 310°C, respectively. The column oven was set at 40°C for 2 min, raised to 160°C at a rate of 10°C/min, then raised to 300°C at 80°C/min. 1-Octanol was measured from calibration curves estimated from a series of standard solutions treated in the same manner as the samples.

2.2.3.2 Biotransformations of *n*-octane and fatty acids by resting *P. putida* and *E. coli* cells containing engineered CYP153A in a fusion construct

2.2.3.2.1 Subcloning of fusion genes

The wild type (CYP153A *M. aq.*-CPR_{BM3}) and mutant (CYP153A *M. aq.* (G307A)-CPR_{BM3}) fusion chimeras were created as pET28a(+) vector constructs (Daniel Scheps, unpublished data). For comparison studies in *P. putida* and *E. coli* strains, the fusion proteins were subcloned into pJOE4782.1 (*Xba*I/*Bsr*GI). The fragments were amplified with the forward primer 5'- C TAG tct aga **ATG** CCA ACA CTG CCC AGA ACA TTT-3' and the reverse primer 5'-G TAC tgt aca **TTA** CCC AGC CCA CAC GTC TTT-3' (restriction sites in lower-case letters; start/stop codons in bold) following a standard PCR protocol. Each digested PCR-amplified fusion gene was ligated with the linearized pJOE vector. Correct constructs were verified by sequencing (GATC-Biotech). Religated pJOE without insert was later used as negative control.

2.2.3.2.2 *n*-Octane and fatty acid oxidations by resting *P. putida* and *E. coli* cells

Strains *P. putida* KT2440, *P. putida* S12, *E. coli* JM109 and *E. coli* BL21(DE3) were included in the comparative study. Competent *P. putida* and *E. coli* cells were transformed with the previously mentioned pJOE-CYP153A *M. aq.*-CPR_{BM3} fusion constructs (containing wild type or mutant CYP) by electroporation and heat shock, respectively. Cells were also transformed with empty religated vector as negative controls to evaluate substrate consumption by the host strains in the absence of monooxygenase.

Freshly-plated transformants were grown overnight in LB_{Kan} and 2 ml of the pre-cultures were used to inoculate 400 ml TB_{Kan}. Cells were incubated at 30°C (*P. putida*) or alternatively at 37°C (*E. coli*) on shakers at 180 rpm. At an OD₆₀₀ of 1.2 - 1.5, cells were induced for recombinant protein expression with 0.2 % L-rhamnose. After 16 - 18 h (OD₆₀₀ = 9-10), cells were harvested and washed twice with 100 mM potassium phosphate buffer pH 7.4 containing 10 g l⁻¹ glycerol. Cells were suspended in 100 mM potassium phosphate buffer pH 7.4 with 10 g l⁻¹ glycerol, 100 µM FeSO₄ and 30 µg ml⁻¹ kanamycin to a final concentration of 100 g_{cww} l⁻¹. A fraction of the cell suspensions (15 ml) was centrifuged, the pellet weighed and stored at -20°C for cell disruption and determination of CYP concentration in cell lysates prior to the start of biotransformations. Cell suspensions (20-25 ml) were also used for cell dry-to-wet weight determinations in triplicates as described elsewhere.¹⁸⁵

Biotransformations of *n*-octane and fatty acids were conducted with solvent-untreated resting cells in the absence or presence of an additional carbon source (glucose/glycerol mix: 0.4 g l⁻¹ glucose and 10 g l⁻¹ glycerol). *In vivo* bioconversions with induced resting cells were carried out in 100 ml shake flasks containing 20 ml fresh cell suspension (100 or 50 g_{cww} l⁻¹). The biotransformation medium consisted of 100 mM potassium phosphate buffer pH 7.4 containing glucose/glycerol mix, 100 µM FeSO₄ and 30 µg ml⁻¹ kanamycin. Biotransformations started by the addition of substrate. For the *n*-octane reaction setups, the substrate and co-solvent DMSO were added to final concentrations of 10 % (v/v) and 2 % (v/v), respectively. Octanoic and dodecanoic acids were added to a final concentration of 5 mM from stock solutions containing 250 mM of the fatty acid in DMSO. In case of oleic acid, the substrate was added directly to the bioconversion mixture in a final concentration of 5 mM, followed by addition of 2 % (v/v) DMSO. Reactions were run on orbital shakers at 30°C and 180 rpm for 20 h.

Five hundred microliter samples were collected at different time points (0, 1, 2, 4, 8, 12 and 20 h after substrate addition) and reactions were immediately stopped by adding 30 µl 37 % HCl. Samples corresponding to *n*-octane bioconversions were treated and analyzed by GC/FID as

described in section 2.3.4.1.3. For samples corresponding to fatty acid bioconversions, internal standard (decanoic acid for the C_{12:0} substrate or tridecanoic acid for the C_{8:0} and C_{18:1} substrates) was added in a final concentration of 1 mM. The reaction mixtures were extracted twice with 2 volumes of diethyl ether. The organic phases were collected, dried with MgSO₄ (anhydrous) and evaporated. Samples were resuspended in 60 µl methyl *tert*-butyl ether, followed by the addition of 60 µl of 1% trimethylchlorosilane in *N,O*-bis(trimethylsilyl)trifluoroacetamide and incubation at 75°C for 30 min for derivatization. Samples were measured by GC/FID as described elsewhere,¹⁷⁴ with the fatty acid substrate and/or products being quantified from calibration curves of standard solutions treated in the same manner as the samples. Occasionally, additional culture samples were taken for OD₆₀₀ measurements and determination of CYP concentrations in whole cells in order to evaluate cell toxicity and enzyme activity over time.¹⁴²

2.2.3.2.3 Determination of hydrogen peroxide formation in cell crude extracts

Quantitation of total (intracellular and extracellular) H₂O₂ was performed by the horseradish peroxidase/phenol/4-aminoantipyrine spectrophotometrical assay, which is based on the absorbance of the quinoneimine product at 510 nm.¹⁸⁶ Reaction mixtures were prepared in 50 mM Tri-HCl buffer pH 7.5 to a final volume of 800 µl and contained 100 µl cell culture, 10 µl BugBuster™ 10X Protein Extraction Reagent (Novagen, Wisconsin, USA), 12.5 mM phenol, 1.25 mM 4-aminoantipyrine and 0.1 mg ml⁻¹ horseradish peroxidase. The absorbance of each sample was set at zero before adding the peroxidase. Hydrogen peroxide concentrations were calculated from a calibration curve with known concentrations of H₂O₂ (2 - 80 µM) that yielded absorbances in the linear range. In order to exclude any potential interference of the BugBuster™ reagent with the enzymatic assay, it was added to all standard solutions.

2.2.3.2.4 Determination of acetate formation in cell cultures

Cell cultures (0.5 ml) were extracted twice with 0.5 ml diethyl ether. The aqueous phase was collected and filtered (0.45 µm) for the determination of acetate concentration using an Agilent 1200 series HPLC system (Agilent Technologies, Waldbronn, Germany) equipped with an Aminex HPX-87H Ion Exclusion Column (300 mm x 78 mm, BIO-RAD, USA). The column was set at 60°C. The mobile phase consisted of 5 mM sulfuric acid in water. The injection volume was 10 µl and compounds were separated at a flow rate of 0.5 ml min⁻¹. Acetate was detected on a RID set at 35°C and a DAD at 210 nm. The concentration of acetate in the samples was calculated using a standard curve of analyte concentrations ranging from 0.25 to 40 mM, treated in the same manner as the samples.

3 Results and Discussion

3.1 Substrate screening of CYP153A biocatalysts

3.1.1 Medium-chain linear alkanes and primary alcohols

CYP153A16 from *Mycobacterium marinum* and CYP153A from *Polaromonas* sp. (CYP153A *P. sp.*) were expressed in soluble form in *E. coli* BL21(DE3), yielding 1.25 and 32 mg active protein l⁻¹ culture, respectively, after purification by immobilized metal affinity chromatography. The reduced protein yield of CYP153A16 might be caused by the use of GTG as start codon (originally present in the *cyp153A16* gene sequence). CO-differential spectral assays indicated that the concentration of purified CYP153A *P. sp.* remained constant at room temperature for at least 4 h, while the characteristic 450 nm-peak of CYP153A16 decreased after 5 min due to lability to sodium dithionite. Nevertheless, the conventional CO-differential spectral assay with sodium dithionite was used as a standard method to determine the concentration of both purified CYP153 enzymes.

The hydroxylation activities of CYP153A16 and CYP153A *P. sp.* were investigated using the well-characterized putidaredoxin reductase (CamA) and putidaredoxin (CamB) from *Pseudomonas putida* as electron transfer partners.¹⁸⁷⁻¹⁸⁹ The redox proteins were selected on the basis of their amino acid sequence similarity (ranging from 63 to 68 %) with the natural FAD-containing oxidoreductases and [2Fe-2S] ferredoxins of CYP153A enzymes from *Mycobacterium marinum* M. and *Polaromonas* sp. strain JS666 (supplementary material table 6.4). In the absence of CamA and CamB, *E. coli* cell lysate containing CYP153A16 showed negligible CYP oxidation activity towards *n*-octane, thereby implying that the constitutive redox partners from *E. coli* could not interact with the CYP153 enzyme or they were not present in a stoichiometrical ratio to support P450 activity. In contrast, when purified CamA and CamB were added to the reaction, the CYP was able to catalyze the hydroxylation of *n*-octane to 1-octanol. Afterwards, the CYP concentration was increased by twofold and different P450-CamA-CamB ratios were tested. The maximum product concentration (140 μ M 1-octanol) was obtained with a P450-CamA-CamB ratio of 1:5:10, while the activity was reduced by 23 – 49 % at ratios of 1:1:5, 1:2:10 and 1:2:20.

CYP153A16 and CYP153A *P. sp.* were screened towards C₅-C₁₂ alkanes and C₆-C₁₂ primary alcohols using CamA and CamB as redox partners within a cofactor regenerating enzyme system. Product distributions are shown in figure 3.1. Amongst the formed products: primary alcohols

(C_n -1ol), secondary alcohols (C_n -2ol), α,ω -diols and products resulting from the further oxidation of primary alcohols (aldehydes and fatty acids) could be identified, while two other byproducts could not be identified (supplementary material table 6.5).

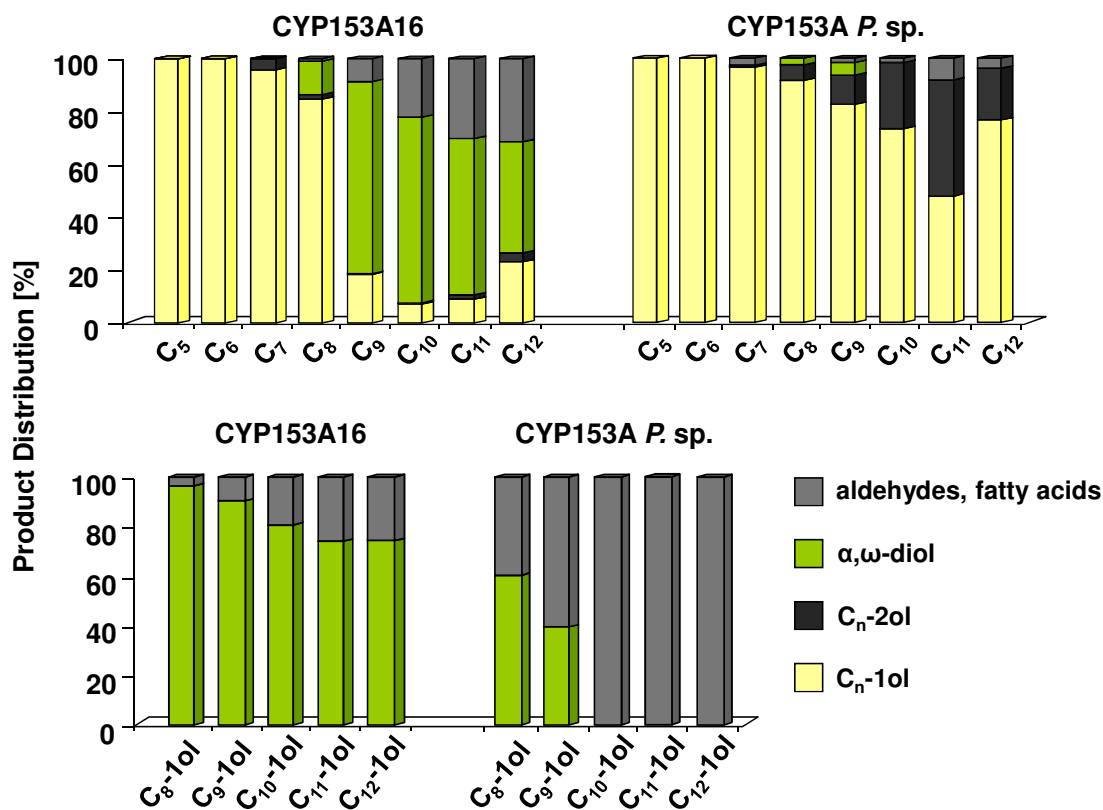


Figure 3.1. Product distributions using *n*-alkanes (above) and primary alcohols (below) as substrates. C_n -1ol, primary alcohol; C_n -2ol, secondary alcohol.

Similarly to previously reported CYP153 enzymes,^{83, 84, 87} the alkane substrate range of CYP153A16 and CYP153A *P. sp.* oscillated between C₅ and C₁₂, with octane being the preferred alkane substrate. C₅ and C₆ alkanes were converted to primary alcohols with low activity but absolute ω -regioselectivity. In case of the primary alcohols, CYP153A16 and CYP153A *P. sp.* could not oxidize 1-hexanol and 1-heptanol, but were able to oxidize those ranging from C₈ to C₁₂. Consistent with the literature, there is a relationship between the substrate chain length and enzyme activity as well as regioselectivity.^{87, 190, 191} In general, ω -regioselectivities tend to decrease for substrates longer than C₁₀. The concentrations of the desired terminally hydroxylated products obtained from alkanes and primary alcohols after 4 h incubation with each P450 system are shown in tables 3.1 and 3.2, respectively.

Table 3.1. Concentrations of primary alcohols (C_n -1ol) and α,ω -diols obtained from alkane oxidation catalyzed by CYP153A enzymes

Substrate (1 mM)	CYP153A16		CYP153A <i>P. sp.</i>	
	C_n -1ol [μ M]	α,ω -diol [μ M]	C_n -1ol [μ M]	α,ω -diol [μ M]
<i>n</i> -Pentane	34 \pm 3 ^a	—	30 \pm 1	—
<i>n</i> -Hexane	24 \pm 1 ^a	—	62 \pm 5	—
<i>n</i> -Heptane	81 \pm 8	—	103 \pm 3	—
<i>n</i> -Octane	120 \pm 9	30 \pm 3	165 \pm 13	16 \pm 1
<i>n</i> -Nonane	35 \pm 2	113 \pm 6	114 \pm 3	16 \pm 1
<i>n</i> -Decane	16 \pm 1	65 \pm 3	99 \pm 4	—
<i>n</i> -Undecane	< 10	N.D. (59 %) ^b	< 10	—
<i>n</i> -Dodecane	< 10	< 10	< 10	—

Reactions were set up for a final volume of 0.5 ml and run at 30°C for 4 h. ^aCYP153A16 produced more 1-pentanol than 1-hexanol in a reproducible manner. ^bPercentage relative to total product estimated from the GC peak areas. — not detected; N.D. not determined

Table 3.2. Concentrations of α,ω -diols obtained from primary alcohol oxidation catalyzed by CYP153A enzymes

Substrate (0.2 mM)	CYP153A16	CYP153A <i>P. sp.</i>
	α,ω -diol [μ M]	α,ω -diol [μ M]
1-Hexanol	—	—
1-Heptanol	—	—
1-Octanol	39 \pm 3	18 \pm 0.2
1-Nonanol	93 \pm 4	16 \pm 1
1-Decanol	80 \pm 6	—
1-Undecanol	N.D. (74 %) ^a	—
1-Dodecanol	43 \pm 2	—

Reactions were set up for a final volume of 0.5 ml and run at 30°C for 4 h. ^aPercentage relative to total product. — not detected; N.D. not determined

The most relevant results of this screening study are related to the different hydroxylation patterns of CYP153A16 and CYP153A *P. sp.*, which can be summarized as follows:

(1) CYP153A16 can produce α,ω -diols from medium-chain *n*-alkanes and primary alcohols, while CYP153A *P. sp* exhibits low to inexistent diterminal hydroxylase activity. CYP153A16 produced α,ω -diols from C_8 - C_{12} alkanes and primary alcohols, while CYP153A *P. sp.* produced diols only from the C_8 and C_9 compounds. Yet the diol yields were

lower than those obtained with CYP153A16 by 2- to 7-fold. As mentioned before, the ability of CYP153A enzymes to hydroxylate the ω -site of primary alcohols has been observed with other enzymes of the same subfamily.^{90, 91} Diols are the result of the ω -hydroxylation of the terminal non-activated methyl group of primary alcohols. This indicates that the -OH group of a C₈-C₁₂ primary alcohol does not hinder the access of the terminal C-H bond to the heme iron and that it does not alter the ferryl reactivity of CYP153A16. However, the hydroxyl group should impair either one or both processes in CYP153A *P. sp.*, as evidenced by its poor catalytic activity towards the ω -site of primary alcohols. The fact that CYP153A *P. sp.* oxidizes a C₁₀-C₁₂ primary alcohol exclusively to the corresponding aldehyde confirms that its hydroxyl group rather than its terminal methyl group is positioned close to the activated iron.

(2) CYP153A16 is more ω -regioselective than CYP153A *P. sp.* When considering both ω -alcohols and α,ω -diols as the total ω -hydroxylated products, CYP153A16 showed 90 – 96 % ω -regioselectivity for C₇-C₉ compounds, while CYP153A *P. sp.*, 83 – 95 %. Although terminal oxidation was the predominant reaction, CYP153A *P. sp.* produced more secondary alcohols (up to 37 % of the total product in the case of longer chain alkanes) than CYP153A16 (< 5 % of secondary alcohols from alkanes of all chain lengths). This implies the presence of more steric constraints in CYP153A16 than in CYP153A *P. sp.* A higher ligand mobility or higher dynamic protein malleability in CYP153A *P. sp.* should allow substrates to bind relatively loosely or in multiple orientations, which generally favours hydroxylation at the more reactive (ω -1)-site.¹⁹²

(3) CYP153A16 has a higher tendency to further oxidize the products derived from alkane hydroxylation, while CYP153A *P. sp.* overoxidizes primary alcohols. After the terminal methyl groups of alkanes were hydroxylated, they were more prone to undergo oxidation to aldehydes and fatty acids by CYP153A16. The concentration of aldehydes and fatty acids found in reactions catalyzed by CYP153A16 (representing a maximum of 32 % of the total product) increased with the length of the carbon chain, while two other unknown byproducts different from aldehydes and fatty acids were obtained from C₉-C₁₂ substrates. CYP153A *P. sp.* yielded smaller proportions of further oxidized products when using alkanes as starting material. Aldehydes or fatty acids were the only further oxidized products yielded by this enzyme. When C₈ and C₉ primary alcohols were used as substrates, a maximum of 40 – 58 % of the total product corresponded to the α,ω -diols, while the remaining products consisted of aldehydes and fatty acids.

3.1.2 Medium- and long-chain linear saturated and monounsaturated fatty acids

Since CYP153A16 could produce diols from primary alcohols, we assumed this enzyme as well as others with highly similar amino acid sequence could ω -hydroxylate fatty acids as well. Following the same reasoning, as CYP153A from *Polaromonas* sp. (CYP153A *P. sp.*) had low to non-existent activity towards primary alcohols; it was expected to perform poorly towards fatty acids.

In this section we screened the fatty acid hydroxylase activities of CYP153A *P. sp.* and CYP153A16. In addition to these enzymes, we selected CYP153A from *Marinobacter aquaeolei* (CYP153A *M. aq.*) due to its high protein sequence similarity with CYP153A16 (79 %) and other reported primary alcohol ω -hydroxylases,⁹⁰ including CYP153 from *Acinetobacter* sp. OC4 (P450aci) (83 %) and CYP153A13a from *Alcanivorax borkumensis* SK2 (91 %) (table 3.3). CYP153A *P. sp.* shares 85 % similarity with CYP153A6 from *Mycobacterium* sp. strain HXN-1500. CYP153A6 is basically known for catalyzing the ω -hydroxylation or epoxidation of linear alkanes, alkenes, cycloalkenes and alicyclic compounds.^{190, 193} No alcohol oxidation activity has been reported for CYP153A6, though it has been shown to support growth of recombinant *Pseudomonas putida* cells on C₁-C₈ primary alcohols.⁷⁷

Table 3.3. Amino acid sequence identities and similarities between the investigated monooxygenases and homologous proteins

CYP	Gene name	aa	Identity		
CYP153s used in this study			CYP153 from <i>A. sp. OC4</i> (497 aa)	CYP153A13a from <i>A. borkumensis</i> SK2 (470 aa)	CYP153A6 from <i>M. sp. HXN-1500</i> (420 aa)
CYP153A <i>P. sp.</i>	Bpro_5301	418	55 %	53 %	77 %
CYP153A16	MMAR_3154	463	68 %	66 %	55 %
CYP153A <i>M. aq.</i>	Maqu_0600	470	69 %	82 %	55 %
CYP	Gene name	aa	Similarity		
CYP153s used in this study			CYP153 from <i>A. sp. OC4</i> (497 aa)	CYP153A13a from <i>A. borkumensis</i> SK2 (470 aa)	CYP153A6 from <i>M. sp. HXN-1500</i> (420 aa)
CYP153A <i>P. sp.</i>	Bpro_5301	418	70 %	72 %	85 %
CYP153A16	MMAR_3154	463	80 %	80 %	69 %
CYP153A <i>M. aq.</i>	Maqu_0600	470	83 %	91 %	71 %

Performed via blastp: <http://blast.ncbi.nlm.nih.gov>

The three monooxygenases were reconstituted *in vitro* using putidaredoxin reductase (CamA) and putidaredoxin (CamB) from *P. putida* and screened towards C_{8:0}-C_{20:0} and 9(Z)/(E)-C_{14:1}-C_{18:1} fatty acids. Preliminary activity assays with purified CYP153A16 indicated that reaction times

longer than 4 h did not contribute to increased conversions. CO differential spectra measurements confirmed that CYP153A16 retained its P450 activity at room temperature for 4 h, while CYP153A *M. aq.* and CYP153A *P. sp.* were stable for 24 h (data not shown). In order to make our enzyme systems comparable, all bioconversions were stopped after 4 h. Substrate conversions and product distributions are detailed in table 3.4 and illustrated in figure 3.2.

Table 3.4. Conversions and product distributions [%] in fatty acid oxidation reactions catalyzed by CYP153A enzymes

CYP153		Saturated								9-Monounsaturated					
		8:0	9:0	10:0	12:0	13:0	14:0	16:0	18:0	20:0	(Z)-14:1	(Z)-16:1	(E)-16:1	(Z)-18:1	(E)-18:1
<i>P. sp.</i>	Conv.	1.5	4.5	1.9	<1.0	<1.0	-	-	-	-	-	-	-	-	-
	α -OH	-	-	-	-	-	-	-	-	-	-	-	-	-	-
	β -OH	-	-	-	-	-	-	-	-	-	-	-	-	-	-
	(ω -1)-OH	-	-	-	-	-	-	-	-	-	-	-	-	-	-
	ω -OH	100	100	100	100	100	-	-	-	-	-	-	-	-	-
	α,ω -DCA	-	-	-	-	-	-	-	-	-	-	-	-	-	-
A16	Conv.	-	-	39.3	71.1	91.8	56.1	6.3	-	-	34.1	32.4	34.6	3.5	1.9
	α -OH	-	-	-	1.3	1.9	1.9	-	-	-	2.1	-	-	-	-
	β -OH	-	-	-	0.3	0.7	0.7	-	-	-	0.7	-	-	-	-
	(ω -1)-OH	-	-	-	5.1	18.8	11.4	-	-	-	24.2	40.5	47.0	-	-
	ω -OH	-	-	100	88.3	68.8	75.1	100	-	-	65.6	59.5	53.0	100	100
	α,ω -DCA	-	-	-	5.0	9.8	10.9	-	-	-	7.4	-	-	-	-
<i>M. aq.</i>	Conv.	-	2.0	52.2	63.7	78.1	83.2	39.8	25.2	4.2	34.2	75.4	93.2	66.3	73.1
	α -OH	-	-	-	-	-	-	-	-	-	-	-	-	-	-
	β -OH	-	-	-	-	-	-	-	-	-	-	-	-	-	-
	(ω -1)-OH	-	-	-	0.9	2.9	2.7	1.0	3.0	-	8.3	4.1	-	0.8	-
	ω -OH	-	100	100	97.4	95.2	96.1	99.0	97.0	100	90.1	95.9	100	99.2	100
	α,ω -DCA	-	-	-	1.7	1.9	1.2	-	-	-	1.6	-	-	-	-

Reactions were run at 30°C for 4 h with 0.2 mM substrate. - not detected

Saturated fatty acids were oxidized by CYP153A *P. sp.* in very low yields (<5 % conversion). CYP153A16 and CYP153A *M. aq.* were considerable more active, with preference towards C_{13:0} and C_{14:0}, respectively. The substrate range of CYP153A16 oscillated between C_{10:0} and C_{16:0}, while CYP153A *M. aq.* had a broader scope, oxidizing those between C_{9:0} and C_{20:0}. Interestingly, CYP153A *P. sp.* could ω -hydroxylate compounds of shorter size (C_{8:0}-C_{13:0}). Monounsaturated fatty acids were only oxidized by CYP153A16 and CYP153A *M. aq.* and not by CYP153A *P. sp.* CYP153A *M. aq.* showed its highest activity towards 9(*E*)-C_{16:1} (93 % conversion), whereas substrate conversions with CYP153A16 were not higher than 35 %. From the substrate range tendencies observed, both enzymes might oxidize 9(*E*)-C_{14:1} and other monounsaturated fatty acids of chain lengths < C_{14:1} and \geq C_{20:1}. This remains unconfirmed since other monoenoic

compounds were not evaluated as substrates. In addition, we noticed differences in the activities towards saturated and monounsaturated fatty acids of the same chain length. For example, CYP153A16 was more active towards 9(*Z*)-C_{16:1} and 9(*E*)-C_{16:1} (~ 34 % conversion) than towards C_{16:0} (6 % conversion). The reason is unknown to us in the absence of a substrate-bound enzyme crystal structure and substrate affinity studies, but the double bond might confer a site for substrate stabilization.

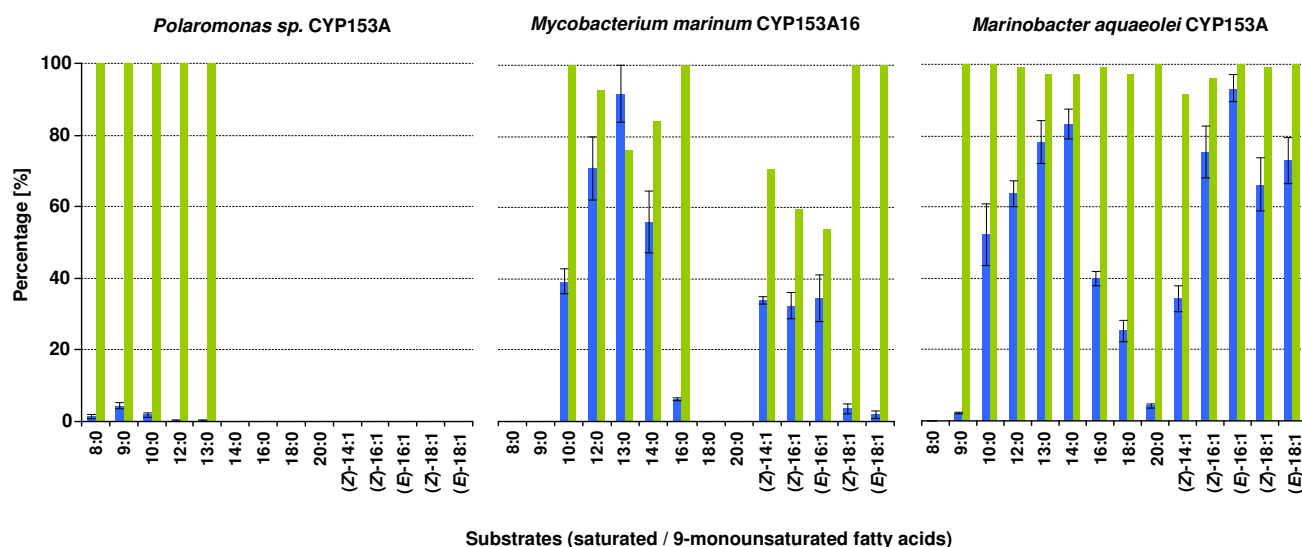


Figure 3.2. Substrate conversions (blue) and ω -regioselectivities (green) in fatty acid oxidation reactions catalyzed by CYP153A monooxygenases.

Concerning regioselectivity, CYP153A *P. sp.* catalyzed hydroxylations exclusively on the ω -position, as expected from its poor activity. Although CYP153A16 and CYP153A *M. aq.* hydroxylated both saturated and monounsaturated fatty acids preferentially on the terminal position, regiospecificities varied depending on the P450 and the chain length of the substrate. CYP153A *M. aq.* was considerably more ω -regioselective than CYP153A16. The latter enzyme produced up to 19 % and 47 % (ω -1)-OHFAs from its preferred C_{13:0} and 9(*E*)-C_{16:1} substrates, respectively. Interestingly, CYP153A16 also catalyzed α - and β -hydroxylations. Considering that these atoms are situated near the carboxyl group, i.e. the opposite extreme of the non-activated terminal carbon, we inferred that iron-catalyzed hydroxylation on such positions could occur if the substrate entered the active site with its carboxyl group coordinated towards the heme group. This type of substrate positioning seems to be less favoured, evidenced by the low yields of α - and β -regioisomers (< 3 % of the total product).

CYP153A16 and CYP153A *M. aq.* could convert C₁₂-C₁₄ ω -OHFAs into α,ω -DCAs. Diacid formation was higher with CYP153A16 (5 – 11 %) than with CYP153A *M. aq.* (< 2 %). Other intermediate

oxidation products such as aldo- or ketoacids were not detected in our experiments. Epoxy products, which might have resulted from the 9(*Z*)-monounsaturated fatty acids, were not found either. In order to verify if using an ω -OHFA as starting material led to higher α,ω -DCA yields, we tested 12-hydroxydodecanoic acid as substrate for CYP153A16. Although the diacid product was not quantified using a calibration curve, diacid yields originating from either 0.2 mM dodecanoic acid or 0.2 mM 12-hydroxydodecanoic acid were estimated from the relative peak areas and they were found to be similar. When the fatty acid was used as substrate, 71 % of it was converted to oxygenated products, 5 % of which corresponded to the diacid (table 3.4). When the ω -OHFA was used as starting material, relative peak areas were 96.4 % for the remaining substrate and 3.6 % for the diacid.

For comparison purposes, we tested CYP153A *M. aq.* against alkanes and primary alcohols. Despite a few variations in product distribution, CYP153A *M. aq.* showed similar oxidation activities as those of CYP153A16 (table 3.5). We could therefore confirm that CYP153A *P. sp.* has low or no catalytic activity towards aliphatic compounds with a polar group at the opposite site of the terminal carbon atom, while CYP153A16 and CYP153A *M. aq.* prefer these substrates over alkanes. CYP153A *P. sp.* can thus be classified as a predominantly alkane ω -hydroxylase, while CYP153A16 and CYP153A *M. aq.* can be referred as predominantly fatty acid ω -hydroxylases.

Table 3.5. Alkane, primary alcohol and fatty acid substrates yielding maximum ratios of ω - and/or α,ω -oxidized products in reactions catalyzed by CYP153A enzymes

CYP153A	Substrate (0.2 mM)	Conv. [%]	Product distribution [%]		
			ω -OH	α,ω^a	others ^b
<i>P. sp.</i>	<i>n</i> -octane	+	91	3	6
	1-octanol	+	n.a.	60	40
	nonanoic acid	+	100	-	-
	monounsaturated fatty acid	-	-	-	-
A16	<i>n</i> -octane	+	85	12	3
	<i>n</i> -nonane	+	18	73	9
	1-nonanol	++	n.a.	90	10
	dodecanoic acid	+++	88	5	7
	9(<i>Z</i>)-tetradecenoic acid	++	66	7	27
<i>M. aq.</i>	<i>n</i> -octane	+	85	14	1
	<i>n</i> -nonane	+	74	25	1
	1-nonanol	++	n.a.	92	8
	dodecanoic acid	+++	97	2	1
	9(<i>E</i>)-hexadecenoic acid	++++	100	-	-

- (no conversion/not detected), + (1 – 30 %), ++ (31 – 60 %), +++ (61 – 90 %), ++++ (> 90 %)

^a α,ω -products: α,ω -diols from *n*-alkanes and 1-alcohols; α,ω -DCAs from fatty acids. ^bOther products: 2-alcohols, aldehydes and fatty acids from alkanes; aldehydes and fatty acids from 1-alcohols; hydroxylated regioisomers from fatty acids. n.a., not applicable.

3.2 Creation of a focused mutant library of CYP153A from *Marinobacter aquaeleoi*

Our *in vitro* substrate screening studies showed that CYP153A *M. aq.* could ω -hydroxylate a broad range of aliphatic compounds, including alkanes, primary alcohols and fatty acids (table 3.5). We therefore took CYP153A *M. aq.* as a model enzyme to create a small focused mutant library aiming altered substrate specificity. More specifically, we targeted the terminal hydroxylation of C₄-C₆ primary alcohols and fatty acids via a shift in substrate range or a higher enzyme activity (figure 3.3).

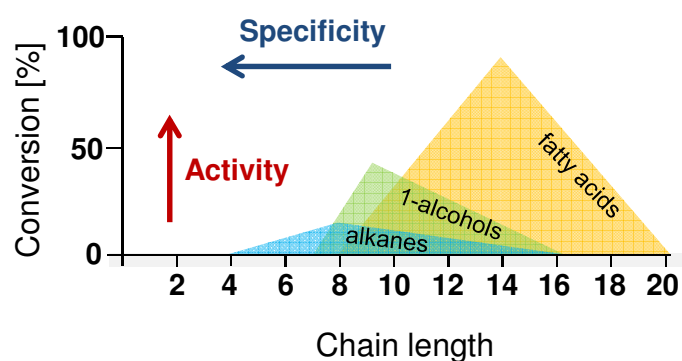


Figure 3.3. Overview of the *in vitro* substrate specificity and range of wild type CYP153A *M. aq.* Enzyme engineering targeted conversion of shorter 1-alcohols and fatty acids by increasing enzyme activity and/or altering substrate range.

The positions were selected based on: 1) multiple protein sequence alignments within the CYP153A subfamily and among other CYP enzymes (e.g. P450 BM3, CYP52A subfamily) (supplementary material figure 6.2), 2) a homology model of CYP153A16 (A. Seifert, unpublished data) and, 3) the existing documentation on the P450 superfamily and the CYP153A subfamily. Nine positions were proposed for substitution with specific residues to generate a library of 19 single mutants. The positions are located on four secondary structures: (1) the BC-loop, (2) the I-helix, (3) the variable substrate recognition site 5 (SRS-5), and (4) the C-terminal β -sheet loop. It is noteworthy indicating that these positions also appear in the homology model of a previously published CYP153A enzyme, CYP153A6 from *Mycobacterium* sp. HXN-1500 (figure 3.4). The rationale for each mutation is presented in table 3.6. From the 19 mutant enzymes, 13 were expressed in similar to slightly lower yields compared to the wild type enzyme, 4 were poorly expressed and 2 were non-expressible (table 3.6).

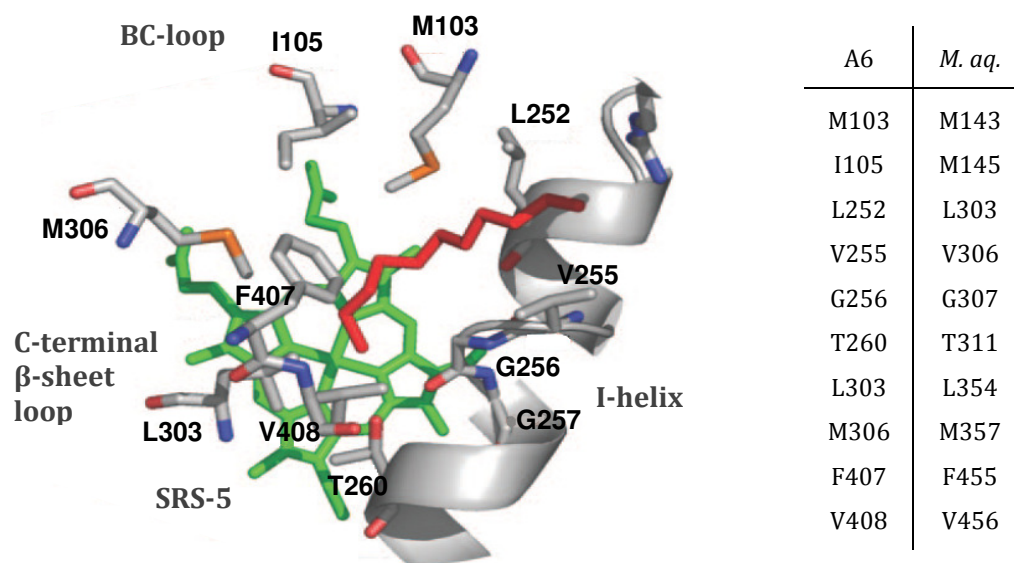


Figure 3.4. Homology model of CYP153A6 from *Mycobacterium* sp. HXN-1500. The model displays key secondary structural regions and 11 residues coordinating undecane (red) towards the heme group (green). The table on the right corner indicates the equivalent positions in CYP153A *M. aq.* Graphic adapted from Funhoff *et al.*¹⁹³

Table 3.6. Focused library of CYP153A *M. aq.*: rationale for mutation and protein expression levels

No.	Secondary Structure	Sequence	Position in wild type	Mutation	Rationale for mutation	Expression level ^a
1	n.a.	Wild type	n.a.	n.a.	n.a.	++
2			M143	R	To resemble Arg242 in P450 _{B₅S} , which anchors the carboxyl group of fatty acids ¹⁹⁴	+++
3				M	To modify hydrophobic interactions with the substrate	++
4	BC-loop	¹⁴³ MFIAMD ¹⁴⁸	I145	F	To resemble P450 BM3	-
5			Equivalent to F87 in P450 BM3 ¹⁹⁵	S	To anchor the carboxyl/ alcohol group of the substrate	+/-
6				T	Similar to I145S, but bulkier	+/-

Table 3.6. (continued)

No.	Secondary Structure	Sequence	Position in wild type	Mutation	Rationale for mutation	Expression level ^a
7				M	To resemble other CYP153A enzymes with Met in this position	++
8		³⁰² TLIVGGNDT ³¹¹	T302	V	To resemble most CYP153A enzymes, which display Ala, Val, Leu, Ile in this position	++
9	I-Helix	Stabilization of shorter compounds	L303	T	To anchor the carboxyl or alcohol group of the substrate	+++
10			V306	T		++
11			G307	A	To resemble the <u>A</u> GxxT motif present in the CYP superfamily ¹⁹⁶	++
12				V	Similar to G307A, but bulkier	++
13				I	Similar to native Leu	+++
14			L354 Position 5 after the ExxR motif. ¹⁹⁶	F	To resemble mutation A328F in P450 BM3, which influences selectivities towards alkanes ¹⁹⁵	+++
15	Substrate recognition site 5 (SRS5)	³⁵¹ QTPLAYMR ³⁵⁸		F	To alter interaction with the substrate or with F465	-
16			M357 Located in close vicinity to F455	Y	Similar to M357F, but polar	+/-
17				N	To resemble the yeast CYP52A subfamily, which displays a conserved Asn	+/-
18	C-terminal	⁴⁵³ SNEV ⁴⁵⁶	F455 Influences orientation of terminal C-H bond towards the heme iron center ¹⁹³	L	To evaluate the influence of smaller hydrophobic residues on substrate positioning	++
19	β -sheet loop			I		++
20				Y	Similar to F455, but polar	++

^aExpression level [mg P450 (g_{cww})⁻¹]: - (no expression), +/- (< 0.5), + (0.5 – 1), ++ (1 – 5), +++ (5 – 10). n.a. not applicable.

The variants including the wild type enzyme were screened towards 1-heptanol and nonanoic acid, as they are two of the shortest compounds within the substrate range of CYP153A *M. aq.* Some variants were additionally screened towards *n*-octane in order to verify if their activity towards this compound (the preferred alkane substrate for the wild type enzyme) changed as well (table 3.7). As cell-free extracts were utilized, it was thus not possible to exclude the influence of alcohol dehydrogenases or oxidases responsible for the overoxidation of the formed products. This occurred most notably when large volumes of cell lysates were used in the reactions. Considerable amounts of heptanoic acid were detected when using 1-heptanol as substrate. This caused substrate conversion levels to be higher than previous *in vitro* results with purified proteins. In addition, higher conversion levels were observed for nonanoic acid when using cell lysates, e.g. wild type enzyme: 14 % conversion with lysate vs. 2 % conversion with purified CYP (table 3.4, table 3.7). This might be attributed to a more efficient electron transfer from the cofactor to the heme iron enzyme caused by the presence of constitutive redox proteins in *E. coli*, which might also act as redox partners of CYP153A *M. aq.*

Table 3.7. Substrate conversions and production distributions in *n*-octane, 1-heptanol and nonanoic acid oxidation reactions with cell-free extracts containing CYP153A *M. aq.* variants

No.	Variant	Conversion ^a , Product distribution [%]			
		<i>n</i> -Octane	1-Heptanol	Nonanoic acid	
1	wt	Conv.	15	7	14
		acid	-	28	-
		(ω -1)-OHFA	-	-	1
		ω -OHFA	-	-	99
		ω -OH	71	-	-
		α ,(ω -1)-diol	-	3	-
		α , ω -diol	29	69	-
2	M143R	Conv.	-	-	-
3	I145M	Conv.	n.d.	< 1	< 1
		ω -OHFA	-	-	100
		α , ω -diol	-	100	-
4	I145F	Conv.	n.e.	n.e.	n.e.
5	I145S	Conv.	n.d.	< 1	< 1
		ω -OHFA	-	-	100
		α , ω -diol	-	100	-
6	I145T^b	Conv.	n.d.	< 1	< 1
		ω -OHFA	-	-	100
		α , ω -diol	-	100	-

Table 3.7. (continued)

No.	Variant	Conversion ^a , Product distribution [%]			
			<i>n</i> -Octane	1-Heptanol	Nonanoic acid
7	T302M	Conv. ω-OHFA α,ω-diol	n.d.	4 - 100	7 - 100
8	T302V	Conv. acid (ω-1)-OHFA ω-OHFA ω-OH α,(ω-1)-diol α,ω-diol	n.d.	n.d.	14 - 1 99 - - -
9	L303T	Conv.	-	-	-
10	V306T	Conv. ω-OHFA α,ω-diol	n.d.	< 1 - 100	< 1 100 -
11	G307A	Conv. acid (ω-1)-OHFA ω-OHFA ω-OH α,(ω-1)-diol α,ω-diol α,ω-diacid	48 - - - 3 - 97 -	67 23 - 14 - 1 62 -	39 - 2 97 - - - 1
12	G307V	Conv.	-	-	-
13	L354I	Conv. acid (ω-1)-OHFA ω-OHFA α,(ω-2)-diol α,(ω-1)-diol α,ω-diol	n.d.	2 24 - - 29 33 14	17 - 76 24 - - -
14	L354F	Conv. acid (ω-1)-OHFA ω-OHFA α,(ω-2)-diol α,(ω-1)-diol α,ω-diol	n.d.	8 37 - - 3 4 56	9 - 17 83 - - -
15	M357F	Conv.	n.e.	n.e.	n.e.
16	M357Y ^b	Conv.	n.d.	-	-
17	M357N ^b	Conv. ω-OHFA α,ω-diol	n.d.	< 1 - 100	< 1 100 -
18	F455L	Conv.	-	-	-
19	F455I	Conv.	-	-	-

Table 3.7. (continued)

No.	Variant	Conversion ^a , Product distribution [%]		
		<i>n</i> -Octane	1-Heptanol	Nonanoic acid
20	F455Y	Conv.	-	-

^aReactions were run with 2 μ M CYP (cell lysate) and additional CamA and CamB to support the reaction.

^bDue to poor protein expression, reactions with these variants were run with 0.2 μ M CYP. The results were contrasted with those obtained with 0.2 μ M wild type enzyme. - no conversion/not detected, n.d. not determined, n.e. not expressible.

The screening test with lysates allowed us to compare each variant with the wild type enzyme and identify positions crucial for enzyme activity and selectivity. Mutations M143R, L303T, G307V, M357Y and F455L/I/Y were the most deleterious ones, resulting in no conversion of the target substrates. Residue F455 can be clearly inferred as determinant for catalysis, as demonstrated by its substitution with tyrosine and two other hydrophobic amino acids. The equivalent position in CYP153A6 has been suggested to cause the alkane chain substrate to adopt a bent conformation, resulting in the approximation of the terminal carbon atom to the heme iron.⁸³ Conversions with the variants mutated on positions I145 and T302 were lower compared to the wild type CYP; however, these enzymes were still able to catalyze ω -hydroxylation reactions. Variants relevant to our scope were G307A (I-helix) and L354I/F (SRS5), which resulted in increased substrate conversion and shifted enzyme regioselectivity, respectively. As indicated in table 3.6, such positions were identified from protein sequence. G307A was proposed considering that a glycine is found in the CYP153A subfamily (first glycine in the GGNDT motif), while in most members of the CYP superfamily a conserved alanine is observed in this position (AGxxT motif).¹⁹⁶ L354, which resides in position 5 after the highly conserved ExxR motif, is equivalent to position A328 in P450 BM3. Isoleucine is alternatively found in the same spot in other CYP153A enzymes, while its substitution with phenylalanine has been shown to modify the selectivity of P450 BM3 towards alkanes.¹⁹⁷ Variants G307A, L354I and L354F were purified and screened towards nonanoic acid (table 3.8).

Table 3.8. Oxidation profiles of CYP153A *M. aq.* wild type and mutants towards 1 mM nonanoic acid

Variant	Conv. [%]	Product distribution [%]	
		(ω -1)-OH	ω -OH
wild type	1.7	2.5	97.5
G307A	26.0	1.1	98.9
L354I	2.0	75.6	24.4
L354F	1.2	17.0	83.0

Reactions were run at 30°C for 4 h with 2 μ M purified CYP, 10 μ M CamA, 20 μ M CamB and cofactor regeneration.

G307A was equally regioselective but significantly more active than the wild-type enzyme. Conversions with L354I/F resulted in higher proportions of the (ω -1)-OH product. This indicates that the residue in position 354 determines the orientation of the substrate close to the heme iron and hence controls where the activated oxygen attacks. *In vitro* bioconversions with C_{8:0}, C_{9:0} and C_{14:0} served us to confirm that G307A was more active than the wild type (table 3.9). We conducted kinetic experiments to investigate if the reason for increased activity was a higher affinity of G307A towards fatty acids (supplementary material figure 6.4). We observed that G307A was more catalytically efficient than the wild type enzyme owing to an increase in k_{cat} rather than changes in the substrate affinity constants (table 3.10).

Table 3.9. Fatty acid oxidation by CYP153A *M. aq.* wild type and variant G307A

Fatty acid (1 mM)	Wild type				G307A			
	Conv. [%]	Product Distribution [%]			Conv. [%]	Product Distribution [%]		
		(ω -1)-OHFA	ω -OHFA	α,ω -DCA		(ω -1)-OHFA	ω -OHFA	α,ω -DCA
C _{8:0}	–	–	–	–	20.3	1.6	98.4	–
C _{9:0}	1.7	2.5	97.5	–	26.0	1.1	98.9	–
C _{14:0}	48.4	2.8	96.8	0.4	68.6	3.1	96.6	0.3

Reactions were run at 30°C for 4 h with 2 μ M purified CYP, 10 μ M CamA, 20 μ M CamB and cofactor regeneration. – no conversion/not detected

Table 3.10. Steady-state kinetic parameters of CYP153A *M. aq.* wild type and variant G307A

Enzyme variant/ Parameter ^a	Fatty acid substrate		
	C _{8:0} ^b	C _{9:0}	C _{14:0}
Wild type			
K_M [mM]	5.15 \pm 0.04	0.217 \pm 0.009	0.036 \pm 0.004
k_{cat} [min ⁻¹]	0.13 \pm 0.01	0.24 \pm 0.02	4.3 \pm 0.2
k_{cat}/K_M [min mM ⁻¹]	0.025	1.1	119
G307A			
K_M [mM]	4.84 \pm 0.36	0.245 \pm 0.008	0.035 \pm 0.004
k_{cat} [min ⁻¹]	2.55 \pm 0.26	4.0 \pm 0.3	7.5 \pm 0.5
k_{cat}/K_M [min mM ⁻¹]	0.527	16.3	214

^aKinetic constants were determined by GC analysis of substrate conversion. Reaction mixtures contained 0.75 - 1 μ M CYP, CamA and CamB in a 1:5:10 ratio, 2 % (*v/v*) DMSO, 1 mM NADH and cofactor regeneration. Substrate concentrations used were within the substrate solubility range.

^bConversion of C_{8:0} to the corresponding ω -OHFA by the wild-type enzyme was detected with >1 mM substrate. Kinetic constants for C_{8:0} were thus measured after adjusting the GC method.

Our mutagenesis study performed by a systematic comparison of protein sequences allowed us to identify key residues influencing activity and regioselectivity in the hydroxylation of primary alcohols and fatty acids. Despite the low turnover rates of CYP153A *M. aq.* wild type or G307A, this enzyme displays similar or higher performance towards linear fatty acids than other bacterial CYPs. For instance, CYP124A from *Mycobacterium tuberculosis*, another reported bacterial fatty acid ω -hydroxylase, was screened towards C_{12:0}, C_{16:0} and C_{20:0}. This enzyme showed a specific activity of 0.07 min⁻¹ towards C_{16:0} at [S] = 5*K_M, while any activity towards C_{12:0} and C_{20:0} was detected.⁹³ Apparent kinetic parameters for AlkB towards nonanoic acid methyl ester have lately been determined.¹⁵ The values, K_S = 0.142 mM and V_{max} = 0.204 mmol min⁻¹(g_{cdw})⁻¹, are difficult to compare with our results since they were determined in whole cell bioconversions. A P450 BM3 variant engineered for terminal alkane hydroxylation displayed a turnover rate of 160 min⁻¹ towards octane.⁹⁷ Even though this mutant was not highly ω -regioselective (52 %), it would be interesting to evaluate its performance towards fatty acids.

Here it is also important to discuss two reports related to our work. In the first report, it was demonstrated that adding mutation G248A to an 8-point mutation variant (F87W/Y96F/T101L/T185M/L244M/V247L/L294M/L358P) of CYP101 (P450cam) from *Pseudomonas putida* caused an increased activity towards small substrates as well as a higher coupling efficiency compared to the wild type. Such mutation was introduced in the light of structural data with the purpose of forcing substrates to bind closer to the heme iron.⁹⁴ We realized that such position is equivalent to G307 in CYP153A *M. aq.* However, the kinetic parameters of P450cam (G248A) were then not investigated; hence it was not clear if the higher activity was caused by an increased substrate affinity. In the second report – published after the creation of our focused mutant library – the X-ray crystal structure of CYP153A7 (P450pyr) from *Sphingopyxis macrogoltabida* (PDB ID 3RWL) was solved.¹⁴⁴ In the same study, position G255 (equivalent to G307 in CYP153A *M. aq.*) was considered within a mutant library in which 20 active site positions were exchanged by iterative saturation mutagenesis in order to find a highly (*S*)-enantioselective variant for *N*-benzyl pyrrolidine hydroxylation. Nonetheless, the most enantioselective candidate was a triple mutant containing mutations in positions different than G255.¹⁴⁴

Additional insights into structure-function relationships within the CYP153A subfamily were provided by aligning the enzymes herein investigated with CYP153A6 and CYP153A7 (supplementary material figure 6.3) and by analyzing the recently published crystal structure of CYP153A7 (figure 3.5).

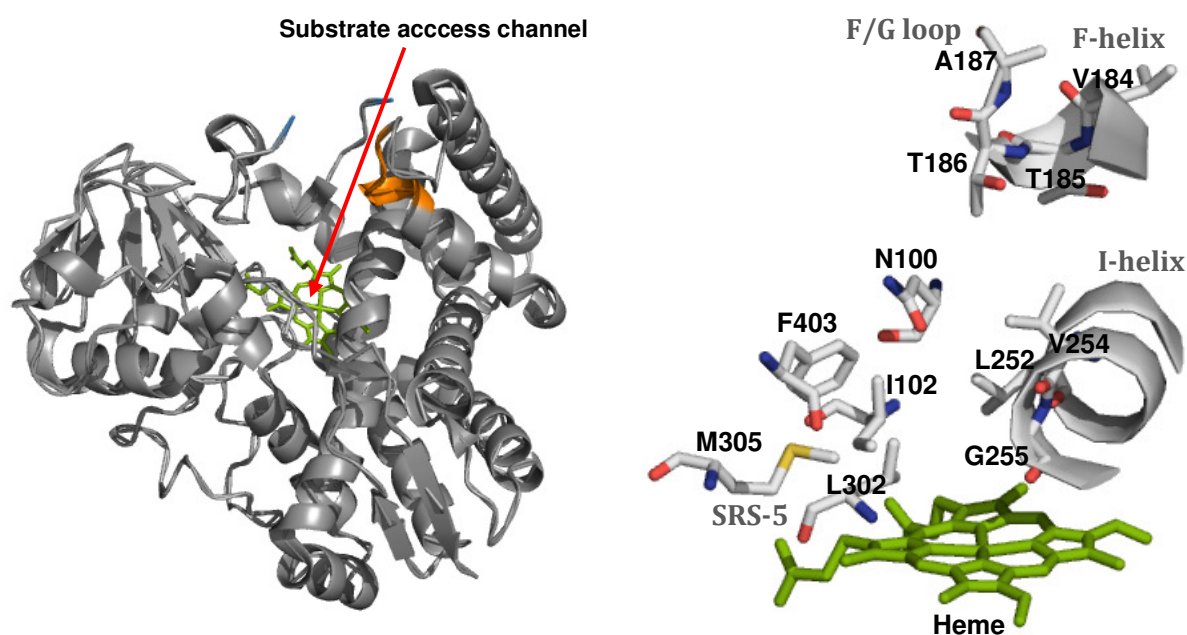


Figure 3.5. Substrate-free crystal structure of CYP153A7 from *Sphingopyxis macrogoltabida* (PDB ID 3RWL).¹⁴⁴ The images were generated by PyMOL. Left: Cartoon representation displaying the heme group (green), a section of the F-helix and adjacent F/G loop (orange) and residues (blue) bordering the reported missing loop (residues 88 – 96) in the published crystal structure. Right: Active site residues, including G255 (I-helix) and L302 (SRS-5) (equivalent to G307 and L354 in CYP153A *M. aq.*). The region ¹⁸⁴VTTA¹⁸⁷ at the C-terminus of the F-helix and F/G loop is located at the entrance of the active site cavity, opposite to the missing loop region.

The region located between the F-helix and the adjacent C-terminal loop (F/G loop) in the CYP153A enzymes is highly variable. The sequences of that region in CYP153A6, CYP153A7 and CYP153A *P. sp.* are similar among each other (VTTAL, VATAL and VTAA) but shorter by 2 amino acids and completely different than those found in CYP153A16 (LATSMEQ) and CYP153A *M. aq.* (RMAGAAS). One or more polar or positively charged residue(s) of this region might be involved in the coordination of the alcohol/carboxyl group of medium-chain primary alcohols or fatty acids in CYP153A16 and CYP153A *M. aq.*, enabling their hydroxylation at the terminal position. This assumption is based on the crystal structure of CYP153A7, since the F/G loop is located at the entrance of the active site (figure 3.5). In other CYPs, a dramatic unfolding of the C-terminus of the F-helix and large movements of the F/G loop have been observed in the presence of substrate, which suggests that the F/G loop and associated elements of structure can move into the active site and shape themselves around active site ligands.¹⁹⁸ The reason why the chain length of the preferred alkane (C₈), primary alcohol (C₉) and fatty acid (C₁₂-C₁₄) substrates is not the same in the investigated fatty acid ω -hydroxylases (table 3.5, figure 3.3) might also be

explained by this hypothesis. The right positioning of *n*-octane towards the active site might be facilitated by its hydrophobicity. However, octanoic acid and shorter fatty acids could be coordinated by a residue of the dynamic F-helix or F/G loop, which would not allow the terminal C-atom reach the heme group of the enzyme. The elucidation of a fatty acid-bound CYP153A structure (e.g., from CYP153A *M. aq.*) and additional mutagenesis studies should contribute to understand this phenomenon.

3.3 Bacterial whole cells for the synthesis of ω -oxygenated aliphatic compounds

3.3.1 Biotransformations of *n*-octane by growing *P. putida* cells containing CYP153A gene clusters

Three alkane hydroxylase operons, comprised by the CYP153A enzymes here investigated and their putative physiological redox partners were cloned into two different vectors for further studies in *Pseudomonas putida* (table 2.2). A derivative of the L-rhamnose-inducible pJOE4782.1 vector and the *n*-alkane-inducible pCom10 vector were selected since these expression systems have been shown to be effective in the production of heterologous proteins in pseudomonads.^{177, 179} In addition, the CYP153A6 alkane hydroxylase system from *Mycobacterium* sp. HXN-1500 has previously been functionally expressed in *Pseudomonas* as a gene cluster (CYP153A6-FdR-Fdx) within vectors of the pCom series.^{77, 88}

The functional expression of the individual components of CYP153A gene clusters in pseudomonads was first verified using the MmFdx→CYP153A16→MmFdR operon. *P. putida* S12, known to display high tolerance towards organic solvents including 1-butanol, was used as host strain.¹⁵⁶ Cells were also transformed with empty vector (negative control) and subjected to the same growth and expression conditions as the gene cluster-containing strain. *P. putida* S12_pJOE-MmAlk cell extracts yielded a concentration of 23 μg active P450 (mg total protein)⁻¹ (equivalent to 3 μM P450 in 7 mg ml⁻¹ total protein) after 16 h expression, which is comparable to a previous report involving CYP153A6 in *n*-octane grown *P. putida* Gpo12 (2.2 μM P450 in 7 mg ml⁻¹ total protein).¹⁹⁹ Negative controls resulted in negligible P450 concentration ($\leq 0.1 \mu\text{M}$). In addition, cell extracts of *P. putida* S12 harboring the gene cluster showed a reductase activity of 130 μmol cytochrome *c* min⁻¹ (mg protein)⁻¹, approximately 4-fold higher than the corresponding negative control. Unfortunately, the ferredoxin component (MmFdx) could not be detected by SDS-PAGE nor quantified in the cell extract, since spectroscopic methods for the determination of ferredoxin concentration are generally performed using purified protein to

avoid the background effect of other redox proteins (e.g., ferredoxin reductases). Cell extracts from *P. putida* S12 containing the MmAlk gene cluster were also proven to be active *in vitro*. After 4 h, 1 mM *n*-octane was oxidized to 1-octanol (13 % conversion, 99 % ω -regioselectivity) using NADH as electron donor in a cofactor regenerating system. Negative controls did not display activity towards *n*-octane.

The *in vivo* hydroxylation activities of recombinant *P. putida* containing the three alkane hydroxylase gene clusters as pJOE or pCom10 vector constructs were investigated. In this section, *P. putida* KT2440 was used as standard platform for whole cell biotransformations given its amenability for genetic manipulation, contrary to strain S12, whose genome has not been published yet. *Pseudomonas putida* KT2440 cells containing the pJOE constructs were grown in rich medium (TB_{Kan}), while those harboring pCom10 vectors were grown in modified M12 mineral medium supplemented with citrate as carbon source (MM-BVT_{Kan}/citrate). To prevent carbon and energy source depletion, cells were fed with glucose or citrate. All recombinant *P. putida* strains grew until a maximum OD₆₀₀ of 2.2 - 2.4 after 12 h of cell growth (6 - 8 h after substrate addition) in both TB_{Kan} and MM-BVT_{Kan}/citrate. *n*-Octane was mainly converted to 1-octanol, while 2-octanol accounted only for 2 - 3.5 % of the total product. 1,8-Octanediol was not detected under the experimental conditions used, presumably due to low accumulation of its precursor, 1-octanol. Recombinant *P. putida* KT2440 with pJOE-MmAlk grown in TB_{Kan} yielded up to 10.4 mg l⁻¹ 1-octanol 18 h after induction/substrate addition, while those containing pJOE-MaqAlk and pJOE-PspAlk reached a maximum of 2.9 and 6.7 mg l⁻¹ 1-octanol 14 h after induction/substrate addition, respectively (table 3.11).

Table 3.11. Concentration of 1-octanol produced by pseudomonads growing in TB_{Kan}

Recombinant <i>P. putida</i> strains	1-Octanol [mg l ⁻¹], time after induction		
	6h	14h	18h
KT2440_pJOE-MmAlk	-	4.1	10.4
KT2440_pJOE-MaqAlk	-	2.9	0.6
KT2440_pJOE-PspAlk	-	6.7	1.5

Recombinant *P. putida* KT2440 with pCom10-MmAlk grown in MM-BVT_{Kan}/citrate produced a maximum of 2.4 mg l⁻¹ 1-octanol 12 h after induction/substrate addition, respectively (table 3.12), while 1-octanol concentration in pCom10-PspAlk cultures reached 18.7 mg l⁻¹ in 12 h. In addition, in most cases it was observed that product formation decreased dramatically 18 h after substrate addition, indicating that 1-octanol was further metabolized by the pseudomonads.

Table 3.12. Concentration of 1-octanol produced by pseudomonads growing in MM-BVT_{Kan}/citrate

Recombinant <i>P. putida</i> strains	1-Octanol [mg l ⁻¹], time after induction		
	4h	12h	18h
KT2440_pCom10-MmAlk	0.7	2.4	1.1
KT2440_pCom10-PspAlk	3.5	18.7	3.6

In an additional experiment performed only with strain KT2440_pJOE-MmAlk grown in MM_{Kan} supplied with 5 g l⁻¹ glucose every 6 h to prevent C-source starvation, the product yield was 2.3 mg l⁻¹ 1-octanol 16 h after induction/substrate addition. This value is similar to that obtained with the same strain in TB medium (2.9 mg l⁻¹ 1-octanol). In order to increase substrate solubility, dimethyl sulfoxide (DMSO) was added in a final concentration of 2 % (v/v). This resulted in a 2-fold increase of the product yield (4.3 mg l⁻¹ 1-octanol). DMSO was thus used as a co-solvent in further experiments.

3.3.2 Biotransformations of *n*-octane and fatty acids by resting *P. putida* and *E. coli* cells containing CYP153A fusion constructs

Aiming to increase the efficiency of electron transfer, CYP153A from *Marinobacter aquaeolei* was fused to the reductase domain of P450 BM3 from *Bacillus megaterium* (CPR_{BM3}). Such construct has been demonstrated to be functional in alkane and fatty acid hydroxylation reactions *in vitro* and *in vivo*, with 3-fold higher coupling efficiency than that of our artificial system of three separate protein components (D. Scheps, unpublished data). As a combined strategy to increase product yields, mutation G307A which is responsible for the higher *in vitro* hydroxylation activity in CYP153A *M. aq.*, has been incorporated in the fusion construct (figure 3.6).

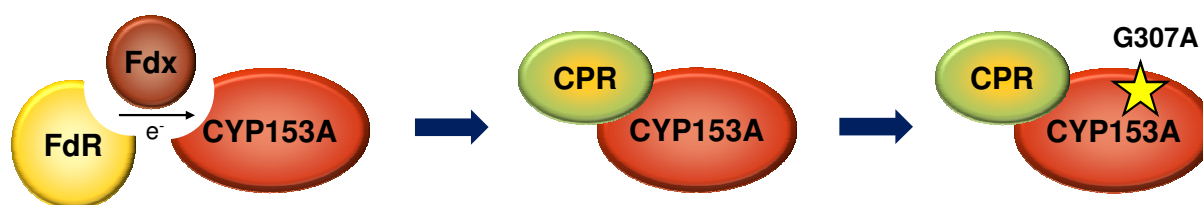


Figure 3.6. Combining two strategies for optimized CYP153A-mediated ω -hydroxylations. CYP153A *M. aq.* harbors mutation G307A fused to CPR_{BM3}. Abbreviations: CPR: Cytochrome P450 Reductase (FAD/FMN-containing reductase domain)

Non-metabolically engineered *P. putida* KT2440, *P. putida* S12, *E. coli* JM109 and *E. coli* BL21(DE3) were transformed with the CYP153A *M. aq.* (G307A)-CPR_{BM3} fusion construct and evaluated as hosts in *n*-alkane and fatty acid ω -oxygenation reactions. Strains JM109 and BL21(DE3) were selected because they perform as suitable hosts for pJOE vector constructs.¹⁷⁸

3.3.2.1 Biotransformations of *n*-octane

To initially assess the biocatalytic performance of the four recombinant strains described above, each one was assayed towards *n*-octane in one single experiment with glucose and glycerol added only at the start of the reaction. Figure 3.7 follows the formation of 1-octanol, 2-octanol, octanal, octanoic acid and 1,8-octanediol during the entire biotransformation. Each strain behaved differently towards the substrate and formed products, thus the highest concentrations of target product (1-octanol) were reached at different time points. Table 3.13 features relevant reaction parameters (biomass and biocatalyst concentrations) as well as product distributions at the time maxima 1-octanol concentrations were observed. *E. coli* resulted in a more effective host for *n*-octane ω -hydroxylation than *P. putida* under the experimental conditions used. In average, *E. coli* yielded 10 times more 1-octanol and 1,8-octanediol than *P. putida*. Strains JM109 and BL21(DE3) produced 130 - 260 mg l⁻¹ 1-octanol and around 55 mg l⁻¹ 1,8-octanediol after 8 h, while KT2440 and S12 yielded a maximum of 3 - 15 mg l⁻¹ 1-octanol and 1.6 - 5 mg l⁻¹ 1,8-octanediol after 1 - 2 h. Cell aggregation was observed in both pseudomonads, which is likely to occur as an energy-dependent stress response due to exposure to *n*-octane and 1-octanol, resulting in a lower capacity for redox biocatalysis. *P. putida* KT2440 cells aggregated after 8 h and product concentrations remained constant or decreased after this time, while *P. putida* S12 cells aggregated after 2 h and yielded very low product concentrations. In addition to this, target hydroxylation products can be degraded by non-engineered pseudomonads, as they are able to utilize primary alcohols as carbon and energy source.^{77, 87} Larger amounts of the aldehyde and fatty acid (40-60 % of the total product) were detected in the pseudomonads, while in *E. coli* these byproducts accounted for less than 12 %. Given that CYP153A *M. aq.* has a low intrinsic ability to oxidize 1-octanol to octanoic acid (table 3.5), overoxidation can be attributed to a higher alcohol dehydrogenase/oxidase activity in the pseudomonads compared to *E. coli*. Possible causes for observing a product plateau in *E. coli* after 8 hours are: equal rates of product formation and degradation, substrate or product toxicity, product inhibition and mass transfer rate limitations caused by the presence of bio-emulsifier released due to cell lysis.²⁰⁰ Alcohols tend to accumulate in the membrane bilayer and cause ion leakage.^{201, 202} Octane and 1-octanol cause changes in cell morphology and membrane physiology, resulting in hole formation in the membrane and reduced viability of both *P. putida* and *E. coli*.^{203, 204}

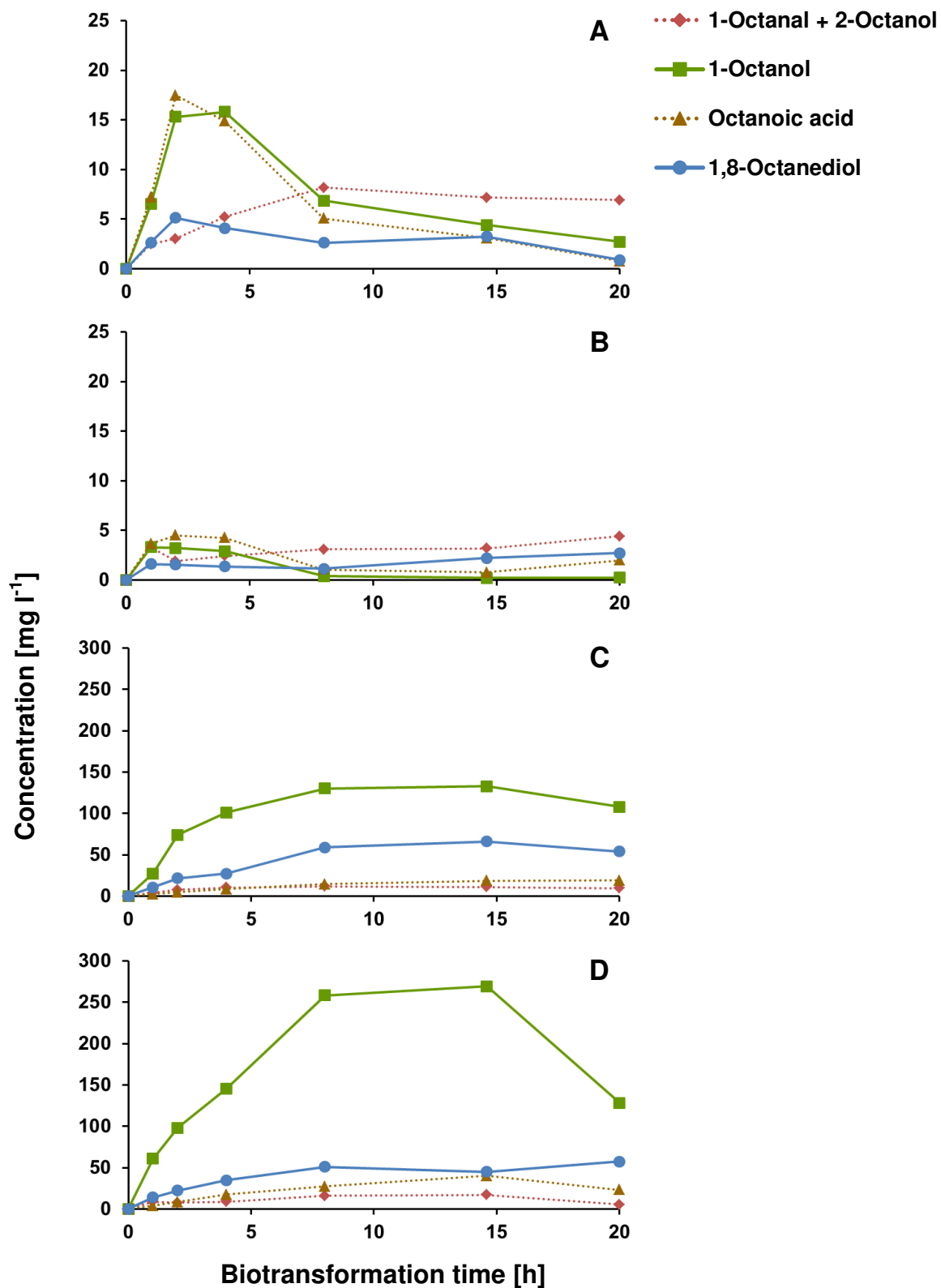


Figure 3.7. Whole cell biotransformations of 10 % (v/v) *n*-octane with resting *P. putida* and *E. coli* cells. (A) *P. putida* KT2440, (B) *P. putida* S12, (C) *E. coli* JM109 and (D) *E. coli* BL21(DE3) harbored the pJOE-CYP153A *M. aq.*(G307A)-CPR_{BM3} vector construct. Cell concentrations were 100 g_{c_{dw}} l⁻¹ (20-24 g_{c_{dw}} l⁻¹). The glucose/glycerol mix was added only at the beginning of the biotransformation.

Table 3.13. Maximum 1-octanol concentrations and product distributions obtained with resting *P. putida* and *E. coli* cells harboring CYP153A *M. aq.* (G307A) fused to CPR_{BM3} in conversions without additional C-source

Parameter	Units	<i>P. putida</i>	<i>P. putida</i>	<i>E. coli</i>	<i>E. coli</i>
		KT2440	S12	JM109	BL21(DE3)
Biotransformation time	h	2	1	8	8
Biomass concentration ¹	g _{cdw} l ⁻¹	20	20	22	24
Active P450 concentration ¹	mg (g _{cdw}) ⁻¹	40.5	56.7	38.9	56.7
Initial substrate concentration	% (v/v)	10	10	10	10
Substrate conversion ²	%	0.05	0.01	0.26	0.43
1-octanol concentration	mg l ⁻¹	15.3	3.3	130	258
1,8-octanediol concentration	mg l ⁻¹	5.1	1.6	59	51
Product distribution					
1-octanal + 2-octanol ³	%	7.8	29.2	5.7	4.6
1-octanol	%	39.6	29.0	62.7	75.0
octanoic acid	%	40.8	29.1	6.3	7.2
1,8-octanediol	%	11.8	12.7	25.2	13.2

¹At start of biotransformation. ²Substrate converted to oxygenated products (not equivalent to substrate consumption). The values were calculated from initial substrate and product concentrations and represent the molar percentage yields. ³Similar retention times of 1-octanal and 2-octanol in GC/FID.

3.3.2.2 Biotransformations of fatty acids

3.3.2.2.1 Dodecanoic acid oxidation without additional C-source by resting *P. putida* and *E. coli* cells containing mutant CYP153A in a fusion construct

In vivo bioconversions of dodecanoic acid by each one of the four recombinant strains described in the previous section were run once. Glucose and glycerol were added only at the start of the reaction. Biotransformations yielded mainly 12-hydroxydodecanoic acid (12-OHFA) and 1,12-dodecanedioic acid (1,12-DCA) as well as small amounts of the subterminally oxygenated product (11-OHFA). Figure 3.8 displays substrate consumption and product formation within a biotransformation time of 20 h as well as product yield coefficients ($Y_{P/S}$) after 8 h.

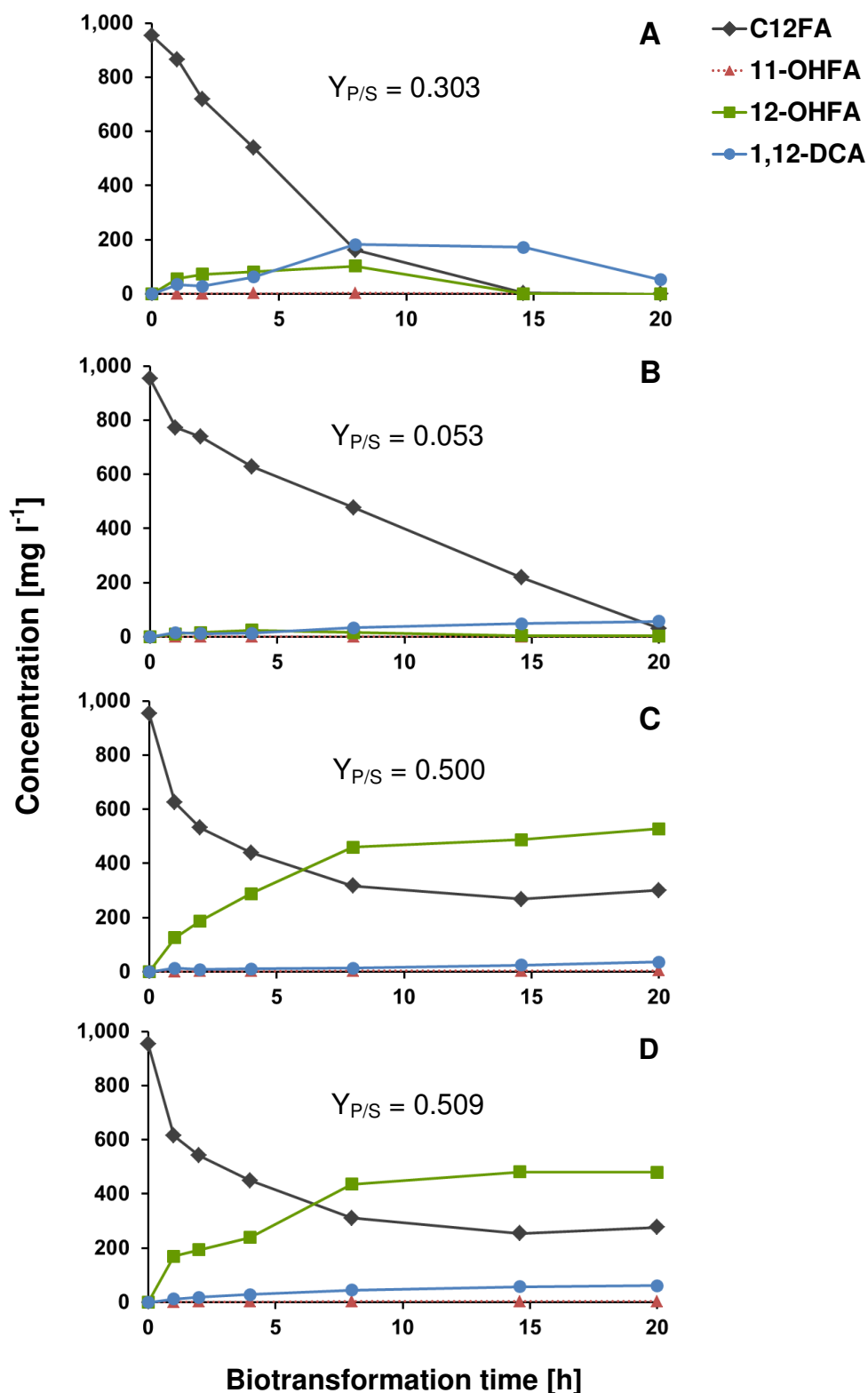


Figure 3.8. Whole cell biotransformations of 1 g l⁻¹ dodecanoic acid with resting *P. putida* and *E. coli* cells. (A) *P. putida* KT2440, (B) *P. putida* S12, (C) *E. coli* JM109 and (D) *E. coli* BL21(DE3) harbored the pJOE-CYP153A *M. aq.*(G307A)-CPR_{BM3} vector construct. Cell concentrations were 100 g_{cww} l⁻¹ (20-24 g_{cdw} l⁻¹). The glucose/glycerol mix was added only at the start of the biotransformation. Product yield coefficients ($Y_{P/S}$) correspond to g of total products per g substrate after 8 h. Abbreviations: C12FA, dodecanoic acid; 11-OHFA, 11-hydroxydodecanoic acid; 12-OHFA, 12-hydroxydodecanoic acid; 1,12-DCA, 1,12-dodecanedioic acid.

In agreement with the results obtained with *n*-octane, *E. coli* strains yielded significantly more ω -hydroxylated product from dodecanoic acid than *P. putida*. The pseudomonads also depleted the substrate completely after 15 - 20 h in the absence of constant carbon source feeding. On one hand, the observation that the 12-OHFA decreased over time is an evidence that it was readily oxidized to 1,12-DCA to enter the β -oxidation pathway for energy generation. The appearance of low 12-OHFA and 1,12-DCA yields in pseudomonads might thus be attributed to a higher rate of product degradation than of product formation, which is likely to occur because CYP153A enzymes are less active than fatty alcohol oxidases. On the other hand, as observed in *n*-octane bioconversions, *P. putida* KT2440 and S12 cells aggregated as well, but this phenomenon began later, 10 hours after the start of biotransformation. This means that the fatty acid and its derived oxidation products do not exert such a burden to the cells as *n*-octane and 1-octanol do. The pseudomonads were thus metabolically active towards dodecanoic acid and derived 12-OHFA by a longer period of time than towards the alkane and primary alcohol. This might be also influenced by the higher solubility of the ω -OHFA product compared to the fatty acid substrate.

E. coli strains consumed 70 % of the substrate within 20 h. From this percentage, 57 - 60 % ended up as oxygenated products, while the remaining 10 - 13 % must have been utilized as carbon and energy source. In contrast with the results observed in *n*-octane oxidation, both *E. coli* JM109 and BL21(DE3) yielded similar 12-OHFA concentrations. Given that the rates of formation of the target product (12-OHFA) dropped after 8 h in all four strains, product concentrations and distributions obtained with each *in vivo* system are compared at this time point (table 3.14). After 8 h, both *E. coli* strains produced in average 450 mg l⁻¹ 12-OHFA. However, the total accumulated 12-OHFA concentrations after 20 h were 528 and 480 mg l⁻¹ for JM109 and BL21(DE3), respectively.

Strain JM109 was less prone to oxidize 12-OHFA to 1,12-DCA than strain BL21(DE3). *P. putida* KT2440 produced up to 103 mg l⁻¹ 12-OHFA, while strain S12 barely yielded 16 mg l⁻¹ 12-OHFA. Both pseudomonads also produced larger amounts of 1,12-DCA (62 - 66 % of the total product) in comparison with *E. coli* (5 - 12 % of the total product). Considering that CYP153A *M. aq.* has low *in vitro* oxidation activity towards ω -OHFAs, constitutive fatty alcohol oxidases (FAOs) seem to be involved in the terminal oxidation of ω -OHFAs in *P. putida* strains.

Table 3.14. Product concentrations and distributions obtained with resting *P. putida* and *E. coli* cells harboring CYP153A *M. aq.* (G307A) fused to CPR_{BM3} in conversions without additional C-source

Parameter	Units	<i>P. putida</i> KT2440	<i>P. putida</i> S12	<i>E. coli</i> JM109	<i>E. coli</i> BL21(DE3)
Biotransformation time	h	8	8	8	8
Biomass concentration ¹	g _{cdw} l ⁻¹	20	20	22	24
Active P450 concentration ¹	mg (g _{cdw}) ⁻¹	40.5	56.7	38.9	56.7
Initial substrate concentration	mg l ⁻¹	954	954	954	954
Substrate conversion ²	%	27	4.7	46.2	46.8
12-OHFA concentration	mg l ⁻¹	103	16	460	436
1,12-DCA concentration	mg l ⁻¹	182	34	14	46
Product distribution					
11-OHFA	%	1.2	1.8	0.7	0.8
12-OHFA	%	37.2	32.3	96.6	90.3
1,12-DCA	%	61.6	65.9	2.7	8.9

¹at start of biotransformation, ²Substrate converted to oxygenated products (not equivalent to substrate consumption). The values were calculated from initial substrate and product concentrations and represent the molar percentage yields.

In order to identify factors responsible for the decreased product formation rates after 8 h, hydrogen peroxide and acetate formation were determined in dodecanoic acid biotransformation mixtures corresponding to *P. putida* KT2440 and *E. coli* JM109 (supplementary material figure 6.5). The concentrations of total (intracellular and extracellular) H₂O₂ after 8 h were 166 μM and 262 μM in *E. coli* JM109 and *P. putida* KT2440 cultures, respectively. After 20 h, up to 274 μM H₂O₂ was quantified in the investigated *E. coli* strain, while 585 μM H₂O₂ was detected in the pseudomonad. Hydrogen peroxide and other reactive oxygen species (ROS) originate from oxidative stress²⁰⁵ and electron uncoupling during P450-mediated biocatalysis (figure 1.3). ROS accumulation results in the damage of DNA, RNA, proteins and lipids. *E. coli* is known to possess an efficient repair machinery when exposed to ROS,²⁰⁶ while *P. putida* KT2440 has high tolerance towards ROS because the high cofactor demand caused by oxidative stress is covered by the NADPH-producing glucose-6-phosphate oxidation step leading to the Entner-Doudoroff pathway.²⁰⁷ Nevertheless, concentrations of 400 μM are known to irreversibly inactivate CYPs *in vitro* by the loss of the heme group.²⁰⁸ The fatty acid α-hydroxylase from *Clostridium acetobutylicum*, with both monooxygenase and peroxygenase activities, has been reported to catalyze reactions in the presence of 200 μM H₂O₂, but becomes inactivated after a few minutes.²⁰⁹ Concerning acetic acid formation, *P. putida* produced 3 to 4 times less acetate than *E. coli*, which is in agreement with the existing literature.²¹⁰ Although glucose was added only at the start of biotransformation, *E. coli* JM109 produced as much as 3.5

g l⁻¹ after 8 h and 4.4 g l⁻¹ after 20 h. *P. putida* KT2440 produced less than 1 g l⁻¹ within 20 h. Acetate concentrations above 2.4 g l⁻¹ are known to reduce biomass production, the proton-motive force and the stability of intracellular proteins.²¹¹ Acetate also reduces the pH of the medium, which might decrease product formation rates. A pH outside the 6.8 – 7.3 range has been reported to cause a 50-fold decrease in fatty acid oxidation rates in reactions catalyzed by CYP119 from *Sulfolobus solfataricus*.²¹²

3.3.2.2.2 Dodecanoic acid oxidation with additional C-source by resting *P. putida* and *E. coli* cells containing wild type and mutant CYP153A in a fusion construct

Further *in vivo* shake flask assays with dodecanoic acid were conducted in *P. putida* KT2440, *E. coli* JM109 and *E. coli* BL21(DE3). *P. putida* S12 was not included given its low performance in hydroxylation reactions under the previous experimental conditions used. On this occasion, each strain contained the fusion construct with CYP153A *M. aq.* either in its wild type form (wt) or as a G307A variant (G307A). In addition, cell concentrations were halved from 100 g_{cww} l⁻¹ to 50 g_{cww} l⁻¹ in order to reduce the amount of costly biocatalyst as well as to minimize mass and oxygen transfer limitations arising from high cell density fermentations. Resting cells were fed with glucose/glycerol at time points 0, 4, 8 and 12 h in order to diminish unproductive substrate consumption, i.e. for biomass and energy production. Although glucose is not the preferred carbon source for *Pseudomonas* strains, this sugar was used in the mix for the sake of preserving similar fermentation conditions as those of *E. coli* cultures. *P. putida* KT2440 and *E. coli* JM109 harboring empty religated pJOE vector (without gene insert) were used as negative controls to measure substrate depletion in the absence of the biocatalyst.

Figure 3.9 exhibits substrate consumption and production formation by *P. putida* KT2440. Cells without the monooxygenase fusion construct depleted the substrate completely in 12 hours despite the presence of additional C-source. In the reactions with the monooxygenase-containing pseudomonads, 65 - 80 % of the fatty acid was consumed within 20 h. From these values, around 20 % resulted in the effective formation of oxygenated products, while the remaining 45 - 60 % was used as carbon and energy source. As explained in section 3.3.2.1, even though dodecanoic acid was still available, we did not observe any significant increase in product yields compared to the previous setup without constant C-source feeding. Under these conditions, biotransformations with the pseudomonads harboring the G307A variant resulted in only 24 % higher product yields compared to the wild type enzyme.

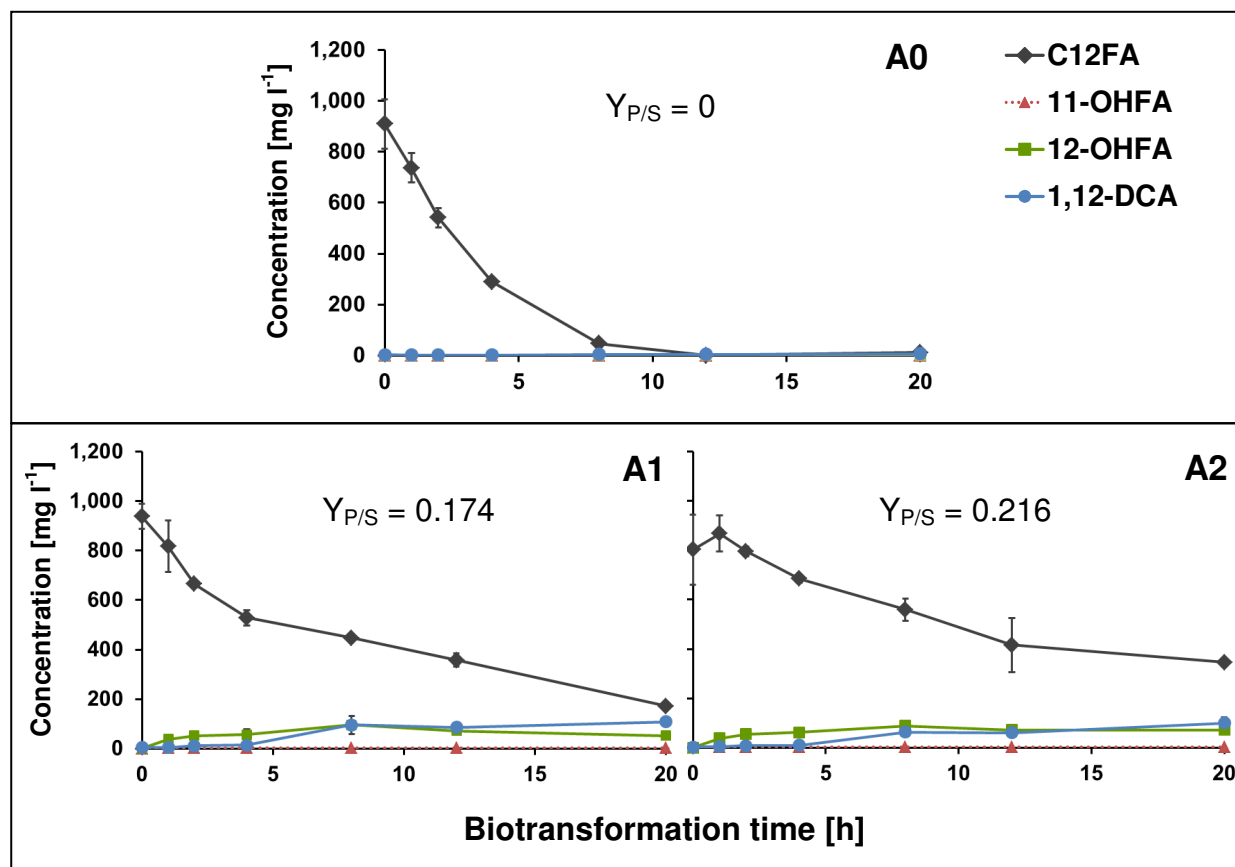


Figure 3.9. Whole cell biotransformations of 1 g l⁻¹ dodecanoic acid with resting *P. putida* cells in the presence of additional C-source. *P. putida* KT2440 cells contained either (A0) empty pJOE, (A1) pJOE-CYP153A *M. aa.*-CPR_{BM3} or (A2) pJOE-CYP153A *M. aa.*(G307A)-CPR_{BM3}. Cell concentrations were 50 g_{cww} l⁻¹ (9.4 – 9.9 g_{cdw} l⁻¹). Cells were fed with additional C-source at 0, 4, 8 and 12 h. Product yield coefficients ($Y_{P/S}$) correspond to g of total products per g substrate. Abbreviations: C12FA, dodecanoic acid; 11-OHFA, 11-hydroxydodecanoic acid; 12-OHFA, 12-hydroxydodecanoic acid; 1,12-DCA, 1,12-dodecanedioic acid.

Once again, aggregation of *P. putida* cells was evident after 10 h of biotransformation. The phenomenon was more dramatic for the cells without CYP (negative control) (supplementary material figure 6.6). As mentioned before, aggregate formation is an energy-dependent survival strategy in front of toxic compounds. Severe aggregation in cells lacking CYP might be attributed to the high energy supply used for the synthesis of extracellular polymeric substances,²¹³ while in the CYP-containing cells, part of the energy ought to be channelled to redox biocatalysis.

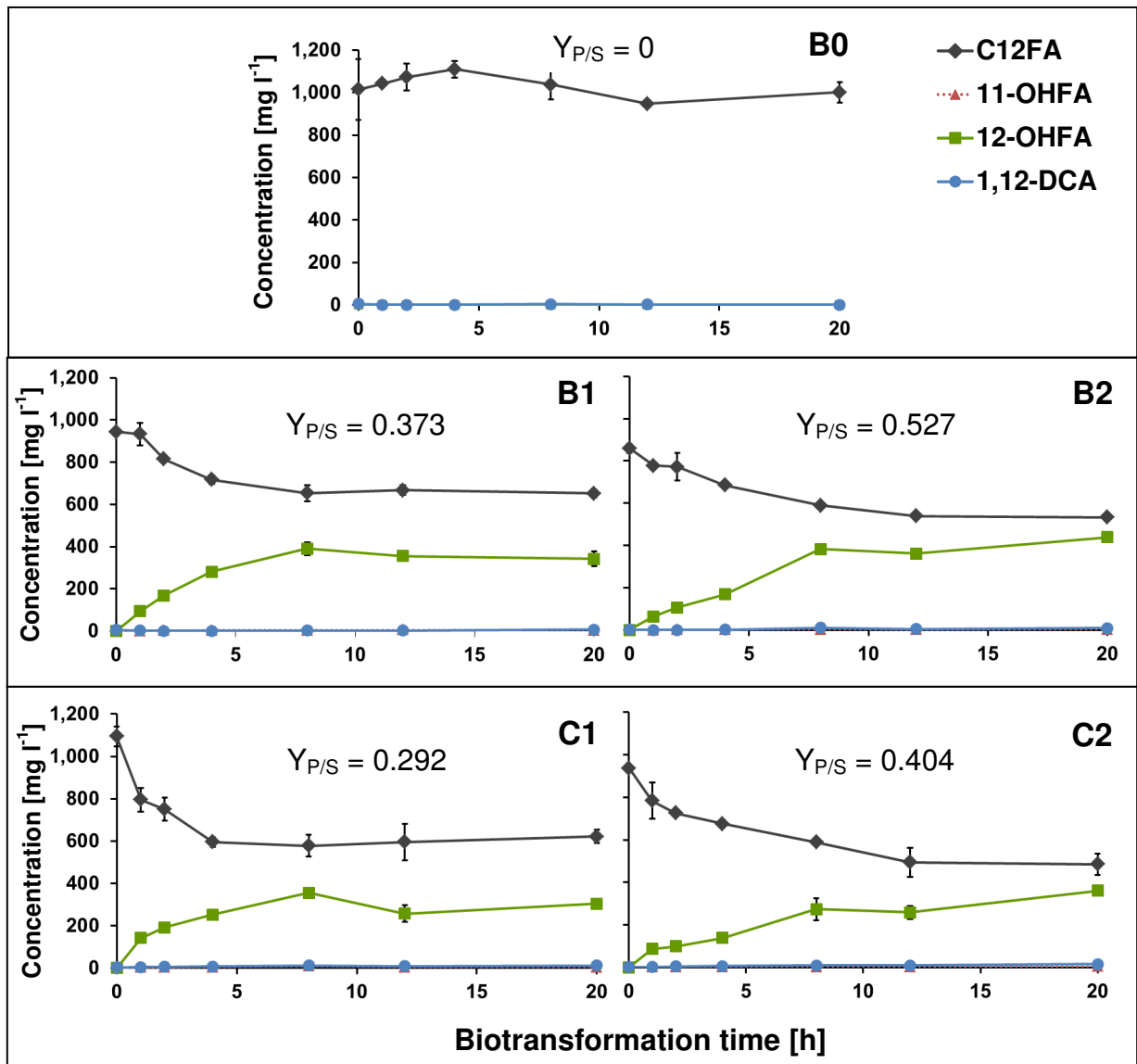


Figure 3.10. Whole cell biotransformations of 1 g l⁻¹ dodecanoic acid with resting *E. coli* cells in the presence of additional C-source. (B) *E. coli* JM109 and (C) *E. coli* BL21(DE3) cells contained either (0) empty pJOE, (1) pJOE-CYP153A *M. aq.*-CPR_{BM3} or (2) pJOE-CYP153A *M. aq.*(G307A)-CPR_{BM3}. Cell suspensions were 50 g_{cww} l⁻¹ (11 - 12.7 g_{cdw} l⁻¹). Cells were fed with additional C-source at 0, 4, 8 and 12 h. Product yield coefficients ($Y_{P/S}$) correspond to g of total products per g substrate. Abbreviations: C12FA, dodecanoic acid; 11-OHFA, 11-hydroxydodecanoic acid; 12-OHFA, 12-hydroxydodecanoic acid; 1,12-DCA, 1,12-dodecanedioic acid.

E. coli containing the empty pJOE vector practically did not consume the substrate when the cells were fed with glycerol and glucose. Total product yields obtained with the G307A variants were 37- 40 % higher than those observed with the wild type (figure 3.10). As observed in table 3.15, CYP concentrations in JM109 and BL21(DE3) reached in average 30 and 40 mg (g_{cdw})⁻¹, respectively. In both strains the G307A variant was expressed in similar levels than the wild type

enzyme. CYP expression levels correlated with the product yields observed, with JM109 and BL21(DE3) producing similar amounts of 12-OHFA (300 – 400 mg l⁻¹). Once again, BL21(DE3) produced more α,ω -DCA than JM109, presumably due to a higher alcohol and/or aldehyde dehydrogenase activity.

Table 3.15. Product concentrations and distributions obtained with resting *P. putida* and *E. coli* cells harboring CYP153A *M. aq.* (wt) or (G307A) fused to CPR_{BM3} in conversions with additional C-source

Parameter	Units	<i>P. putida</i>		<i>E. coli</i>		<i>E. coli</i>	
		KT2440	G307A	JM109	G307A	BL21(DE3)	G307A
		wt	G307A	wt	G307A	wt	G307A
Biotransformation time	h	20	20	20	20	20	20
Biomass concentration ¹	g _{cdw} l ⁻¹	9.5	9.9	11.3	10.9	12.7	12.1
Active P450 concentration ¹	mg (g _{cdw}) ⁻¹	46.6	40.3	27.6	33.5	39.5	40.0
Initial substrate concentration	mg l ⁻¹	938	803	944	859	1095	938
Substrate conversion ²	%	15.4	19.3	34.5	48.7	27.1	37.3
12-OHFA concentration	mg l ⁻¹	53	72	342	439	305	360
1,12-DCA concentration	mg l ⁻¹	108	100	7	9	13	15
Product distribution							
11-OHFA	%	1.2	1.1	1.1	0.8	1.3	1.1
12-OHFA	%	33.7	43.2	97.0	97.2	95.0	95.2
1,12-DCA	%	65.1	55.7	1.9	2.0	3.7	3.8

¹at start of biotransformation. ²Substrate converted to oxygenated products (not equivalent to substrate consumption). The values were calculated from initial substrate and product concentrations and represent the molar percentage yields.

3.3.2.2.3 Dodecanoic, octanoic and oleic acid oxidation with additional C-source by resting *E. coli* cells containing wild type and mutant CYP153A in a fusion construct

A short fatty acid (octanoic acid) and a long monounsaturated fatty acid (oleic acid) were selected as substrates for biotransformations with *E. coli* JM109 containing the fusion construct in their CYP153A *M. aq.* (wt) and (G307A) versions. Dodecanoic acid was tested again for comparison purposes, as other measurements were included on this occasion. In order to investigate the stability of the *in vivo* systems, cell densities, cell viability and whole cell P450 concentrations were determined over time as well. Although the yields of ω -OHFA products from octanoic and oleic acids were significantly lower compared to those obtained with dodecanoic acid, ω -OHFA concentrations reached by mutant G307 were respectively 34 to 61 %

higher compared to the wild type enzyme (figures 3.11 - 3.13). *E. coli* harboring empty vector consumed octanoic and oleic acid over time, even though cells were fed with glucose and glycerol every 4 hours. Cell densities did not change significantly over time, indicating that the host strain remained stable during biotransformation. In addition, cell viability tests showed no logarithmic decrease in the number of colony forming units after 4, 8 and 20 h (data not shown). Growing *E. coli* cells have been reported to be susceptible towards $C_{2:0}$ - $C_{8:0}$ and $C_{12:0}$ - $C_{18:0}$,²¹⁴ but resting cells appear to be more robust. CO differential spectral analysis of whole cells indicated a 50 % decrease in active CYP concentration in the case of cultures exposed to dodecanoic and oleic acids, thereby indicating that intrinsic biocatalyst stability depends on the fatty acid.

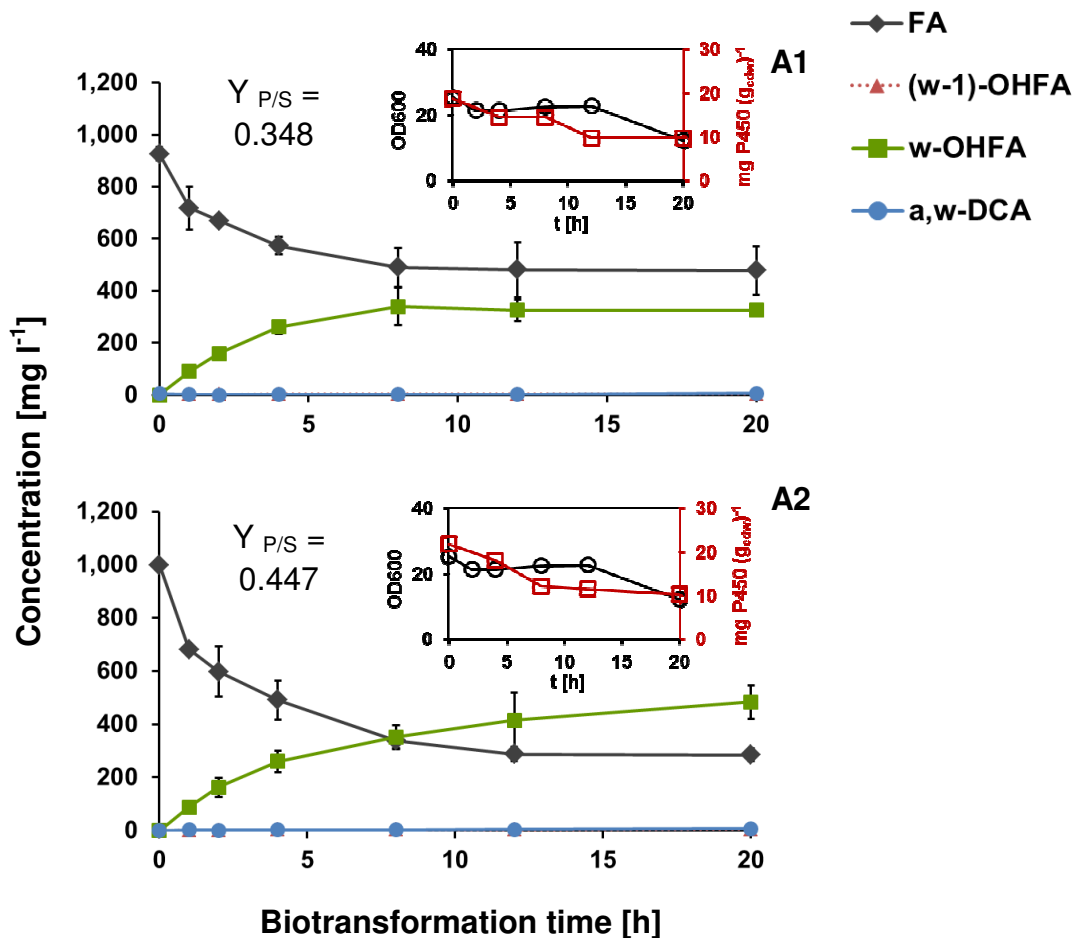


Figure 3.11. Whole cell biotransformations of 1 g l⁻¹ dodecanoic acid with resting *E. coli* JM109 cells. Cells contained (A1) pJOE-CYP153A *M. aq.*-CPR_{BM3} or (A2) pJOE-CYP153A *M. aq.*(G307A)-CPR_{BM3}. Cell concentrations were 11 g_{cdw} l⁻¹. Cells were fed with additional C-source at 0, 4, 8 and 12 h. Product yield coefficients ($Y_{P/S}$) correspond to g of total products per g substrate. Abbreviations: FA, fatty acid substrate; (ω -1)-OHFA, subterminally hydroxylated fatty acid; ω -OHFA, terminally hydroxylated fatty acid; α,ω -DCA, dicarboxylic acid.

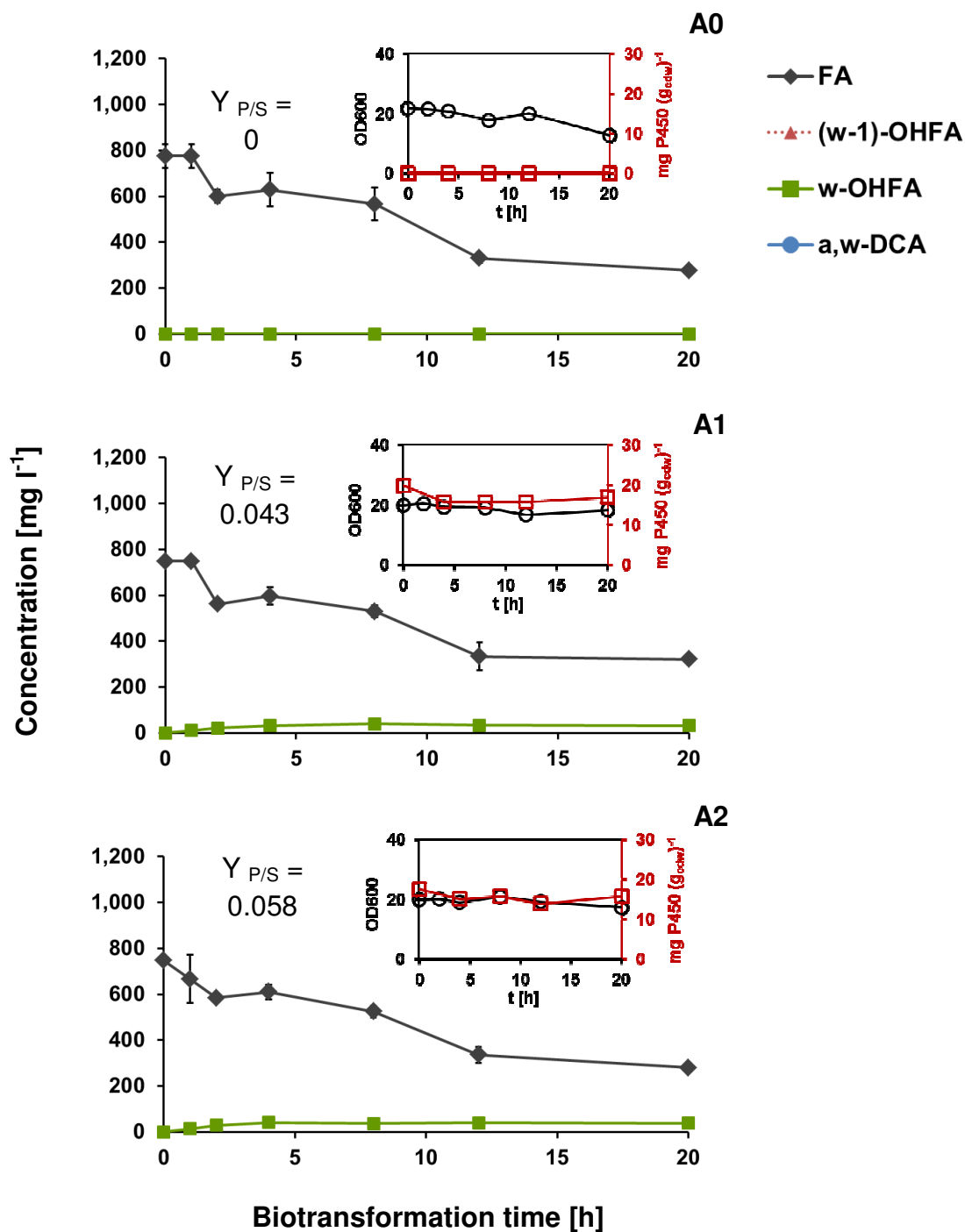


Figure 3.12. Whole cell biotransformations of 0.75 g l⁻¹ octanoic acid with resting *E. coli* JM109 cells. Cells contained (A0) empty pJOE, (A1) pJOE-CYP153A *M. aq.* -CPR_{BM3} or (A2) pJOE-CYP153A *M. aq.* (G307A)-CPR_{BM3}. Cell concentrations were 11 g_{cdw} l⁻¹. Cells were fed with additional C-source at 0, 4, 8 and 12 h. Product yield coefficients ($Y_{P/S}$) correspond to g of total products per g substrate. Abbreviations: FA, fatty acid substrate; (w-1)-OHFA, subterminally hydroxylated fatty acid; w-OHFA, terminally hydroxylated fatty acid; α,ω -DCA, dicarboxylic acid.

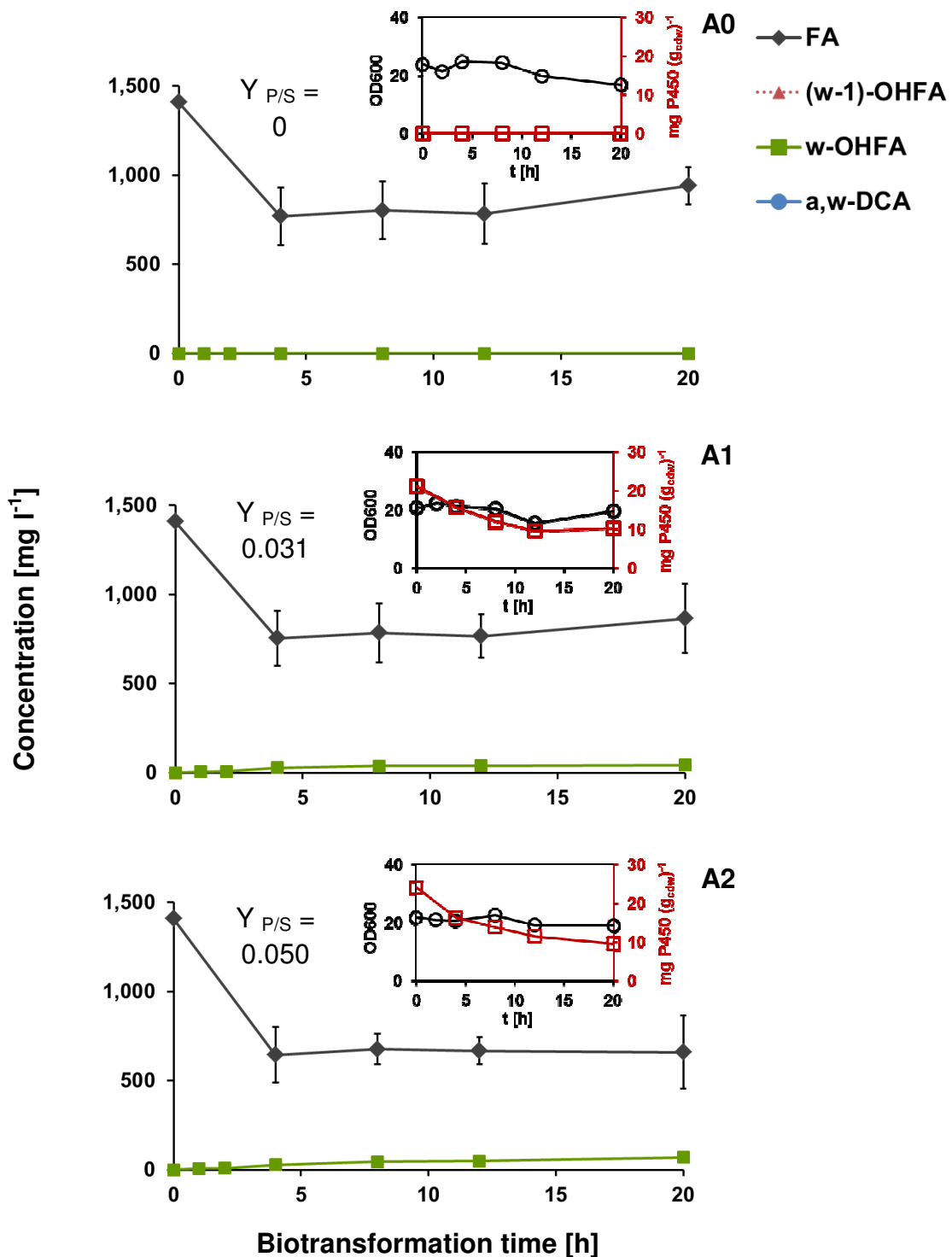


Figure 3.13. Whole cell biotransformations of 1.4 g l⁻¹ oleic acid with resting *E. coli* JM109 cells. Cells contained (A0) empty pJOE, (A1) pJOE-CYP153A *M. aq.*-CPR_{BM3} or (A2) pJOE-CYP153A *M. aq.* (G307A)-CPR_{BM3}. Cell concentrations were 11 g_{cdw} l⁻¹. Cells were fed with additional C-source at 0, 4, 8 and 12 h. Product yield coefficients (Y_{P/S}) correspond to g of total products per g substrate. Abbreviations: FA, fatty acid substrate; (ω-1)-OHFA, subterminally hydroxylated fatty acid; ω-OHFA, terminally hydroxylated fatty acid; α,ω-DCA, dicarboxylic acid.

As indicated in table 3.16, CYP concentrations were in average 20 mg (g_{cdw})⁻¹ at the start of biotransformation. Maximum ω -OHFA yields for the G307A variant towards octanoic and oleic acids were 43 and 70 mg l⁻¹ after 20 h, respectively. Considering that *E. coli* consumes octanoic and oleic acids, the use of β -oxidation knockout for biotransformations with these substrates seems imperative.

Table 3.16. Product concentrations and distributions obtained with resting *E. coli* JM109 cells harboring CYP153A *M. aq.* (wt) or (G307A) fused to CPR_{BM3} in conversions with additional C-source

Parameter	Units	Octanoic acid		Dodecanoic acid		Oleic acid	
		wt	G307A	wt	G307A	wt	G307A
		Biotransformation time	h	20	20	20	20
Biomass concentration ¹	g _{cdw} l ⁻¹	11.0	11.0	11.0	11.0	11.0	11.0
Active P450 concentration ¹	mg (g _{cdw}) ⁻¹	19.9	17.5	18.8	21.7	21.2	24.2
Initial substrate concentration	mg l ⁻¹	750	741	908	998	1412	1412
Substrate conversion ²	%	3.8	4.5	32.2	41.3	2.9	4.7
ω -OHFA concentration	mg l ⁻¹	32	43	309	438	44	70
α,ω -DCA concentration	mg l ⁻¹	—	—	4	5	—	—
Product distribution							
(ω -1)-OHFA	%	—	—	1.0	0.7	—	—
ω -OHFA	%	100	100	97.7	98.3	100	100
α,ω -DCA	%	—	—	1.3	1.0	—	—

¹at start of biotransformation. ²Substrate converted to oxygenated products (not equivalent to substrate consumption). The values were calculated from initial substrate and product concentrations and represent the molar percentage yields.

In summary, the best results of the *in vivo* shake flask bioconversions herein presented were achieved with resting *E. coli* JM109 cells harboring the engineered CYP153A *M. aq.*(G307A)-CPR_{BM3} fusion construct towards dodecanoic acid after 8 h ($Y_{p/s}$ = 0.45 – 0.5; \geq 96 % ω -regioselectivity). Biotransformations were run at 30°C, 180 rpm. Experimental conditions resulting in higher product yields included the use of 11 g_{cdw} l⁻¹ cells, 1 g l⁻¹ substrate and 2 % (v/v) DMSO. Higher cell or substrate concentrations did not contribute to increase product yields significantly. Cells were fed with glucose/glycerol (0.4 g l⁻¹/ 1 g l⁻¹) every 4 h to minimize substrate depletion.

4 Conclusion and outlook

We have investigated biocatalysts for the synthesis of industrially relevant ω -oxyfunctionalized medium- and long-chain length aliphatic compounds. Prokaryotic CYP153A enzymes were selected on the basis of their high ω -regiospecificity, expression in soluble form (suitable for *in vitro* studies) and straightforward application within a bacterial system.

CYP153A enzymes from *Polaromonas* sp. JS666, *Mycobacterium marinum* M. and *Marinobacter aquaeolei* VT8 were investigated. The CYP153A enzyme from *M. marinum* is herein referred as CYP153A16, based on the CYP nomenclature system.¹²⁸ There are no former reports on CYP153A16; however, one CYP153 enzyme from *M. marinum* (referred as CYP153A14) was formerly expressed in *Pseudomonas putida* and demonstrated to ω -oxidize C₆-C₁₀ alkanes, among other compounds.¹⁹⁰ The monooxygenases from *Polaromonas* sp. and *M. aquaeolei* have not been assigned a CYP systematic name yet, thus the terms CYP153A *P.* sp. and CYP153A *M. aq.* were adopted in agreement with the Cytochrome P450 Engineering Database (CYPED).²¹⁵ CYP153A *P.* sp. and CYP153A *M. aq.* have not been characterized prior to this work, but *Polaromonas* sp. and *M. aquaeolei* are known to grow on and metabolize alkanes²¹⁶ and alkanes/fatty acids,²¹⁷⁻²¹⁹ respectively.

The monooxygenases were first screened towards C₅-C₁₂ alkanes and C₆-C₁₂ primary alcohols. CYP153A16 and CYP153A *M. aq.* were found to oxidize alkanes to primary alcohols and these further to α,ω -diols. CYP153A *P.* sp. was active towards the investigated alkanes, but lacked the ability to terminally hydroxylate primary alcohols. Diol formation has been documented for CYP153 from *Acinetobacter* sp. OC4 (P450aci) and CYP153A13a (P450balk).^{90, 91} In a more recent study, CYP153A13a was shown to ω -hydroxylate C₈-C₁₂ alkanes, though α,ω -diols were not observed as products.⁸⁹ Our findings are consistent with the fact that P450aci shares higher protein sequence similarity with CYP153A16 and CYP153A *M. aq.* (≥ 80 %) than with CYP153A *P.* sp. (70 %). Likewise, there is a high amino acid sequence similarity between CYP153A *P.* sp. and CYP153A6 from *Mycobacterium* sp HXN-1500, which has never been reported to yield diols. Our substrate screening studies towards C₈-C₂₀ saturated and 9(*Z*)/(*E*)-C_{14:1}-C_{18:1} monounsaturated fatty acids provided further insights into the capabilities of CYP153A enzymes. We demonstrated that primary alcohol ω -hydroxylases CYP153A16 and CYP153A *M. aq.* are also able to convert fatty acids to ω -OHFAs. CYP153A *M. aq.* exhibited higher flexibility towards fatty acids of different size and saturation level. A combined rational design approach enabled us to

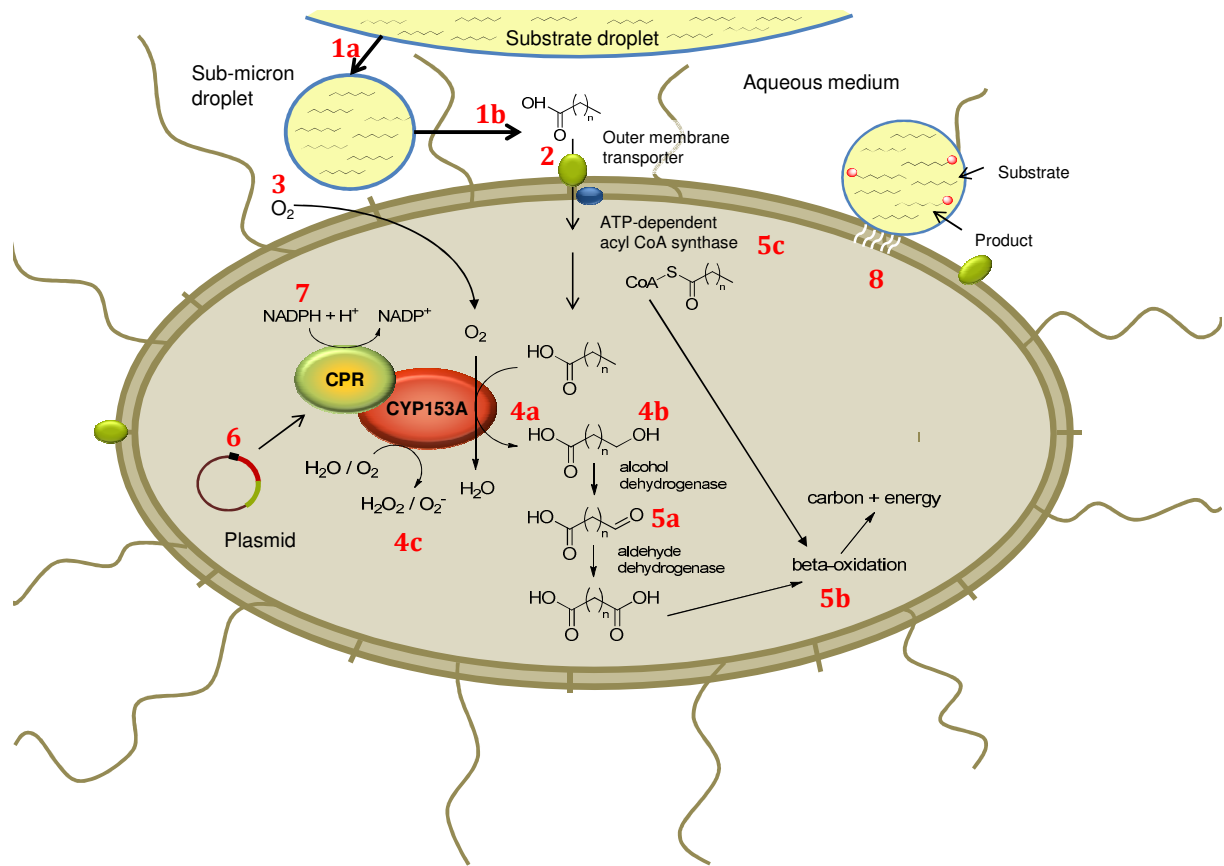
identify key residues for the activity and selectivity of CYP153A *M. aq.* An important aim was achieved by the creation of variant G307A, which was able to ω -oxygenate shorter primary alcohols and fatty acids owing to a higher catalytic efficiency compared to the wild type enzyme.

The biotechnological potential of CYP153A *M. aq.* can be estimated by comparing its activity with those of yeast CYP52 alkane/fatty acid ω -hydroxylases. We are though unable to perform such comparison as previous publications have focused on studying CYP52 activity under different conditions, using either insect/yeast microsomal fractions^{14, 81} or improved whole yeast cells.^{4, 136} However, the low intrinsic oxidation activity of CYP153A *M. aq.* towards ω -OHFAs contrasts the behaviour of CYP52 enzymes, known to be *per se* responsible for the overoxidation of ω -OHFAs to diacids without the intervention of other oxidoreductases.^{17, 220} This means CYP153A *M. aq.* allows more control of the reaction, which is an ideal feature for ω -OHFA synthesis. Compared to the most active bacterial CYPs known from the literature, i.e. CYP102A enzymes, the performance of CYP153 enzymes is still low. Nevertheless, attempts to mutate the former enzymes for alkane terminal oxidation have resulted in low ω -regiospecificities,^{96, 97} indicating that engineered CYPs from other bacterial families are yet not able to compete against CYP153A enzymes in terms of selectivity. The fact that CYP153A6 was formerly evolved for increased activity towards short-chain alkanes without affecting its selectivity⁷⁷ is a proof that these enzymes are overall promising biocatalysts which can be tailored for higher activity and altered substrate specificity.

As CYP activity also relies on coupling efficiency, it is important to consider that product yields shown in our *in vitro* reactions belong to the non-natural CamA-CamB-CYP153A electron transfer chain. Even though CamA/CamB are known to interact reasonably well with CYP153A enzymes,⁹¹ higher oxidation activities should be expected by using physiological redox partners or an artificial reductase in a single polypeptide chain arrangement. Here this limitation was tackled by the application of a fusion construct comprised by the CYP153A monooxygenase and the reductase domain of CYP102A1 (P450 BM3).

Oxygenation reactions with the fusion proteins were carried out in *P. putida* and *E. coli*. The pseudomonads were included mainly due to their higher solvent tolerance and redox capacity. A comparative study with non-improved strains showed that higher concentrations of primary alcohols and ω -OHFAs were accumulated by *E. coli* than by *P. putida*. The fusion protein containing mutation G307A did not display the same efficiency *in vivo* as *in vitro*, but it performed better than the wild type enzyme. Figure 4.1 illustrates potential limitations in a whole cell fatty acid ω -hydroxylation reaction with our established fusion construct and proposed strategies to overcome them. Given the high tendency of *P. putida* to consume the

substrate and the target products, production yields should be increased by the use of solvent-treated knock-out strains. These cells should have a higher tolerance towards the substrate/product and a more efficient metabolism for redox biocatalysis.



Limitations

- 1 Mass transport**
 - a. Interfacial area
 - b. Substrate solubility
- 2 Substrate uptake**
- 3 Oxygen transfer**
- 4 Enzyme effects**
 - a. Low turnover/stability
 - b. Product inhibition
 - c. Uncoupling
- 5 Host metabolic effects**
 - a. Overoxidation
 - b. β -oxidation
 - c. Fatty acid activation
- 6 Protein production**
 - Plasmid instability
 - Poor induction
- 7 Cofactor availability**
- 8 Substrate and/or product toxicity**

Figure 4.1. Limitations in whole cell fatty acid ω -hydroxylations catalyzed by CYP153A-CPR systems. Possible solutions for each bottleneck are: (1a-b) addition of surfactants; (2) overexpression of the constitutive fatty acid transporter/co-expression of a heterologous one; (3) stirred-tank reactor design; (4a) enzyme engineering to increase activity and stability; (4c) heme-reductase linker engineering to maximize electron transfer efficiency, co-expression of ROS-scavenging enzymes; (4b, 8) reaction configuration in a two-phase system to prevent product inhibition/toxicity; (5) deletion of selected enzymes to prevent substrate and product depletion; (6) selection of an adequate vector or gene integration into the chromosome; (7) overexpression of a constitutive cofactor-regenerating enzyme/co-expression of a heterologous one or increase the flux of NADPH-producing reactions; (8) use of solvent-tolerant and solvent-adapted host strains. Based on van Beilen *et al.*,¹³⁹ Grant *et al.*²²¹ and D. Scheps *et al.*, *Microb Technol*, 2013, manuscript accepted.

Additional efforts in both *P. putida* and *E. coli* should be oriented to maximize mass transfer and transport of the substrate across the membrane. In fact, substrate solubilization and uptake is not completely relieved by the addition of surfactants and cosolvents.^{222, 223} Recently, the co-expression of the outer membrane protein transporter AlkL of *P. putida* Gpo1 has been shown to increase AlkB monooxygenase-based reaction rates towards methyl dodecanoate by 62-fold.²²² Another issue is cellular cofactor availability, which can be increased by protein and metabolic engineering as well. An elegant strategy described for *E. coli* consists of modifying an NADPH-dependent monooxygenase for dual NADH/NADPH specificity. At the same time, increasing the flux of the NADPH-producing pentose phosphate pathway and eliminating NADH-utilizing processes resulted in a more efficient utilization of the energy source in redox biocatalysis.²²⁴

Hydrogen peroxide and other ROS accumulated in *P. putida* as a response to stress or as a side-product of the CYP-mediated reaction can be immediately removed *in situ* by co-expressing catalase and other ROS-scavenging enzymes (e.g., superoxide dismutase). ROS generated by electron uncoupling could be minimized by increasing the coupling efficiency of the fusion construct. Varying the length of the polypeptide linker between the heme and the reductase domains has been reported to influence the coupling efficiency of chimeric fusion proteins.^{225, 226} However, one *in vitro* study on a human CYP fused to the CPR from P450 BM3 suggests that uncoupling is an intrinsic property of the heme domain and that the covalent linkage of the reductase in a single polypeptide chain has little influence on activity coupled to product formation, with factors like cofactor concentration, pH and ionic strength having a significant role in uncoupling.²²⁷ Acetate formation in *E. coli* can be minimized by using a low acetate-producing strain. At high glucose concentrations, growing JM109 cells have been reported to accumulate up to 11 g l⁻¹ acetate, while growing BL21(DE3) cells produce around 3 g l⁻¹ (≥ 2.4 g l⁻¹ is detrimental).²¹¹ Other strategies to reduce acetate production in high-cell density *E. coli* fermentations can be applied at the bioprocess level (use of alternative C-sources and feeding approaches) and at the genetic level (regulation of futile cycles, anapleurotic pathways, coenzyme levels, acetate-producing and ATP-consuming pathways), with the latter giving the best results.²²⁸

To conclude, we have reported the selective ω -hydroxylation of a broad set of alkanes, primary alcohols and fatty acids by bacterial CYP153A enzymes. The hydroxylation activity of a CYP153A candidate was increased by a rational design approach and the construction of a catalytic self-sufficient monooxygenase. Although *E. coli* appeared to be a more effective host than *P. putida*, higher product titers could be obtained with adapted and improved pseudomonads. Finally, further protein, strain and process engineering strategies will eventually lead to the generation

of an alternative bacterial-based platform for the production of commercially attractive primary alcohols, α,ω -diols and ω -OHFAs.

5 References

1. K. Noweck and W. Grafahrend. Fatty alcohols, in *Ullmann's Encyclopedia of Industrial Chemistry*. 2002, Wiley-VCH Verlag GmbH & Co. KGaA.
2. A. Abe and K. Sugiyama. Growth inhibition and apoptosis induction of human melanoma cells by omega-hydroxy fatty acids. *Anticancer Drugs*, 2005. **16**(5): 543.
3. S. Huf, S. Krugener, T. Hirth, S. Rupp, and S. Zibek. Biotechnological synthesis of long-chain dicarboxylic acids as building blocks for polymers. *Eur J Lipid Sci Technol*, 2011. **113**(5): 548.
4. W. Lu, J.E. Ness, W. Xie, X. Zhang, J. Minshull, and R.A. Gross. Biosynthesis of monomers for plastics from renewable oils. *J Am Chem Soc*, 2010. **132**(43): 15451.
5. A.V. Rawlings. Trends in stratum corneum research and the management of dry skin conditions. *Int J Cosmet Sci*, 2003. **25**(1-2): 63.
6. C. Liu, F. Liu, J. Cai, W. Xie, T.E. Long, S.R. Turner, A. Lyons, and R.A. Gross. Polymers from fatty acids: Poly(omega-hydroxyl tetradecanoic acid) synthesis and physico-mechanical studies. *Biomacromolecules*, 2011. **12**(9): 3291.
7. D.J. Cole-Hamilton. Nature's polyethylene. *Angew Chem Int Ed*, 2010. **49**(46): 8564.
8. Y. Doi, K. Sudesh, and H. Abe. Synthesis, structure and properties of polyhydroxyalkanoates: biological polyesters. *Prog Polym Sci*, 2000. **25**(10): 1503.
9. U. Edlund and A.C. Albertsson. Polyesters based on diacid monomers. *Adv Drug Deliv Rev*, 2003. **55**(4): 585.
10. R.A. Gross, W. Lu, J. Ness, and J. Minshull. Production of an alpha-carboxyl-omega-hydroxy fatty acid using a genetically modified *Candida* strain DNA Twopointo, Inc., 2012. U.S. Patent 8,158,391.
11. A.K. Mohanty and R. Bhardwaj. Advances in the properties of polylactides based materials: A review. *J Biobased Mater Bio*, 2007. **1**(2): 191.
12. D.L. Craft, K.M. Madduri, M. Eshoo, and C.R. Wilson. Identification and characterization of the CYP52 family of *Candida tropicalis* ATCC 20336, important for the conversion of fatty acids and alkanes to alpha,omega-dicarboxylic acids. *Appl Environ Microbiol*, 2003. **69**(10): 5983.
13. P. Fickers, P.H. Benetti, Y. Wache, A. Marty, S. Mauersberger, M.S. Smit, and J.M. Nicaud. Hydrophobic substrate utilisation by the yeast *Yarrowia lipolytica*, and its potential applications. *FEMS Yeast Res*, 2005. **5**(6-7): 527.

14. U. Scheller, T. Zimmer, E. Kargel, and W.H. Schunck. Characterization of the *n*-alkane and fatty acid hydroxylating cytochrome P450 forms 52A3 and 52A4. *Arch Biochem Biophys*, 1996. **328**(2): 245.
15. M. Schrewe, A.O. Magnusson, C. Willrodt, B. Bühler, and A. Schmid. Kinetic analysis of terminal and unactivated C-H bond oxyfunctionalization in fatty acid methyl esters by monooxygenase-based whole-cell biocatalysis. *Adv Synth Catal*, 2011. **353**(18): 3485.
16. Q. Cheng, D. Sanglard, S. Vanhanen, H.T. Liu, P. Bombelli, A. Smith, and A.R. Slabas. *Candida* yeast long chain fatty alcohol oxidase is a c-type haemoprotein and plays an important role in long chain fatty acid metabolism. *Biochim Biophys Acta*, 2005. **1735**(3): 192.
17. U. Scheller, T. Zimmer, D. Becher, F. Schauer, and W.H. Schunck. Oxygenation cascade in conversion of *n*-alkanes to alpha,omega-dioic acids catalyzed by cytochrome P450 52A3. *J Biol Chem*, 1998. **273**(49): 32528.
18. U. Antczak, J. Gora, T. Antczak, and E. Galas. Enzymatic Lactonization of 15-Hydroxypentadecanoic and 16-Hydroxyhexadecanoic Acids to Macrocyclic Lactones. *Enzyme Microb Technol*, 1991. **13**(7): 589.
19. E.J. Corey and K.C. Nicolaou. Efficient and Mild Lactonization Method for Synthesis of Macrolides. *J Am Chem Soc*, 1974. **96**(17): 5614.
20. K.C. Nicolaou. Synthesis of Macrolides. *Tetrahedron*, 1977. **33**(7): 683.
21. Y.X. Yang, W.H. Lu, X.Y. Zhang, W.C. Xie, M.M. Cai, and R.A. Gross. Two-Step Biocatalytic Route to Biobased Functional Polyesters from omega-Carboxy Fatty Acids and Diols. *Biomacromolecules*, 2010. **11**(1): 259.
22. M. Renz. Ketonization of carboxylic acids by decarboxylation: Mechanism and scope. *Eur J Org Chem*, 2005(6): 979.
23. V. Alphand, G. Carrea, R. Wohlgemuth, R. Furstoss, and J.M. Woodley. Towards large-scale synthetic applications of Baeyer-Villiger monooxygenases. *Trends Biotechnol*, 2003. **21**(7): 318.
24. A. Baeyer and V. Villiger. Impact of Caro's reagent on ketones. *Berichte Der Deutschen Chemischen Gesellschaft*, 1900. **33**: 124.
25. A. Baeyer and V. Villiger. The effect of Caro' reagent on ketone. *Berichte Der Deutschen Chemischen Gesellschaft*, 1900. **33**: 858.
26. M. Renz and B. Meunier. 100 years of Baeyer-Villiger oxidations. *Eur J Org Chem*, 1999(4): 737.
27. M. Eh and I. Wöhrle. Macrocyclic ketones. Symrise GmbH & Co. KG, 2004. U.S. Patent 6,815,413 B2.
28. O. Roelen. Eine neue Synthese von Aldehyden und deren Derivaten, ausgehend von Olefinen, Kohlenoxyd und Wasserstoff. *Angew Chem*, 1948. **60**(3): 62.

29. R.D.M. L.H. Slaugh. 1966. US Patent 3,239,566.
30. D. Evans, J.A. Osborn, and Wilkinso.G. Hydroformylation of Alkenes by Use of Rhodium Complex Catalysts. *Journal of the Chemical Society a -Inorganic Physical Theoretical*, 1968(12): 3133.
31. R.L. Pruett and J.A. Smith. A Low-Pressure System for Producing Normal Aldehydes by Hydroformylation of Alpha Olefins. *J Org Chem*, 1969. **34**(2): 327.
32. B. Reuben and H. Wittcoff. The SHOP Process - an Example of Industrial Creativity. *J Chem Educ*, 1988. **65**(7): 605.
33. J.O. Metzger. Fats and oils as renewable feedstock for chemistry. *Eur J Lipid Sci Technol*, 2009. **111**(9): 865.
34. J.O. Metzger and U. Bornscheuer. Lipids as renewable resources: current state of chemical and biotechnological conversion and diversification. *Appl Microbiol Biotechnol*, 2006. **71**(1): 13.
35. S. Warwel, H.G. Jagers, and S. Thomas. Metathesis of Unsaturated Fatty-Acid Esters - a Simple Approach to Long-Chained Dicarboxylic-Acids. *Fett Wissenschaft Technologie-Fat Science Technology*, 1992. **94**(9): 323.
36. T. Yokota and A. Watanabe. Process for producing omega-hydroxy fatty acids Nippon Mining Co., Ltd. , 1992. U.S. Patent 5,191,096.
37. L. Cotarca, P. Maggioni, and A. Nardelli. Process for producing an omega-functionalized aliphatic carboxylic acid and intermediate products of said process. Industrie Chimiche Caffaro, S.p.A. , 1999. U.S. Patent 5,872,267.
38. M.M.S. Stephan and B. Mohar. Simple preparation of highly pure monomeric omega-hydroxycarboxylic acids. *Org Process Res Dev*, 2006. **10**(3): 481.
39. K. Suzuki, T. Eto, T. Osuka, S. Abe, and S. Yoshikawa. Process for the Preparation of Omega-hydroxy Fatty Acids from Omega-hydroxy (or acyloxy)-alkyl-gamma-Butyrolactones. Soda Koryo Kabushiki Kaisha, 1981. U.S. Patent 4,246,182.
40. J.A. Labinger and J.E. Bercaw. Understanding and exploiting C-H bond activation. *Nature*, 2002. **417**(6888): 507.
41. J.A. Labinger. Selective alkane oxidation: hot and cold approaches to a hot problem. *J Mol Catal A Chem*, 2004. **220**(1): 27.
42. J.M. Thomas. Heterogeneous catalysis: Enigmas, illusions, challenges, realities, and emergent strategies of design. *J Chem Phys*, 2008. **128**(18): 182502 (1).
43. C. Hall and R.N. Perutz. Transition metal alkane complexes. *Chem Rev*, 1996. **96**(8): 3125.
44. R.K. Grasselli. Fundamental principles of selective heterogeneous oxidation catalysis. *Topics in Catalysis*, 2002. **21**(1-3): 79.
45. P. Battioni, J.P. Renaud, J.F. Bartoli, M. Reinaartiles, M. Fort, and D. Mansuy. Monooxygenase-like oxidation of hydrocarbons by H₂O₂ catalyzed by manganese

- porphyrins and imidazole - Selection of the best catalytic system and nature of the active oxygen species. *J Am Chem Soc*, 1988. **110**(25): 8462.
46. M. Bordeaux, A. Galarneau, and J. Drone. Catalytic, mild, and selective oxyfunctionalization of linear alkanes: current challenges. *Angew Chem Int Ed* 2012. **51**(43): 10712.
 47. B.R. Cook, T.J. Reinert, and K.S. Suslick. Shape selective alkane hydroxylation by metalloporphyrin catalysts. *J Am Chem Soc*, 1986. **108**(23): 7281.
 48. M. Costas. Selective C-H oxidation catalyzed by metalloporphyrins. *Coord Chem Rev*, 2011. **255**(23-24): 2912.
 49. N.F. Goldshleger, A.A. Shteinman, A.E. Shilov, and V.V. Eskova. Reactions of alkanes in solutions of chloride complexes of platinum. *Russ J Phys Chem*, 1972. **46**(5): 785.
 50. K. Miki and T. Furuya. Catalytic hydroxylation of alkanes by immobilized mononuclear iron carboxylate. *Chem Commun*, 1998(1): 97.
 51. A.E. Shilov and A.A. Shteinman. Activation of saturated hydrocarbons by metal complexes in solutions. *Kinet Catal*, 1977. **18**(5): 924.
 52. J.M. Thomas, R. Raja, G. Sankar, and R.G. Bell. Molecular-sieve catalysts for the selective oxidation of linear alkanes by molecular oxygen. *Nature*, 1999. **398**(6724): 227.
 53. S.M. Yiu, W.L. Man, and T.C. Lau. Efficient catalytic oxidation of alkanes by Lewis acid/[Os(VI)(N)Cl₄]- using peroxides as terminal oxidants. Evidence for a metal-based active intermediate. *J Am Chem Soc*, 2008. **130**(32): 10821.
 54. S.M. Yiu, Z.B. Wu, C.K. Mak, and T.C. Lau. FeCl₃-activated oxidation of alkanes by [Os(N)O₃]-. *J Am Chem Soc*, 2004. **126**(45): 14921.
 55. M.J. Coon. Omega oxygenases: nonheme-iron enzymes and P450 cytochromes. *Biochem Biophys Res Commun*, 2005. **338**(1): 378.
 56. Z. Li and D.L. Chang. Recent advances in regio- and stereoselective biohydroxylation of non-activated carbon atoms. *Curr Org Chem*, 2004. **8**(17): 1647.
 57. J.B. van Beilen and E.G. Funhoff. Alkane hydroxylases involved in microbial alkane degradation. *Appl Microbiol Biotechnol*, 2007. **74**(1): 13.
 58. J. Colby and H. Dalton. Resolution of the methane mono-oxygenase of *Methylococcus capsulatus* (Bath) into three components. Purification and properties of component C, a flavoprotein. *Biochem J*, 1978. **171**(2): 461.
 59. J. Green and H. Dalton. Substrate specificity of soluble methane monooxygenase. Mechanistic implications. *J Biol Chem*, 1989. **264**(30): 17698.
 60. J.C. Murrell, B. Gilbert, and I.R. McDonald. Molecular biology and regulation of methane monooxygenase. *Arch Microbiol*, 2000. **173**(5-6): 325.

61. R. Balasubramanian, S.M. Smith, S. Rawat, L.A. Yatsunyk, T.L. Stemmler, and A.C. Rosenzweig. Oxidation of methane by a biological dicopper centre. *Nature*, 2010. **465**(7294): 115.
62. R.L. Lieberman, K.C. Kondapalli, D.B. Shrestha, A.S. Hakemian, S.M. Smith, J. Telser, J. Kuzelka, R. Gupta, A.S. Borovik, S.J. Lippard, B.M. Hoffman, A.C. Rosenzweig, and T.L. Stemmler. Characterization of the particulate methane monooxygenase metal centers in multiple redox states by X-ray absorption spectroscopy. *Inorg Chem*, 2006. **45**(20): 8372.
63. S. Park, N.N. Shah, R.T. Taylor, and M.W. Droege. Batch cultivation of *Methylosinus trichosporium* OB3b: II. Production of particulate methane monooxygenase. *Biotechnol Bioeng*, 1992. **40**(1): 151.
64. G.M. Stephens and H. Dalton. The role of the terminal and subterminal oxidation pathways in propane metabolism by bacteria. *J Gen Microbiol*, 1986. **132**: 2453.
65. T. Kotani, Y. Kawashima, H. Yurimoto, N. Kato, and Y. Sakai. Gene structure and regulation of alkane monooxygenases in propane-utilizing *Mycobacterium* sp. TY-6 and *Pseudonocardia* sp. TY-7. *J Biosci Bioeng*, 2006. **102**(3): 184.
66. T. Kotani, T. Yamamoto, H. Yurimoto, Y. Sakai, and N. Kato. Propane monooxygenase and NAD⁺-dependent secondary alcohol dehydrogenase in propane metabolism by *Gordonia* sp. strain TY-5. *J Bacteriol*, 2003. **185**(24): 7120.
67. D.J. Arp. Butane metabolism by butane-grown '*Pseudomonas butanovora*'. *Microbiology-Uk*, 1999. **145**: 1173.
68. R.B. Cooley, B.L. Dubbels, L.A. Sayavedra-Soto, P.J. Bottomley, and D.J. Arp. Kinetic characterization of the soluble butane monooxygenase from *Thauera butanivorans*, formerly '*Pseudomonas butanovora*'. *Microbiology*, 2009. **155**(Pt 6): 2086.
69. B.L. Dubbels, L.A. Sayavedra-Soto, and D.J. Arp. Butane monooxygenase of '*Pseudomonas butanovora*': purification and biochemical characterization of a terminal-alkane hydroxylating diiron monooxygenase. *Microbiology*, 2007. **153**(Pt 6): 1808.
70. N. Hamamura, R.T. Storfa, L. Semprini, and D.J. Arp. Diversity in butane monooxygenases among butane-grown bacteria. *Appl Environ Microbiol*, 1999. **65**(10): 4586.
71. L.A. Sayavedra-Soto, D.M. Doughty, E.G. Kurth, P.J. Bottomley, and D.J. Arp. Product and product-independent induction of butane oxidation in *Pseudomonas butanovora*. *FEMS Microbiol Lett*, 2005. **250**(1): 111.
72. M.K. Sluis, L.A. Sayavedra-Soto, and D.J. Arp. Molecular analysis of the soluble butane monooxygenase from '*Pseudomonas butanovora*'. *Microbiology-Sgm*, 2002. **148**: 3617.
73. N. Hamamura and D.J. Arp. Isolation and characterization of alkane-utilizing *Nocardioides* sp. strain CF8. *FEMS Microbiol Lett*, 2000. **186**(1): 21.
74. E.L. Johnson and M.R. Hyman. Propane and n-butane oxidation by *Pseudomonas putida* GPo1. *Appl Environ Microbiol*, 2006. **72**(1): 950.

75. J.B. van Beilen, J. Kingma, and B. Witholt. Substrate specificity of the alkane hydroxylase system of *Pseudomonas oleovorans* Gpo1. *Enzyme Microb Technol*, 1994. **16**(10): 904.
76. J.B. van Beilen, S. Panke, S. Lucchini, A.G. Franchini, M. Rothlisberger, and B. Witholt. Analysis of *Pseudomonas putida* alkane-degradation gene clusters and flanking insertion sequences: evolution and regulation of the alk genes. *Microbiology*, 2001. **147**(Pt 6): 1621.
77. D.J. Koch, M.M. Chen, J.B. van Beilen, and F.H. Arnold. *In vivo* evolution of butane oxidation by terminal alkane hydroxylases AlkB and CYP153A6. *Appl Environ Microbiol*, 2009. **75**(2): 337.
78. N. Lopes Ferreira, H. Mathis, D. Labbe, M. Frederic, C.W. Greer, and F. Fayolle-Guichard. n-Alkane assimilation and tert-butyl alcohol (TBA) oxidation capacity in *Mycobacterium austroafricanum* strains. *Appl Microbiol Biotechnol*, 2007. **75**(4): 909.
79. W.E. Phillips and J.J. Perry. Metabolism of normal-butane and 2-butanone by *Mycobacterium vaccae*. *J Bacteriol*, 1974. **120**(2): 987.
80. Y. Nie, J. Liang, H. Fang, Y.Q. Tang, and X.L. Wu. Two novel alkane hydroxylase-rubredoxin fusion genes isolated from a *Dietzia* bacterium and the functions of fused rubredoxin domains in long-chain n-alkane degradation. *Appl Environ Microbiol*, 2011. **77**(20): 7279.
81. W.H. Eschenfeldt, Y. Zhang, H. Samaha, L. Stols, L.D. Eirich, C.R. Wilson, and M.I. Donnelly. Transformation of fatty acids catalyzed by cytochrome P450 monooxygenase enzymes of *Candida tropicalis*. *Appl Environ Microbiol*, 2003. **69**(10): 5992.
82. O. Asperger, A. Naumann, and H.P. Kleber. Occurrence of cytochrome P450 in *Acinetobacter* strains after growth on normal hexadecane. *FEMS Microbiol Letters*, 1981. **11**(4): 309.
83. E.G. Funhoff, U. Bauer, I. Garcia-Rubio, B. Witholt, and J.B. van Beilen. CYP153A6, a soluble P450 oxygenase catalyzing terminal-alkane hydroxylation. *J Bacteriol*, 2006. **188**(14): 5220.
84. E.G. Funhoff, J. Salzmänn, U. Bauer, B. Witholt, and J.B. van Beilen. Hydroxylation and epoxidation reactions catalyzed by CYP153 enzymes. *Enzyme Microb Technol*, 2007. **40**(4): 806.
85. M. Kubota, M. Nodate, M. Yasumoto-Hirose, T. Uchiyama, O. Kagami, Y. Shizuri, and N. Misawa. Isolation and functional analysis of cytochrome P450 CYP153A genes from various environments. *Biosci Biotechnol Biochem*, 2005. **69**(12): 2421.
86. T. Maier, H.H. Forster, O. Asperger, and U. Hahn. Molecular characterization of the 56-kDa CYP153 from *Acinetobacter* sp. EB104. *Biochem Biophys Res Commun*, 2001. **286**(3): 652.

87. J.B. van Beilen, E.G. Funhoff, A. van Loon, A. Just, L. Kaysser, M. Bouza, R. Holtackers, M. Rothlisberger, Z. Li, and B. Witholt. Cytochrome P450 alkane hydroxylases of the CYP153 family are common in alkane-degrading eubacteria lacking integral membrane alkane hydroxylases. *Appl Environ Microbiol*, 2006. **72**(1): 59.
88. J.B. van Beilen, R. Holtackers, D. Luscher, U. Bauer, B. Witholt, and W.A. Duetz. Biocatalytic production of perillyl alcohol from limonene by using a novel *Mycobacterium* sp. cytochrome P450 alkane hydroxylase expressed in *Pseudomonas putida*. *Appl Environ Microbiol*, 2005. **71**(4): 1737.
89. M. Bordeaux, A. Galarneau, F. Fajula, and J. Drone. A regioselective biocatalyst for alkane activation under mild conditions. *Angew Chem Int Ed* 2011. **50**(9): 2075.
90. T. Fujii, T. Narikawa, F. Sumisa, A. Arisawa, K. Takeda, and J. Kato. Production of alpha, omega-alkanediols using *Escherichia coli* expressing a cytochrome P450 from *Acinetobacter* sp. OC4. *Biosci Biotechnol Biochem*, 2006. **70**(6): 1379.
91. N. Fujita, F. Sumisa, K. Shindo, H. Kabumoto, A. Arisawa, H. Ikenaga, and N. Misawa. Comparison of two vectors for functional expression of a bacterial cytochrome P450 gene in *Escherichia coli* using CYP153 genes. *Biosci Biotechnol Biochem*, 2009. **73**(8): 1825.
92. M. Nodate, M. Kubota, and N. Misawa. Functional expression system for cytochrome P450 genes using the reductase domain of self-sufficient P450RhF from *Rhodococcus* sp. NCIMB 9784. *Appl Microbiol Biotechnol*, 2006. **71**(4): 455.
93. J.B. Johnston, P.M. Kells, L.M. Podust, and P.R. Ortiz de Montellano. Biochemical and structural characterization of CYP124: a methyl-branched lipid omega-hydroxylase from *Mycobacterium tuberculosis*. *PNAS*, 2009. **106**(49): 20687.
94. F. Xu, S.G. Bell, J. Lednik, A. Insley, Z. Rao, and L.L. Wong. The heme monooxygenase cytochrome P450cam can be engineered to oxidize ethane to ethanol. *Angew Chem Int Ed* 2005. **44**(26): 4029.
95. E.T. Farinas, U. Schwaneberg, A. Glieder, and F.H. Arnold. Directed evolution of a cytochrome P450 monooxygenase for alkane oxidation. *Adv Synth Catal*, 2001. **343**(6-7): 601.
96. O. Lentz, A. Feenstra, T. Habicher, B. Hauer, R.D. Schmid, and V.B. Urlacher. Altering the Regioselectivity of Cytochrome P450 CYP102A3 of *Bacillus subtilis* by Using a New Versatile Assay System. *ChemBioChem*, 2006. **7**(2): 345.
97. P. Meinhold, M.W. Peters, A. Hartwick, A.R. Hernandez, and F.H. Arnold. Engineering cytochrome P450 BM3 for terminal alkane hydroxylation. *Adv Synth Catal*, 2006. **348**(6): 763.

98. N. Kawakami, O. Shoji, and Y. Watanabe. Use of perfluorocarboxylic acids to trick cytochrome P450BM3 into initiating the hydroxylation of gaseous alkanes. *Angew Chem Int Ed* 2011. **50**(23): 5315.
99. F.E. Zilly, J.P. Acevedo, W. Augustyniak, A. Deege, U.W. Hausig, and M.T. Reetz. Tuning a p450 enzyme for methane oxidation. *Angew Chem Int Ed* 2011. **50**(12): 2720.
100. N.M. Broadway, F.M. Dickinson, and C. Ratledge. The enzymology of dicarboxylic acid formation by *Corynebacterium* sp. strain 7e1c grown on *n*-alkanes. *J Gen Microbiol*, 1993. **139**: 1337.
101. G. Cardini and P. Jurtschuk. Cytochrome P450 involvement in the oxidation of *n*-octane by cell-free extracts of *Corynebacterium* sp. strain 7E1C. *J Biol Chem*, 1968. **243**(22): 6070.
102. G. Cardini and P. Jurtschuk. The enzymatic hydroxylation of *n*-octane by *Corynebacterium* sp. strain 7E1C. *J Biol Chem*, 1970. **245**(11): 2789.
103. S. Torres, C.R. Fjetland, and P.J. Lammers. Alkane-induced expression, substrate binding profile, and immunolocalization of a cytochrome P450 encoded on the *nifD* excision element of *Anabaena* 7120. *BMC Microbiol*, 2005. **5**: 16.
104. T.H. Smits, S.B. Balada, B. Witholt, and J.B. van Beilen. Functional analysis of alkane hydroxylases from Gram-negative and Gram-positive bacteria. *J Bacteriol*, 2002. **184**(6): 1733.
105. J.H. Maeng, Y. Sakai, Y. Tani, and N. Kato. Isolation and characterization of a novel oxygenase that catalyzes the first step of *n*-alkane oxidation in *Acinetobacter* sp strain M-1. *J Bacteriol*, 1996. **178**(13): 3695.
106. A. Tani, T. Ishige, Y. Sakai, and N. Kato. Gene structures and regulation of the alkane hydroxylase complex in *Acinetobacter* sp strain M-1. *J Bacteriol*, 2001. **183**(5): 1819.
107. L. Feng, W. Wang, J. Cheng, Y. Ren, G. Zhao, C. Gao, Y. Tang, X. Liu, W. Han, X. Peng, R. Liu, and L. Wang. Genome and proteome of long-chain alkane degrading *Geobacillus thermodenitrificans* NG80-2 isolated from a deep-subsurface oil reservoir. *PNAS*, 2007. **104**(13): 5602.
108. L. Li, X. Liu, W. Yang, F. Xu, W. Wang, L. Feng, M. Bartlam, L. Wang, and Z. Rao. Crystal structure of long-chain alkane monooxygenase (LadA) in complex with coenzyme FMN: unveiling the long-chain alkane hydroxylase. *J Mol Biol*, 2008. **376**(2): 453.
109. Y. Dong, J. Yan, H. Du, M. Chen, T. Ma, and L. Feng. Engineering of LadA for enhanced hexadecane oxidation using random- and site-directed mutagenesis. *Appl Microbiol Biotechnol*, 2012. **94**(4): 1019.
110. M. Merckx, D.A. Kopp, M.H. Sazinsky, J.L. Blazyk, J. Muller, and S.J. Lippard. Dioxygen activation and methane hydroxylation by soluble methane monooxygenase: A tale of two irons and three proteins. *Angew Chem Int Ed*, 2001. **40**(15): 2782.

111. I.E. Staijen, V. Hatzimanikatis, and B. Witholt. The AlkB monooxygenase of *Pseudomonas oleovorans* – synthesis, stability and level in recombinant *Escherichia coli* and the native host. *Eur J Biochem*, 1997. **244**(2): 462.
112. P.R. Ortiz de Montellano. Cytochrome P450: structure, mechanism, and biochemistry. 3rd ed. ed. 2005, New York: Kluwer Academic/Plenum Publishers.
113. I.G. Denisov, T.M. Makris, S.G. Sligar, and I. Schlichting. Structure and chemistry of cytochrome P450. *Chem Rev*, 2005. **105**(6): 2253.
114. F. Hannemann, A. Bichet, K.M. Ewen, and R. Bernhardt. Cytochrome P450 systems-biological variations of electron transport chains. *Biochim Biophys Acta*, 2007. **1770**(3): 330.
115. E. O'Reilly, V. Kohler, S.L. Flitsch, and N.J. Turner. Cytochromes P450 as useful biocatalysts: addressing the limitations. *Chem Commun*, 2011. **47**(9): 2490.
116. G.A. Roberts, G. Grogan, A. Greter, S.L. Flitsch, and N.J. Turner. Identification of a new class of cytochrome P450 from a *Rhodococcus* sp. *J Bacteriol*, 2002. **184**(14): 3898.
117. R. Bernhardt. Cytochromes P450 as versatile biocatalysts. *J Biotechnol*, 2006. **124**(1): 128.
118. G. Grogan. Cytochromes P450: exploiting diversity and enabling application as biocatalysts. *Curr Opin Chem Biol*, 2011. **15**(2): 241.
119. V.B. Urlacher and M. Girhard. Cytochrome P450 monooxygenases: an update on perspectives for synthetic application. *Trends Biotechnol*, 2012. **30**(1): 26.
120. J.A. Hogg. Steroids, the steroid community, and Upjohn in perspective: a profile of innovation. *Steroids*, 1992. **57**(12): 593.
121. D.H. Peterson and H.C. Murray. Microbiological oxygenation of steroids at carbon 11. *J Am Chem Soc*, 1952. **74**(7): 1871–1872.
122. K. Petzoldt, K. Annen, H. Laurent, and R. Wiechert. Process for the preparation of 11-beta-hydroxy steroids. Schering Aktiengesellschaft (Berlin, Germany), 1982. U.S. Patent 4,353,985.
123. J.B. van Beilen, W.A. Duetz, A. Schmid, and B. Witholt. Practical issues in the application of oxygenases. *Trends Biotechnol*, 2003. **21**(4): 170.
124. C. Dingler, L. W., G. Krei, B. Cooper, and B. Hauer. Preparation of (R)-2-(4-hydroxyphenoxypropionic acid by biotransformation. *Pestic Sci*, 1996. **46**: 33.
125. W. Ladner, H.R. Staudenmaier, B. Hauer, U. Müller, U. Pressler, J. Meyer, and H. Siegel. Process for the hydroxylation of aromatic acids using strains of the fungus *Beauveria*. BASF Aktiengesellschaft (Ludwigshafen, Germany), 1999. U.S. Patent 5,928,912.
126. V.B. Urlacher and S. Eiben. Cytochrome P450 monooxygenases: perspectives for synthetic application. *Trends Biotechnol*, 2006. **24**(7): 324.

127. F. Pinot. Cytochrome P450 metabolizing fatty acids in living organisms. *FEBS J*, 2011. **278**(2): 181.
128. D.R. Nelson. The cytochrome P450 homepage. *Hum Genomics*, 2009. **4**(1): 59.
129. S. Mauesberger, M. Ohkuma, W.-H. Schunck, and M. Tagaki. *Candida maltosa*, in *Non-Conventional Yeasts in Biotechnology*, K. Wolf, Editor. 1996, Springer: Berlin Heidelberg New York. p. 411.
130. I.N. Van Bogaert, S. Groeneboer, K. Saerens, and W. Soetaert. The role of cytochrome P450 monooxygenases in microbial fatty acid metabolism. *FEBS J*, 2011. **278**(2): 206.
131. M. Ohkuma, S. Muraoka, T. Tanimoto, M. Fujii, A. Ohta, and M. Takagi. CYP52 (cytochrome P450alk) multigene family in *Candida maltosa*: identification and characterization of eight members. *DNA Cell Biol*, 1995. **14**(2): 163.
132. M. Ohkuma, T. Tanimoto, K. Yano, and M. Takagi. CYP52 (cytochrome P450alk) multigene family in *Candida maltosa*: molecular cloning and nucleotide sequence of the two tandemly arranged genes. *DNA Cell Biol*, 1991. **10**(4): 271.
133. K. Hanley, L.V. Nguyen, F. Khan, G.P. Pogue, F. Vojdani, S. Panda, F. Pinot, V.B. Oriedo, L. Rasochova, M. Subramanian, B. Miller, and E.L. White. Development of a plant viral-vector-based gene expression assay for the screening of yeast cytochrome P450 monooxygenases. *Assay Drug Dev Techn*, 2003. **1**(1): 147.
134. T. Iida, A. Ohta, and M. Takagi. Cloning and characterization of an n-alkane-inducible cytochrome P450 gene essential for n-decane assimilation by *Yarrowia lipolytica*. *Yeast*, 1998. **14**(15): 1387.
135. T. Iida, T. Sumita, A. Ohta, and M. Takagi. The cytochrome P450ALK multigene family of an n-alkane-assimilating yeast, *Yarrowia lipolytica*: cloning and characterization of genes coding for new CYP52 family members. *Yeast*, 2000. **16**(12): 1077.
136. M.S. Smit, M.M. Mokgoro, E. Setati, and J.M. Nicaud. alpha,omega-Dicarboxylic acid accumulation by acyl-CoA oxidase deficient mutants of *Yarrowia lipolytica*. *Biotechnol Lett*, 2005. **27**(12): 859.
137. H. Takai, R. Iwama, S. Kobayashi, H. Horiuchi, R. Fukuda, and A. Ohta. Construction and characterization of a *Yarrowia lipolytica* mutant lacking genes encoding cytochromes P450 subfamily 52. *Fungal Genetics and Biology*, 2012. **49**(1): 58.
138. J.B. van Beilen and E.G. Funhoff. Expanding the alkane oxygenase toolbox: new enzymes and applications. *Curr Opin Biotechnol*, 2005. **16**(3): 308.
139. J.B. van Beilen, Z. Li, W.A. Duetz, T.H.M. Smits, and B. Witholt. Diversity of alkane hydroxylase systems in the environment. *Oil Gas Sci Technol - Revue d'IFP*, 2003. **58**(4): 427.

140. T.H. Smits, M. Rothlisberger, B. Witholt, and J.B. van Beilen. Molecular screening for alkane hydroxylase genes in Gram-negative and Gram-positive strains. *Environ Microbiol*, 1999. **1**(4): 307.
141. T. Plaggemeier, Elimination der Schwer Wasserlöslichen Modellabluftinhaltsstoffe n-Hexan und Toluol in Biorieselbettverfahren. 2000, Universitaet Stuttgart.
142. R.K. Gudimanchi, C. Randall, D.J. Opperman, O.A. Olaofe, S.T. Harrison, J. Albertyn, and M.S. Smit. Whole-cell hydroxylation of n-octane by *Escherichia coli* strains expressing the CYP153A6 operon. *Appl Microbiol Biotechnol*, 2012.
143. T. Otomatsu, L.M. Bai, N. Fujita, K. Shindo, K. Shimizu, and N. Misawa. Bioconversion of aromatic compounds by *Escherichia coli* that expresses cytochrome P450 CYP153A13a gene isolated from an alkane-assimilating marine bacterium *Alcanivorax borkumensis*. *J Mol Catal B-Enzymatic*, 2010. **66**(1-2): 234.
144. S.Q. Pham, G. Pompidor, J. Liu, X.D. Li, and Z. Li. Evolving P450_{pyr} hydroxylase for highly enantioselective hydroxylation at non-activated carbon atom. *Chem Commun* 2012. **48**(38): 4618.
145. D. Chang, H.J. Feiten, K.H. Engesser, J.B. van Beilen, B. Witholt, and Z. Li. Practical syntheses of N-substituted 3-hydroxyazetidines and 4-hydroxypiperidines by hydroxylation with *Sphingomonas* sp. HXN-200. *Org Lett*, 2002. **4**(11): 1859.
146. Y.T. Lee, R.F. Wilson, I. Rupniewski, and D.B. Goodin. P450_{cam} visits an open conformation in the absence of substrate. *Biochemistry*, 2010. **49**(16): 3412.
147. K. Faber. Biotransformations in organic chemistry. 2004, Berlin, Germany: Springer.
148. D.J. Leak, R.A. Sheldon, J.M. Woodley, and P. Adlercreutz. Biocatalysts for selective introduction of oxygen. *Biocatalysis and Biotransformation*, 2009. **27**(1): 1.
149. A. Schmid, J.S. Dordick, B. Hauer, A. Kiener, M. Wubbolts, and B. Witholt. Industrial biocatalysis today and tomorrow. *Nature*, 2001. **409**(6817): 258.
150. D. Meyer, B. Buhler, and A. Schmid. Process and catalyst design objectives for specific redox biocatalysis. *Adv Appl Microbiol*, 2006. **59**: 53.
151. J.A.M. de Bont. Solvent-tolerant bacteria in biocatalysis. *Trends in Biotechnology*, 1998. **16**(12): 493.
152. S. Isken and J.A.M. de Bont. Bacteria tolerant to organic solvents. *Extremophiles*, 1998. **2**(3): 229.
153. I. Pobleto-Castro, J. Becker, K. Dohnt, V.M. dos Santos, and C. Wittmann. Industrial biotechnology of *Pseudomonas putida* and related species. *Appl Microbiol Biotechnol*, 2012. **93**(6): 2279.
154. B. Rosche, X.Z. Li, B. Hauer, A. Schmid, and K. Buehler. Microbial biofilms: a concept for industrial catalysis? *Trends Biotechnol*, 2009. **27**(11): 636.

155. T. del Castillo, J.L. Ramos, J.J. Rodriguez-Herva, T. Fuhrer, U. Sauer, and E. Duque. Convergent peripheral pathways catalyze initial glucose catabolism in *Pseudomonas putida*: genomic and flux analysis. *J Bacteriol*, 2007. **189**(14): 5142.
156. J. Ruhl, A. Schmid, and L.M. Blank. Selected *Pseudomonas putida* strains able to grow in the presence of high butanol concentrations. *Appl Environ Microbiol*, 2009. **75**(13): 4653.
157. L.M. Blank, G. Ionidis, B.E. Ebert, B. Bühler, and A. Schmid. Metabolic response of *Pseudomonas putida* during redox biocatalysis in the presence of a second octanol phase. *FEBS J*, 2008. **275**(20): 5173.
158. B.E. Ebert, F. Kurth, M. Grund, L.M. Blank, and A. Schmid. Response of *Pseudomonas putida* KT2440 to increased NADH and ATP demand. *Appl Environ Microbiol*, 2011. **77**(18): 6597.
159. S. Isken, A. Derks, P.F.G. Wolffs, and J.A.M. de Bont. Effect of organic solvents on the yield of solvent-tolerant *Pseudomonas putida* S12. *Appl Environ Microbiol*, 1999. **65**(6): 2631.
160. D. Kuhn, B. Buhler, and A. Schmid. Production host selection for asymmetric styrene epoxidation: *Escherichia coli* vs. solvent-tolerant *Pseudomonas*. *J Ind Microbiol Biotechnol*, 2012. **39**(8): 1125.
161. A. Schmid, A. Kollmer, R.G. Mathys, and B. Witholt. Developments toward large-scale bacterial bioprocesses in the presence of bulk amounts of organic solvents. *Extremophiles*, 1998. **2**(3): 249.
162. D.D. Axe and J.E. Bailey. Transport of lactate and acetate through the energized cytoplasmic membrane of *Escherichia coli*. *Biotechnol Bioeng*, 1995. **47**(1): 8.
163. L.M. Blank, B.E. Ebert, K. Buehler, and B. Buhler. Redox biocatalysis and metabolism: molecular mechanisms and metabolic network analysis. *Antioxidants & Redox Signaling*, 2010. **13**(3): 349.
164. R. Gross, K. Lang, K. Buhler, and A. Schmid. Characterization of a biofilm membrane reactor and its prospects for fine chemical synthesis. *Biotechnol Bioeng*. **105**(4): 705.
165. B. Halan, A. Schmid, and K. Buehler. Real-time solvent tolerance analysis of *Pseudomonas* sp. strain VLB120{Delta}C catalytic biofilms. *Appl Environ Microbiol*. **77**(5): 1563.
166. B. Halan, A. Schmid, and K. Buehler. Maximizing the productivity of catalytic biofilms on solid supports in membrane aerated reactors. *Biotechnol Bioeng*. **106**(4): 516.
167. M.K. Julsing, D. Kuhn, A. Schmid, and B. Buhler. Resting cells of recombinant *E. coli* show high epoxidation yields on energy source and high sensitivity to product inhibition. *Biotechnol Bioeng*. **109**(5): 1109.
168. A.M. McIver, S.V. Garikipati, K.S. Bankole, M. Gyamerah, and T.L. Peebles. Microbial oxidation of naphthalene to cis-1,2-naphthalene dihydrodiol using naphthalene dioxygenase in biphasic media. *Biotechnol Prog*, 2008. **24**(3): 593.

169. A.Z. Walton and J.D. Stewart. An efficient enzymatic Baeyer-Villiger oxidation by engineered *Escherichia coli* cells under non-growing conditions. *Biotechnol Prog*, 2002. **18**(2): 262.
170. A.Z. Walton and J.D. Stewart. Understanding and improving NADPH-dependent reactions by nongrowing *Escherichia coli* cells. *Biotechnol Prog*, 2004. **20**(2): 403.
171. D. Kuhn, M.A. Kholiq, E. Heinzle, B. Buhler, and A. Schmid. Intensification and economic and ecological assessment of a biocatalytic oxyfunctionalization process. *Green Chemistry*, 2010. **12**(5): 815.
172. H.J. Heipieper, G. Neumann, S. Cornelissen, and F. Meinhardt. Solvent-tolerant bacteria for biotransformations in two-phase fermentation systems. *Appl Microbiol Biotechnol*, 2007. **74**(5): 961.
173. D. Scheps, S. Honda Malca, H. Hoffmann, B.M. Nestl, and B. Hauer. Regioselective omega-hydroxylation of medium-chain *n*-alkanes and primary alcohols by CYP153 enzymes from *Mycobacterium marinum* and *Polaromonas* sp. strain JS666. *Org Biomol Chem*, 2011. **9**(19): 6727.
174. S. Honda Malca, D. Scheps, L. Kuhnel, E. Venegas-Venegas, A. Seifert, B.M. Nestl, and B. Hauer. Bacterial CYP153A monooxygenases for the synthesis of omega-hydroxylated fatty acids. *Chem Commun*, 2012. **48**(42): 5115.
175. T. Omura and R. Sato. The carbon monoxide-binding pigment of liver microsomes I. Evidence for its hemoprotein nature. *J Biol Chem*, 1964. **239**: 2370.
176. T. Omura and R. Sato. The carbon monoxide-binding pigment of liver microsomes II. Solubilization, purification and properties. *J Biol Chem*, 1964. **239**: 2379.
177. M. Jeske and J. Altenbuchner. The *Escherichia coli* rhamnose promoter rhaP(BAD) is in *Pseudomonas putida* KT2440 independent of Crp-cAMP activation. *Appl Microbiol Biotechnol*, 2010. **85**(6): 1923.
178. T. Stumpp, B. Wilms, and J. Altenbuchner. Ein neues L-Rhamnose-induzierbares Expressionsystem für *Escherichia coli*. *Biospektrum*, 2000. **6**: 33.
179. T.H. Smits, M.A. Seeger, B. Witholt, and J.B. van Beilen. New alkane-responsive expression vectors for *Escherichia coli* and *Pseudomonas*. *Plasmid*, 2001. **46**(1): 16.
180. J. Brass, C. Kiziak, J. Klein, and R. Ostendorp. Rhamnose Promoter Expression System. 2008. US Patent 2008/0206817 A1.
181. S. Vomund, Ganzzellbiotransformation von *n*-Octan zu 2-Octanol mit rekombinanten *Pseudomonas putida* in 2-Phasen-System. 2010, Institut für Technische Biochemie, Universitaet Stuttgart: Germany.
182. K. Iwasaki, H. Uchiyama, O. Yagi, T. Kurabayashi, K. Ishizuka, and Y. Takamura. Transformation of *Pseudomonas putida* by electroporation. *Biosci Biotechnol Biochem*, 1994. **58**(5): 851.

183. B. van Gelder and E.C. Slater. The extinction coefficient of cytochrome *c*. *Biochim Biophys Acta*, 1962. **58**: 593.
184. L. Yuste, I. Canosa, and F. Rojo. Carbon-source-dependent expression of the PalkB promoter from the *Pseudomonas oleovorans* alkane degradation pathway. *J Bacteriol*, 1998. **180**(19): 5218.
185. C.H. Posten and C.L. Cooney. Growth of Microorganisms, in *Biotechnology: Biological Fundamentals*, H.J. Rehm, Editor. 2008, Wiley-VCH
186. F. Xu, S.G. Bell, Z. Rao, and L.L. Wong. Structure-activity correlations in pentachlorobenzene oxidation by engineered cytochrome P450cam. *Protein Eng Des Sel*, 2007. **20**(10): 473.
187. J.A. Peterson, M.C. Lorence, and B. Amarneh. Putidaredoxin reductase and putidaredoxin. Cloning, sequence determination, and heterologous expression of the proteins. *J Biol Chem*, 1990. **265**(11): 6066.
188. P.W. Roome and J.A. Peterson. The oxidation of reduced putidaredoxin reductase by oxidized putidaredoxin. *Arch Biochem Biophys*, 1988. **266**(1): 41.
189. P.W. Roome, Jr., J.C. Philley, and J.A. Peterson. Purification and properties of putidaredoxin reductase. *J Biol Chem*, 1983. **258**(4): 2593.
190. E.G. Funhoff, J. Salzmann, U. Bauer, B. Witholt, and J.B. van Beilen. Hydroxylation and epoxidation reactions catalyzed by CYP153 enzymes. *Enzyme and Microbial Technology*, 2007. **40**(4): 806.
191. U. Hoch, Z. Zhang, D.L. Kroetz, and P.R. Ortiz de Montellano. Structural determination of the substrate specificities and regioselectivities of the rat and human fatty acid omega-hydroxylases. *Arch Biochem Biophys*, 2000. **373**(1): 63.
192. J.B. Johnston, H. Ouellet, L.M. Podust, and P.R. Ortiz de Montellano. Structural control of cytochrome P450-catalyzed omega-hydroxylation. *Arch Biochem Biophys*. **507**(1): 86.
193. E.G. Funhoff, U. Bauer, I. Garcia-Rubio, B. Witholt, and J.B. van Beilen. CYP153A6, a soluble P450 oxygenase catalyzing terminal-alkane hydroxylation. *J Bacteriol*, 2006. **188**(14): 5220.
194. I. Matsunaga, A. Ueda, T. Sumimoto, K. Ichihara, M. Ayata, and H. Ogura. Site-directed mutagenesis of the putative distal helix of peroxygenase cytochrome P450. *Archives of Biochemistry and Biophysics*, 2001. **394**(1): 45.
195. A. Seifert, S. Vomund, K. Grohmann, S. Kriening, V.B. Urlacher, S. Laschat, and J. Pleiss. Rational design of a minimal and highly enriched CYP102A1 mutant library with improved regio-, stereo- and chemoselectivity. *Chembiochem*, 2009. **10**(5): 853.
196. J. Mestres. Structure conservation in cytochromes P450. *Proteins-Structure Function and Bioinformatics*, 2005. **58**(3): 596.

197. E. Weber, A. Seifert, M. Antonovici, C. Geinitz, J. Pleiss, and V.B. Urlacher. Screening of a minimal enriched P450 BM3 mutant library for hydroxylation of cyclic and acyclic alkanes. *Chem Commun*, **47**(3): 944.
198. T.L. Poulos. Cytochrome P450 flexibility. *Proc Natl Acad Sci U S A*, 2003. **100**(23): 13121.
199. J.B. van Beilen, R. Holtackers, D. Luscher, U. Bauer, B. Witholt, and W.A. Duetz. Biocatalytic production of perillyl alcohol from limonene by using a novel *Mycobacterium* sp. cytochrome P450 alkane hydroxylase expressed in *Pseudomonas putida*. *Appl Environ Microbiol*, 2005. **71**(4): 1737.
200. C. Grant, J.M. Woodley, and F. Baganz. Whole-cell bio-oxidation of *n*-dodecane using the alkane hydroxylase system of *P. putida* GPo1 expressed in *E. coli*. *Enzyme Microb Technol*, 2011. **48**(6-7): 480.
201. J. Sikkema, J.A.M. DeBont, and B. Poolman. Mechanisms of membrane toxicity of hydrocarbons. *Microbiol Rev*, 1995. **59**(2): 201.
202. F.J. Weber and J.A.M. deBont. Adaptation mechanisms of microorganisms to the toxic effects of organic solvents on membranes. *Biochim Biophys Acta* 1996. **1286**(3): 225.
203. O. Favre-Bulle, T. Schouten, J. Kingma, and B. Witholt. Bioconversion of *n*-octane to octanoic acid by a recombinant *Escherichia coli* cultured in a two-liquid phase bioreactor. *Bio/technology*, 1991. **9**(4): 367.
204. B. Witholt. Synthesis of apolar organic compounds by *Pseudomonas* spp. and *Escherichia coli* in two-liquid-phase fermentations, in *Pseudomonas: molecular biology and biotechnology*, E. Galli, S. Silver, and B. Witholt, Editors. 1992, ASM Press: Washington, DC. p. 301–313.
205. E. Cabiscol, J. Tamarit, and J. Ros. Oxidative stress in bacteria and protein damage by reactive oxygen species. *Int Microbiol*, 2000. **3**(1): 3.
206. B. Demple and J. Halbrook. Inducible repair of oxidative DNA damage in *Escherichia coli*. *Nature*, 1983. **304**(5925): 466.
207. M. Chavarría, P.I. Nikel, D. Pérez-Pantoja, and V. de Lorenzo. The Entner-Doudoroff pathway empowers *Pseudomonas putida* KT2440 with a high tolerance to oxidative stress. *Environ Microbiol*, 2012: DOI: 10.1111/1462.
208. L.Z. Karpetz, N.V. Adrianov, Karuzina, II, S. Dzhuzenova Ch, and A.I. Archakov. Effects of hydrogen peroxide on cytochrome P-450 inactivation. *Biull Eksp Biol Med*, 1988. **105**(5): 547.
209. M. Girhard, S. Schuster, M. Dietrich, P. Durre, and V.B. Urlacher. Cytochrome P450 monooxygenase from *Clostridium acetobutylicum*: a new alpha-fatty acid hydroxylase. *Biochem Biophys Res Commun*, 2007. **362**(1): 114.

210. D. Kuhn, B. Buhler, and A. Schmid. Production host selection for asymmetric styrene epoxidation: *Escherichia coli* vs. solvent-tolerant *Pseudomonas*. *J Ind Microbiol Biotechnol*, 2012. **39**(8): 1125.
211. Y.J. Son, J.N. Phue, L.B. Trinh, S.J. Lee, and J. Shiloach. The role of Cra in regulating acetate excretion and osmotic tolerance in *E. coli* K-12 and *E. coli* B at high density growth. *Microb Cell Fact*, 2011. **10**: 52.
212. Z. Su, J.H. Horner, and M. Newcomb. Rates of fatty acid oxidations by P450 compound I are pH dependent. *Chembiochem*, 2012. **13**(14): 2061.
213. J. Klebensberger, O. Rui, E. Fritz, B. Schink, and B. Philipp. Cell aggregation of *Pseudomonas aeruginosa* strain PAO1 as an energy-dependent stress response during growth with sodium dodecyl sulfate. *Arch Microbiol*, 2006. **185**(6): 417.
214. M. Marounek, E. Skrivanova, and V. Rada. Susceptibility of *Escherichia coli* to C2-C18 fatty acids. *Folia Microbiol (Praha)*, 2003. **48**(6): 731.
215. D. Sirim, F. Wagner, A. Lisitsa, and J. Pleiss. The cytochrome P450 engineering database: Integration of biochemical properties. *BMC Biochem*, 2009. **10**: 27.
216. T.E. Mattes, A.K. Alexander, P.M. Richardson, A.C. Munk, C.S. Han, P. Stothard, and N.V. Coleman. The genome of *Polaromonas* sp. strain JS666: insights into the evolution of a hydrocarbon- and xenobiotic-degrading bacterium, and features of relevance to biotechnology. *Appl Environ Microbiol*, 2008. **74**(20): 6405.
217. N.B. Huu, E.B. Denner, D.T. Ha, G. Wanner, and H. Stan-Lotter. *Marinobacter aquaeolei* sp. nov., a halophilic bacterium isolated from a Vietnamese oil-producing well. *Int J Syst Bacteriol*, 1999. **49 Pt 2**: 367.
218. M. Soltani, P. Metzger, and C. Largeau. Fatty acid and hydroxy acid adaptation in three gram-negative hydrocarbon-degrading bacteria in relation to carbon source. *Lipids*, 2005. **40**(12): 1263.
219. R.M. Willis, B.D. Wahlen, L.C. Seefeldt, and B.M. Barney. Characterization of a fatty acyl-CoA reductase from *Marinobacter aquaeolei* VT8: a bacterial enzyme catalyzing the reduction of fatty acyl-CoA to fatty alcohol. *Biochemistry*, 2011. **50**(48): 10550.
220. S. Picataggio, T. Rohrer, K. Deanda, D. Lanning, R. Reynolds, J. Mielenz, and L.D. Eirich. Metabolic engineering of *Candida tropicalis* for the production of long-chain dicarboxylic acids. *Biotechnology*, 1992. **10**(8): 894.
221. C. Grant, A.C. Pinto, H.P. Lui, J.M. Woodley, and F. Baganz. Tools for characterizing the whole-cell biooxidation of alkanes at microscale. *Biotechnol Bioeng*, 2012. **109**(9): 2179.
222. M.K. Julsing, M. Schrewe, S. Cornelissen, I. Hermann, A. Schmid, and B. Buhler. Outer membrane protein AlkL boosts biocatalytic oxyfunctionalization of hydrophobic substrates in *Escherichia coli*. *Appl Environ Microbiol*, 2012. **78**(16): 5724.

223. H. Nikaido. Molecular basis of bacterial outer membrane permeability revisited. *Microbiol Mol Biol Rev*, 2003. **67**(4): 593.
224. R. Fasan, N.C. Crook, M.W. Peters, P. Meinhold, T. Buelter, M. Landwehr, P.C. Cirino, and F.H. Arnold. Improved product-per-glucose yields in P450-dependent propane biotransformations using engineered *Escherichia coli*. *Biotechnol Bioeng*, 2011. **108**(3): 500.
225. A. Robin, V. Kohler, A. Jones, A. Ali, P.P. Kelly, E. O'Reilly, N.J. Turner, and S.L. Flitsch. Chimeric self-sufficient P450cam-RhFRed biocatalysts with broad substrate scope. *Beilstein J Org Chem*, 2011. **7**: 1494.
226. A. Robin, G.A. Roberts, J. Kisch, F. Sabbadin, G. Grogan, N. Bruce, N.J. Turner, and S.L. Flitsch. Engineering and improvement of the efficiency of a chimeric [P450cam-RhFRed reductase domain] enzyme. *Chem Commun*, 2009(18): 2478.
227. D. Degregorio, S.J. Sadeghi, G. Di Nardo, G. Gilardi, and S.P. Solinas. Understanding uncoupling in the multiredox centre P450 3A4-BMR model system. *J Biol Inorg Chem*, 2011. **16**(1): 109.
228. M. De Mey, S. De Maeseneire, W. Soetaert, and E. Vandamme. Minimizing acetate formation in *E. coli* fermentations. *J Ind Microbiol Biotechnol*, 2007. **34**(11): 689.

6 Supplementary material

6.1 Genes, vectors and strains

6.1.1 Genes

MmAlk gene cluster (MmFdx→CYP153A16→MmFdr)

Gene IDs: MMAR_3155→MMAR_3154→MMAR_3153

```

ATGGCAGTTGTCACATTTGTCTCCCACGGCGGCGAGAAGTATGAGGCGCCTCTCGAGGAAGGTCAGTCACTGATGCGGG
TCGCGACCAACAATGCGGTGCCCGGCATCGACGGCGACTGCGGAGGCGAAGCCGCGTGCGGCACCTGCCATGTGATCGT
CGATCCGCAATGGTCCGATCGGGTCGGCTCTCCGGGGCCAATGAAGAGGAGATGCTCGCGATGAACCCCGAGCGTCAG
CCGACCTCCC GGCTGTCTGCCAGATGCAGGTCTCTGAGGCGTGGGACGGTTTGATCGTCCATCTGCCCGAGTTCCAAC
TGTGATGACGAAAAGAGAGGTGAGACGTGAGCAATATTCGCGAGGCAGTCACTGCCAAGGCTCAGGCAACAATTCCGATG
GACCGAATAATCCAGGGCGCCACCTCTACGACAGAACCGGGCGCTGGGTCAACGGCACCAACGGTGAAAAAATCTTCA
TCGAGCGACCGATCCCGCGGCTGACGAGGTGAACTGACCGACATCGACCTTAGCAATCCTTTCTCTATCGTCAGGG
TCGCTGGAAGTCTATTACGAGCGCCTACGCAACGAGGCTCCCGTGCACTATCAGGCCACAGCGCGTTCGGCCCGTTC
TGGTCGGTGACGCGGCATGCCGACATCGTGGCCGTCGACAAGAACCACGAGGTCTTCTCCTCCGAGCCGTTTCATCGTCA
TCGGGAGCCCGCGCTTCTCGACATTGCGATGTTTCATCGCGATGGACCCCCAAAACACGACCGGCAACGGCAGGC
TGTCAGGGTGTGGTTCGACACGAAGAACCCTGCGTGAGATGGAGGGCCTCATCCGCGAGCGGGTGGTAGACGTGCTCGAC
GCTCTGCCGCTTGGCGAACCGTTCAACTGGGTGCAGCACGTCTCGATCGAGCTAACCGCGCGCATGCTGGCCACGCTGC
TGGACTTCCCGTTCGAGCAGCGGCGCAAGCTCGTCCAATGGTCCGATCTCGCCACCTCCATGGAGCAAGCCAACGGTGG
GCCCTCGGACAACGACGAGATATTTGCGGGCATGGTTCGATATGGCTAGAGGTCTCAGCGCTCACTGGCGGGACAAGGCA
GCCCGGACAGCTGCCGAGAGCTGCCCGGCTTCGATCTGATCACCATGTTGCAGAGCGACGAGAGCACCAAGGACCTGA
TCGATCGCCGATGGAGTCTTGGGCAACTTGGTATTGCTGATCGTGGGTGGCAACGATACGACCCGCAATTCATGAG
CGGTGGTGTTCGGCGCTGAACGAGTTCCTGACCAGTTTGAAGAAGCTGAAGGCGAACCCCGAGCTGATCCCCAACATG
GTCTCGGAGATCATCCGGTGGCAAACCCCGCTCGCGCATATGCGCCGGATCGCCAAGGCCGACACTGTGCTCAACGGGC
AGTTCATCCGCAAGGGCGACAAGTCTGATGTGGTACGCCTCGGGCAACCGCGACGAGCGGTGTTTCGATCGGCCCG
ATGACCTGATTATCGATCGGGCCAACGCCGTAACCACATCTCCTTCGGTTTCGGCGTGACCCGCTGTATGGGTAACCG
GCTGGCCGAGATGCAGTTGCGGATCCTGTGGGAGGAGCTGCTTCCGCGGTTTCGAGAACATCGAGGTGCTCGGTGAGCCC
GAGTACGTGCAGTCCAACCTCGTGAGGGGGATCAGTAAGCTGATGGTCCGCTCACCCGAAAGGTGGCGCATGACCGT
GCAGCGAGCGGTTCATCGCGGGGGCCAGCCACGCGGGCACCCAGCTCGCCGCCAGTCTTCGCGGAGAAGGGTGGGACGGC
GAAATCGTCTCGTCGGCGATGAGTCGGCGTTGCCCTACCAGCGGCCCCCGCTGTCCAAGTCGTACCTGGCCGACAAAT
GCGAATGGCCGAACTCGCGATCCGCAACTCGGATTTCTACGCCAAGCAGCGGATCCGACTCCTGGATGCGACGGTGGC
GGCGGTGACCCGCTCGGCTGGTTCATGTCGTGCTGAGTACCGGGCGACGCACTGCCCTACGACAAGCTCGCGCTGTGCACT
GGCGCCCGGCTCGTTCGGCTCCCCACCCGGGAGCGGACCTGGCCGGAGTCTTCTACCTACGCACCCGCGCGGACGGCG
AGATGATCCGAGAGGCCCGCCGGCCCGGGCGTCGGCGGTGATCGTTCGGCGGCGGTACATCGGACTGGAGACAGCCGC
CTCGTTGCGTGCACCTGGGTCTGGAGGTCAACCTGCTCGAGGCGACCGGGCGCGTCTTGAACGGGTACCCGCCCGGAG
GTATCGGAGTCTTCGACCCGATCCACCGGGAGGAGGGCGTCAACATCCGGACGGGCACGCTGGTTCGAGGCTCTGTCCG
GCGACGGCAGGGTCCGCGAAGTAATCCTGGCCGTGGCGAATCAATTCGCCCGACCTCGTCAATTGTCGGCATCGGCGT
GGAGCCGAACACCGAGCTCGCCGCCACCGGGGCTGGTTCGTCGACAACGGCGTTCGTGATCGACGATCAGGCCCGGACT
AGCGACCCCGACATCGTGGCCGCCGGGACTGCGCCAGCCACGACATGGCCCGTTACGGCCGTCGCATCCGCTGGAGT
CCGTGCCGAGCGCGGCCGAGCAGGCCAAGGTCGCCGCCGCGACCGTCTGTGGGAAGTCCAAGAAGATAGCGGCCCTTCC
ATGGTTCGGTTCAGATCAATACGACCTCAAGTCCAGATCGCCGGTCTCAACACCGGGTACGACGAGGTCTGCTCCTCAGC
GGCGACCCGACCCGGGAGCGCGACTTACCTGCTTCTACCTCCGTGCCGGGAGCTTCTTGCCGCCGACTGCATCAACC
GTCCCGCGACTTCATGTTTCAGCAAGCGGGTTCATCACGCGCAAGTCCCGTTCGAACGGGCCGAACTGGTGTCTCGCCGG
CTCGGACTGA

```

MaqAlk gene cluster (MaqFdx→CYP153A *M. aq.*→MaqFdR)

Gene IDs: Maqu_0599→Maqu_0600→Maqu_0601

ATGGGCGGTACAGATGGGCCGGAATATGCACATGTCGCAGAATTCAAAGCTGGTTCCTCGGTAATGCAAATCGCTGTTG
 ATAGCGCCATTCCTGGTATCGACGGGGATTGTGGGGGGAGTGCGCCTGCGGTACCTGCCACGTTATCGTCACGAACGA
 ATGGTTCAGCAAGACAGGCACGCCTGGCAATGAGGAAGAACAATGCTGTCAATGACACCGGAGCGGGCGAGCACTTCG
 CGCTGGGCTGCCAGGTGGTACTGACTGATGAAATGGACGGCATGACCGTGCATTTACCCGAGTTCAGATGTGAACAC
 AGGAGGACGCATGCCAACACTGCCAGAACATTTGACGACATTCAGTCCCGACTGATTAACGCCACCTCCAGGGTGGTG
 CCGATGCAGAGGCAAATTCAGGGACTGAAATCTTAATGAGCGCCAAGAGGAAGACCTTCGGCCCACGCCGACCGATGC
 CCGAATTCGTTGAAAACCCATCCCGGACGTTAACACGCTGGCCCTTGAGGACATCGATGTCAGCAATCCGTTTTTATA
 CCGGCAGGGTCAGTGGCGCGCCTATTTCAAACGGTTGCGTGTAGAGCGCCGGTCCATTACCAGAAGAACAGCCCTTTC
 GGCCCTTCTGGTGGTAACTCGGTTTGAAGACATCTGTTTCGTGGATAAGAGTCACGACCTGTTTTCCGCCGAGCCGC
 AAATCATCTCGGTGACCTCCGGAGGGGCTGTCGGTGGAAATGTTTCATAGCGATGGATCCGCCGAAAACACGATGTGCA
 GCGCAGCTCGGTGCAGGGAGTAGTGGCACCGAAAAACCTGAAGGAGATGGAGGGGCTGATCCGATCACGCACCGCGGAT
 GTGCTTGACAGCTGCCTACAGACAAACCCTTTAACTGGGTACCTGCTGTTTCCAAGGAACACAGGCCGCATGCTGG
 CGACGCTTCTGGATTTTCTTACGAGGAACGCCACAAGCTGGTTGAGTGGTCCGACAGAATGGCAGGTGCAGCATCGGC
 CACCGCGGGGAGTTTGCCGATGAAAATGCCATGTTTACGACGCGCGCAGACATGGCCCGGTCTTTCTCCAGGCTTTGG
 CGGGACAAGGAGCGCGCCGCGCAGCAGGCGAGGAGCCCGGTTTCGATTTGATCAGCCTGTTGCAGAGCAACAAAGAAA
 CGAAAGACCTGATCAATCGGCCGATGGAGTTTATCGGTAATTTGACGCTGCTCATAGTCGGCGGCAACGATACGACGCG
 CAACTCGATGAGTGGTGGCCTGGTGGCCATGAACGAATTTCCCGAGGAAATTTGAAAAATGAAGGCAAAACCGGAGTTG
 ATTCGAACATGGTGTGGAAATCATCCGCTGGCAAACGCCGCTGGCCTATATGCGCCGAATCGCCAAGCAGGATGTGCG
 AACTGGGCGGCCAGACCATCAAGAAGGGTGATCGAGTTGTGATGTGGTACGCGTCGGGTAACCGGGACGAGCGCAAAT
 TGACAACCCCGATCAGTTCATATTGATCGCAAGGACGCACGAAACCACATGTCGTTCCGGCTATGGGGTTACCGTTGC
 ATGGGCAACCGTCTGGCTGAACTGCAACTGCGCATCTCTGGGAAGAAATACTCAAGCGTTTTGACAACATCGAAGTCG
 TCGAAGAGCCCAGCGGGTGCAGTCCAACCTTCGTGCGGGGCTATTCCAGGTTGATGGTCAAACCTGACACCGAACAGTTA
 ATTAACCGATTGACCAGGATGGCATCCGAACGTGTGGAGAGTCCAATCCCAGGGCACAGCGAAAAGAGATAGCCTATGGT
 AAGCAAACGTAAAGAGAGGACGGTCATTGTTGGCGGTGGGCACGCAGCAGGTGCCCTCTGACAGCCTTACTCCAAAA
 AAATATCAACATGAGGTCGTTCTGGTGGGGAATGAACCTCATCCGCCCTACCATCGACCGCCGCTGTCCAAGAATTACC
 TGACAGGAGACGTTGATCAGGAGTGCCTGTACCTGAAAACCGCGCTCGGTATACGAGAACGCAGGCCATCAGTTGCGGCT
 CGGTGTGCGCTCGAACAATTTGATCGGGACAGTAGCACCATCAGCTTGTGCGATCAGAGCAGGCTGCAATACGATCGA
 CTGGTCCGGCCACCGGTACACCTTCGACACCTGAACGCGCCCGGGGCTGACTTAAATGGCATTTCATTACCTGCACG
 ACATAGCTGATTCAGAGGTACTGCGTGAACAGTTAGTTGCTGGAAAGCGCCTGGTCTGCTGGGTGGTGGTTACATCGG
 CCTTGAGGTGGCGCCAGTGCCAACAAAAAGGTGTTAATGTACGGTGTGTAAGCCCGAACGCTTTATGCAGCGC
 GTTACGGGCCCAGAAATATCAGCGTTCCTTTACGACAAACACCGTGGCGCCGGCGTGGACGTACGTTGAAACACAGCGG
 TAACCGGCTTCGAAGCGGGCGATCAGGGGCATGTGGCTGGCGTGACGTTGGCGGACGGAAGCACCGTACCAGCCGACAT
 CGTCTTGTGTCGATCGGCATTATCCCGAAACCGCTCTGGCTAAGGACGCCGCGCTGCCCTGTGATAACGGTATTATT
 GTTGACGAATTTACCGTACCGAGGACCCCGCCATCTTGGCGATCGGTGACTGCACCCGGCACCGGAATCTTTTCTTCG
 AGAAGATGCAACGACTCGAGTCTGTGCCAATGCTGTGATCAGGCTCGTACAGCCGCGGCAACCCTGATGGGTGAGGA
 GAAACCCTATGATAGCGTTCATGGTCTGGTCAAACCAGTACGATGTTGCTGTCAGATGGTAGGATTGTGCAAAAT
 CATGATCAGCGAGTGGTTCGAGGCACCCCGAGGATAAAGGATTTGCCGTGTTCTATCTCCGGAAGGCTGTGTTATTG
 CTGTTGACGCGGTCAACCTGCCCTTGCCTTTTTTGGTAGGCAAGACTCGTTCAACAACGCAGAACGATCAACCCGGA
 ACTAATAGAGGATCCGGATACTGAACTGAAATCTTTGGTGAACGGAAGGCTCCAGAGTTGA

PspAlk gene cluster (CYP153A *P. sp.*→PspFdR→PspFdx)

Gene IDs: Bpro_5301→Bpro_5300→Bpro_5299

ATGAGTGAAGCGATTGTGGTAAACAACCAAAACGACCAAAGCAGGGCATAACGCGATCCCGCTTGAGGACATTGATGTAA
 GCAATCCGGAGCTGTTTTGCGGACAATACGATGTGGGGTTATTTTTGAGCGTCTGCGCCGCGAAGACCCCGTGCATTACTG
 TAAGGACAGCTTGTGGTCCGTACTGGTCCGTGACCAAGTTCAAGGACATCATGCAGGTGGAGACCCATCCGGAGATA
 TTTTCATCCGAGGGCAATATCACCATCATGGAGTCCAATGCGGGGTAACCCGCGCATGTTTCATTGCGATGGATCCGC
 CCAAGCACGACGTGCAGCGCATGGCGGTGAGTCCGATCGTGGCGCCGGAACCTCGCCAAGCTCGAAGGTCTGATCCG
 CGAGCGTACCGGTCGTGCGCTGGATGGCTGCCGATCAACGAGACCTTTGACTGGGTCAAGCTCGTTTCGATCAACCTG
 ACGACGCAGATGCTGGCGACGCTGTTTGATTTCCCTTGGGAAGACCGTGCCAAGCTGACGCGCTGGTCCGATGTCGCGA
 CGGGCTGGTCCGACGGGCATTATTGATTCGGAAGAGCAGCGCATGGAGGAGCTCAAGGGGTGCGTGAATACATGAC
 CCGGCTGTGGAACGAGCGCGTCAATGTGCCACCGGGCAATGATCTGATATCGATGATGGCGCACACCGAGTCCATGCGC
 AACATGACGCCGGAAGAGTTTCTGGGCAACCTCATTTTGTGATCGTCCGGCGCAATGACACGACCCGCAACTCGATGA
 CCGGCGGCTGCTGGCGCTCAACGAAAATCCGGACGAATACCGCAAGCTGTGCGCCAACCCGGCGCTGATCGCCTCCAT
 GGTGCCGGAGATCGTTCGTTGGCAGACACCGCTGGCGCACATGCGGCGTACCGCGCTGCAGGACACCGAGCTCGGCGGC
 AAGTCCATTTCGAAGGGTGACAAGGTATCATGTGGTATGTCTCCGGCAACCGTGATCCCGAAGCGATTGAAAATCCGG
 ACGGTTTCATCATTGATCGCGCAAGCCGCGCCATCACCTCTCGTTCGGTTTCGGCATTCACCGCTGCGTGGGCAACCG
 TCTCGCCGAGTTGCAGCTGCGCATCGTTTGGGAGGAGTTGCTCAAGCGCTGGCCCAATCCAGGTGAGATCGAGGTCGTT
 GCGCGCCCCGAGCGCGTGTGTCGCCCTTTGTGAAGGGCTATGAGTCGCTGCCCGTCCGCATCAACGCTTGAAGCCGCG
 CTGATCGTGAGCGAAACTGTGATTATTGCCGGCGCCGGTCAAGCGCGCCGGCCAGGCGGTTGCGAGCCTGCGGCAAGAGG
 GATTCGACGGGCGCATCGTGTGGTCCGGCCGAGCCGGTGTGCGGTATCAGCGCCCGCCGCTGTGCAAGGCATTTTTT
 GCGGGCACCTTGCCGCTGGAGCGATTGTTCCGAAAGCCCGCGGCATTCTACGAGCAGGCGGTGTGGACACGCTGCT
 CGGGGTGGCCGTCACCGAACTTGATGCCGCCCGCGGCAGGTGAGGCTGGACGATGGCCGCGAAGTGGCGTTTGATCAT
 CTGCTGCTGGCGACTGGCGGGCGTCCCGTCCGGTCTGACTGCCCGGGTGGCGACCATCCGCGCCTGCACTATCTGCGCA
 CCGTGGCTGATGTTGACGGCATTCTGCGCTGCGTCCCGGGCCCGGCTGGTGTGATCGGGCGGGCTACGTCGG
 ACTCGAGATCGCCCGTGGCCGCAAACTGGGGCTCGCGGTGACCGTGTGGAAGCGCGCCGACGGTGTGGCGCGT
 GTCACTTGTCCGGCCGTGGCGCGCTTCTTCGAAAGCGTGCACCGGCAGGCGGGCGTGACGATCCGCTGCGCGACGACGG
 TCTCCGGCATCGAGGGCGATGCTTCGCTGGCGCGGGTCTGACCGGGCGATGGCGAACGCATTGACGCCGACCTGGTCAT
 TGCCGGCATCGGTCTGCTGCCGAACGTCGAGTTGGCGCAGGCCGCGGGTCTGGTCTGCGACAACGGCATCGTCTGAC
 GAGGAATGCCGACCTCTGTGCCCGGCATTTTCGCGGCTGGCGACTGCACGCAGCATCCGAACCGGATCTACGACAGTC
 GGCTGCGTCTCGAATCGGTGCACAACGCCATTGAGCAGGGCAAGACGGCGGGCGGCCATGTGTGGCAAGGCCAGGCC
 GTATCGGCAGGTGCCGTGGTTCTGGTCCGATCAGTACGACCTCAAGTTACAAACCGGGGACTCAACCGCGGCTATGAC
 CAGGTCGTGATCGGGGCGAGTACCGACAACCGTTTCGTTTGGCGGCTTCTACCTGCGCGACGGGCGATTGCTTGCCGTCG
 ATGCGGTCAACCGCCGGTCGAGTTTCATGGTGGCCAAAGCGCTGATTGCGAACCGCACCGTCAATCGCGCCCGAGCGGCT
 CGCCGACGAGCGTATCGCAGCGAAGGACCTGGCCGGCTGATGTGCGTGTGCCGGCCATGGATTTAATTTTATCGAAGT
 ATCAATTCACAAGGGCGCTGCCAAGGCGGCCCATTTTGGAAAATCAACATGACAAAAGTTACTTTTATTGAACACAA
 TGGTACGGTCCGCAACGTGGACGTGACGACGGCCTGTCCGTGATGGAGGCCCGCTCAACAACCTGGTGGCGGGCATC
 GATGGCGACTGCGGTGGCGCCTGCGCCTGCGCCACCTGCCATGTGCACATCGACGCCCGCTGGCTGGACAAGTTGCCGC
 CGATGGAGGCGATGGAAAAGTCGATGCTTGTGTTTCCGAGGGCCGCAACGAAAGCTCGCGCCTGGGTTGTGAGATCAA
 GCTCAGCCCCGCGCTTGACGGCATTGTGGTGGCAGCCGCTCGGCCAGCACTGA

6.1.2 Vectors

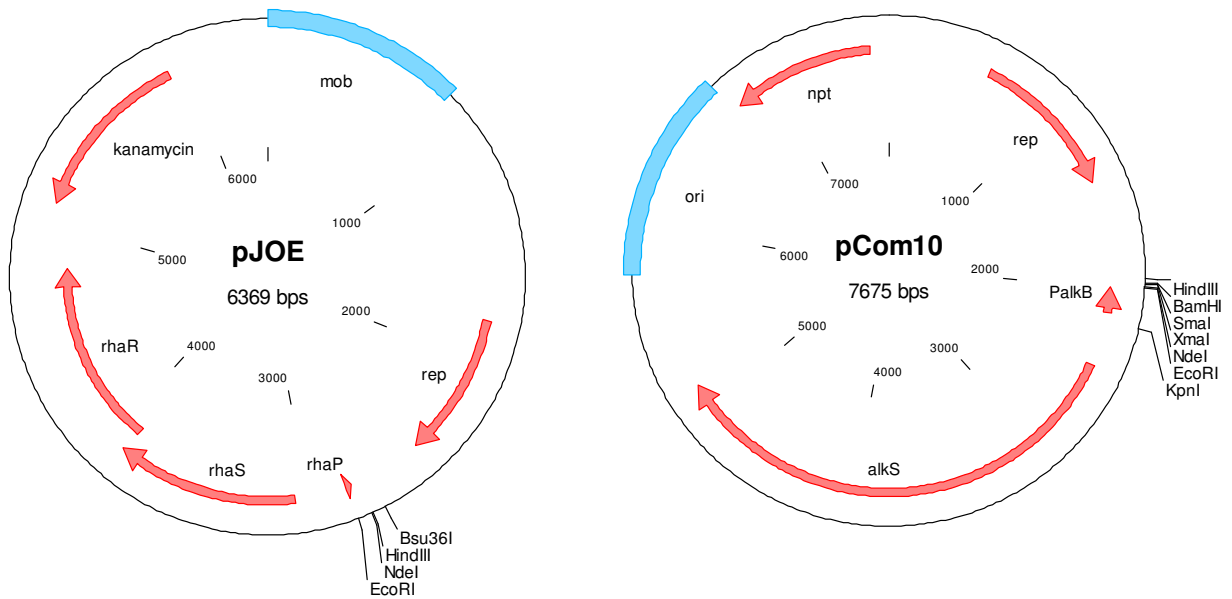


Figure 6.1. Maps of non-commercial vectors used in this study: pJOE and pCom10. The pJOE vector series, developed at the University of Stuttgart, contain the L-rhamnose promoter (*rhaP_{BAD}*) from the catabolic operon *rhaBAD* as well as transcriptional activators *rhaR* and *rhaS*. pJOE vectors have reported protein expression yields of 20 % in *E. coli* and *Pseudomonas* strains.^{177, 178} The pCom vector series were developed in the Swiss Federal Institute of Technology Zurich (ETH Zürich). They contain the *PalkB* promoter which originally controls the expression of the *alkBFGHIJKL* operon located in the OCT plasmid from *P. putida* Gpo1. The AlkS protein activates transcription from *PalkB* upon exposure to C₇-C₁₂ *n*-alkanes, alkenes, ethyl acetate or dicyclopropyl ketone. pCom10 is a medium to high copy number plasmid able to yield recombinant protein levels as high as 25 % in *E. coli* and *Pseudomonas*.¹⁷⁹

Table 6.1. Vector constructs used in this work

Name	Gene Insert	Available at ITB?	ITB No.
pET28a(+)-CamA	Putidaredoxin reductase (CamA) from <i>P. putida</i> ATCC 17453	Yes	pITB692
pET28a(+)-CamB	Putidaredoxin (CamB) from <i>P. putida</i> ATCC 17453	Yes	pITB691
pKK223-3-CYP153A16	CYP153A16 (MMAR_3154) from <i>Mycobacterium marinum</i> M. ATCC BAA-535	Yes	pITB442
pET28a(+)-CYP153A <i>P. sp.</i>	CYP153A <i>P. sp.</i> (Bpro_5301) from <i>Polaromonas sp.</i> JS666 ATCC BAA-500	Yes	pITB376
pET28a(+)-CYP153A <i>M. aq.</i> T302M	Focused mutant library of CYP153A <i>M. aq.</i> (Maqu_0600) from <i>Marinobacter aquaeolei</i> VT8 DSM 11845	Yes	pITB719
pET28a(+)-CYP153A <i>M. aq.</i> T302V	Focused mutant library of CYP153A <i>M. aq.</i> (Maqu_0600) from <i>Marinobacter aquaeolei</i> VT8 DSM 11845	Yes	pITB751
pET28a(+)-CYP153A <i>M. aq.</i> V306T	Focused mutant library of CYP153A <i>M. aq.</i> (Maqu_0600) from <i>Marinobacter aquaeolei</i> VT8 DSM 11845	Yes	pITB726
pET28a(+)-CYP153A <i>M. aq.</i> M357Y	Focused mutant library of CYP153A <i>M. aq.</i> (Maqu_0600) from <i>Marinobacter aquaeolei</i> VT8 DSM 11845	Yes	pITB720
pET28a(+)-CYP153A <i>M. aq.</i> F455I	Focused mutant library of CYP153A <i>M. aq.</i> (Maqu_0600) from <i>Marinobacter aquaeolei</i> VT8 DSM 11845	Yes	pITB721
pET28a(+)-CYP153A <i>M. aq.</i> F455L	Focused mutant library of CYP153A <i>M. aq.</i> (Maqu_0600) from <i>Marinobacter aquaeolei</i> VT8 DSM 11845	No†	-
pJOE [pJOE4782.1 (malE ⁻ , eGFP ⁻)]	None. Empty religated vector lacking malE (maltose binding protein) and eGFP (enhanced green fluorescent protein)	Yes	pITB437
pJOE-BM3	CYP102A1 or P450 BM3 (CPXB_BACME) from <i>Bacillus megaterium</i> DSM 319	Yes	pITB438
pJOE-MmAlk	MmAlk operon: Ferredoxin (MMAR_3155), CYP153A16 (MMAR_3154), ferredoxin reductase (MMAR_3153) from <i>Mycobacterium marinum</i> M. ATCC BAA-535	Yes	pITB439

Table 6.1. Vector constructs used in this work (continued)

Name	Gene Insert	Available at ITB?	ITB No.
pJOE-MaqAlk	MaqAlk operon: Ferredoxin (Maqu_0599), CYP153A <i>M. aq.</i> (Maqu_0600), ferredoxin reductase (Maqu_0601) from <i>Marinobacter aquaeolei</i> VT8 DSM 11845	Yes	pITB457
pJOE-PspAlk	PspAlk operon: CYP153A <i>P. sp.</i> (Bpro_5301), ferredoxin reductase (Bpro_5300), ferredoxin (Bpro_5299) from <i>Polaromonas sp.</i> JS666 ATCC BAA-500	Yes	pITB458
pCom10-alkB-BMO2	AlkB (alkane-1-monooxygenase, BMO2 mutant), AlkF (rubredoxin 1), AlkG (rubredoxin 2) from <i>P. putida</i> Gpo1	Yes	-
pCom10-MmAlk	MmAlk operon	Yes	pITB459
pCom10-MaqAlk	MaqAlk operon	Yes	pITB460
pCom10-PspAlk	PspAlk operon	Yes	pITB461
pJOE-CYP153A <i>M. aq.</i> -CPR	CYP153A <i>M. aq.</i> fused to the reductase domain (CPR) of P450 BM3 from <i>Bacillus megaterium</i> DSM 319	Yes	pITB468
pJOE-CYP153A <i>M. aq.</i> (G307A)-CPR	CYP153A <i>M. aq.</i> (G307A variant) fused to the reductase domain (CPR) of P450 BM3 from <i>Bacillus megaterium</i> DSM 319	Yes	pITB469
pKK223-3-MmAlk	MmAlk operon	Yes	pITB750

†Available only as cell-free extract.

6.1.3 Strains

Table 6.2. Strains used in this work

Name	Description / Use	Available at ITB?	ITB No.
JM105_pKK223-3-153A16	Expression of CYP153A16 in <i>E. coli</i> JM105	Yes	ITB442
BL21 (DE3)_pET28a(+)- <i>M. aq.</i> -Enz-N-Term	Expression of CYP153A <i>M. aq.</i> in <i>E. coli</i> BL21(DE3)	Yes	ITB372
BL21 (DE3)_pET28a(+)- <i>P. sp.</i> -Enz-C-Term	Expression of CYP153A <i>P. sp.</i> in <i>E. coli</i> BL21(DE3)	No†	-
BL21 (DE3)_pET28a(+)-CYP153A <i>M. aq.</i> M143R	Focused mutant library of CYP153A <i>M. aq.</i>	Yes	ITB383
BL21 (DE3)_pET28a(+)-CYP153A <i>M. aq.</i> I145M	Focused mutant library of CYP153A <i>M. aq.</i>	yes	ITB392
BL21 (DE3)_pET28a(+)-CYP153A <i>M. aq.</i> I145F	Focused mutant library of CYP153A <i>M. aq.</i>	Yes	ITB393
BL21 (DE3)_pET28a(+)-CYP153A <i>M. aq.</i> I145T	Focused mutant library of CYP153A <i>M. aq.</i>	Yes	ITB394
BL21 (DE3)_pET28a(+)-CYP153A <i>M. aq.</i> I145S	Focused mutant library of CYP153A <i>M. aq.</i>	Yes	ITB399
BL21 (DE3)_pET28a(+)-CYP153A <i>M. aq.</i> L303T	Focused mutant library of CYP153A <i>M. aq.</i>	Yes	ITB388
BL21 (DE3)_pET28a(+)-CYP153A <i>M. aq.</i> L354F	Focused mutant library of CYP153A <i>M. aq.</i>	Yes	ITB389
BL21(DE3)_pET28a(+)-CYP153A <i>M. aq.</i> L354I	Focused mutant library of CYP153A <i>M. aq.</i>	Yes	ITB390
BL21 (DE3)_pET28a(+)-CYP153A <i>M. aq.</i> F455Y	Focused mutant library of CYP153A <i>M. aq.</i>	Yes	ITB391
BL21 (DE3)_pET28a(+)-CYP153A <i>M. aq.</i> G307A	Focused mutant library of CYP153A <i>M. aq.</i>	Yes	ITB396
BL21 (DE3)_pET28a(+)-CYP153A <i>M. aq.</i> G307V	Focused mutant library of CYP153A <i>M. aq.</i>	Yes	ITB397
BL21 (DE3)_pET28a(+)-CYP153A <i>M. aq.</i> M357N	Focused mutant library of CYP153A <i>M. aq.</i>	Yes	ITB398
DH5 α _pET28a(+)-CYP153A <i>M. aq.</i> M357F	Focused mutant library of CYP153A <i>M. aq.</i>	Yes	ITB470
JM109_pJOE	<i>E. coli</i> JM109 with religated pJOE vector (negative control)	Yes	ITB437
JM109_pJOE-MmAlk	Expression of the MmAlk operon in <i>E. coli</i>	Yes	ITB439
S12_pJOE	<i>P. putida</i> S12 with religated pJOE vector (negative control)	Yes	ITB440

Table 6.2. Strains used in this work (continued)

Name	Description / Use	Available at ITB?	ITB No.
S12_pJOE-MmAlk	Expression of the MmAlk operon in <i>P. putida</i> S12	Yes	ITB441
DH5 α _pJOE-MaqAlk	Propagation of pJOE_MaqAlk in <i>E. coli</i>	Yes	ITB457
DH5 α _pJOE-PspAlk	Propagation of pJOE_PspAlk in <i>E. coli</i>	Yes	ITB458
DH5 α _pCom10-MmAlk	Propagation of pCom10_MmAlk in <i>E. coli</i>	Yes	ITB459
DH5 α _pCom10-MaqAlk	Propagation of pCom10_MaqAlk in <i>E. coli</i>	Yes	ITB460
DH5 α _pCom10-PspAlk	Propagation of pCom10_PspAlk in <i>E. coli</i>	Yes	ITB461
KT2440_pJOE	<i>P. putida</i> KT2440 with religated pJOE vector (negative control)	Yes	ITB450
KT2440_pJOE-MmAlk	Expression of the MmAlk operon in <i>P. putida</i> KT2440	Yes	ITB451
KT2440_pJOE-MaqAlk	Expression of the MaqAlk operon in <i>P. putida</i> KT2440	Yes	ITB452
KT2440_pJOE-PspAlk	Expression of the PspAlk operon in <i>P. putida</i> KT2440	Yes	ITB423, ITB453
KT2440_pCom10-MmAlk	Expression of the MmAlk operon in <i>P. putida</i> KT2440	Yes	ITB454
KT2440_pCom10-MaqAlk	Expression of the MaqAlk operon in <i>P. putida</i> KT2440	Yes	ITB455
KT2440_pCom10-PspAlk	Expression of the PspAlk operon in <i>P. putida</i> KT2440	Yes	ITB422, ITB456
DH5 α _pJOE-CYP153A <i>M. aq.</i> (G307A)-CPR	Propagation of the pJOE_CYP153A <i>M. aq.</i> (G307A)-CPR fusion construct in <i>E. coli</i>	Yes	ITB462
KT2440_pJOE-CYP153A <i>M. aq.</i> -CPR	Expression of the CYP153A <i>M. aq.</i> -CPR fusion construct in <i>P. putida</i> KT2440	Yes	ITB463
KT2440_pJOE-CYP153A <i>M. aq.</i> (G307A)-CPR	Expression of the CYP153A <i>M. aq.</i> (G307A)-CPR fusion construct in <i>P. putida</i> KT2440	Yes	ITB464
S12_pJOE-CYP153A <i>M. aq.</i> (G307A)-CPR	Expression of the CYP153A <i>M. aq.</i> (G307A)-CPR fusion construct in <i>P. putida</i> S12	Yes	ITB465
JM109_pJOE-CYP153A <i>M. aq.</i> -CPR	Expression of the CYP153A <i>M. aq.</i> -CPR fusion construct in <i>E. coli</i> JM109	Yes	ITB466
JM109_pJOE-CYP153A <i>M. aq.</i> (G307A)-CPR	Expression of the CYP153A <i>M. aq.</i> (G307A)-CPR fusion construct in <i>E. coli</i> JM109	Yes	ITB467

Table 6.2. Strains used in this work (continued)

Name	Description / Use	Available at ITB?	ITB No.
BL21(DE3)_pJOE-CYP153A <i>M. aq.</i> -CPR	Expression of the CYP153A <i>M. aq.</i> -CPR fusion construct in <i>E. coli</i> BL21(DE3)	Yes	ITB468
BL21(DE3)_pJOE-CYP153A <i>M. aq.</i> (G307A)-CPR	Expression of the CYP153A <i>M. aq.</i> (G307A)-CPR fusion construct in <i>E. coli</i> BL21(DE3)	Yes	ITB469

†Available only as vector construct (pITB376).

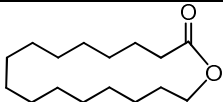
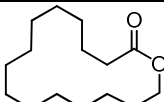
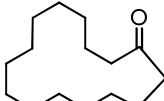
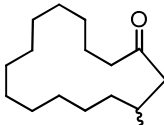
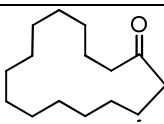
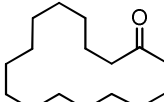
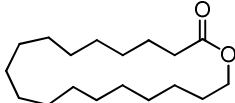
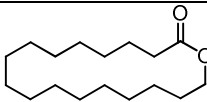
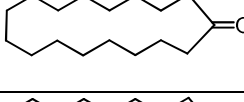
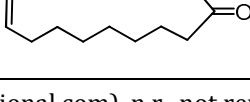
6.2 Multiple protein sequence alignments

CYP153A1	FDAAVDAAKHFAELWHRKAAQKSAGAEMGYDLISLMQSNEATKDLIYR--PMEFMGNL	VLL	331
CYP153AspOC4	FDAAVDAAKHFAELWHRKAAQKSAGAEMGYDLISLMQSNEATKDLIYR--PMEFMGNL	VLL	331
CYP153A13a	FDDAADMAWAFSKLWRDKEARQKAGEEPGFDLISMLQSNEDTKDLINR--PLEFIGNL	LALL	304
CYP153Maq	FDDAADMARSF SRLWRDKEARRAAGEEPGFDLISLLQSNKETKDLINR--PMEFIGNL	L	304
CYP153A16	FRGMVDMARGLSAHWRDKAARTAAAGELPGFDLITMLQSEDESTKDLIDR--PMEFLGNL	VLL	295
CYP153M.gamma	RTIMGEMLQSFTQLWHDHKANDRES----FDLIRMLQRDPKTONMVDE--PF SYLGNL	MLL	259
CYP153A6	MAELMECATYFTELWNQVRNAEPKN-----DLISMAHSESTRHMA---PEEYLGNI	VLL	253
CYP153Psp	MEELKGCQVYMTRLWNERVNVPPGN-----DLISMAHTESMRNMT---PEEFLGNL	ILL	251
CYP153A8	RAELIECAMYFKGLWEQRINAEPKN-----DLISMAHSPATRDMP---FLEFLGNL	LLL	255
CYP153A11	RQELIECAMYFKGLWQRI DRSEGS----DLITMANSPATREMP---FLEFLGNL	LLL	260
CYP153A7	KTELLECAAYFQVLWNERVVKDPGN-----DLISMLAHSPATRNT---PEEYLGNI	VLL	252
CYP52A10	FKRCNKIVHKFSDYYIKKALTATPEELEKHS--SYFLYELAKQTRD--PIVLRDQSLNI		312
CYP52A11	FKRCNKIVHKFSDYYIKKALTATPEELEKHS--SYFLYELAKQTRD--PIVLRDQSLNI		312
CYP52A17	FRDCTKSVHKFTNYVQKALDASPEELEKQS--GYVFLYELVKQTRD--PNVLRDQSLNI		310
CYP52A4	FNKSIKTVHKFADFVQKALSLTDDDLKQE--GYVFLYELAKQTRD--PKVLRDQLNI		331
CYP52A3	FRDCNAKVHKLAQYFVNTALNATEKEVEEKS KGGYVFLYELVKQTRD--PKVLRDQSLNI		317
CYP124	MQVSADIGAYATALAEDRRVNHDD-----LTSSLVEAEVDGERLS--SREIASFF	ILL	264
P450BM3	KRQFQEDIKVMNDLVDKIIADRKASGEQSDDLLTHMLNGKDPETGEPLDDENIRYQIITF		262
P450Bsbeta	PRAEEWIEVMIEDARAGLLKTTSGT-----ALHEMAFHTQEDGSQ LDS---RMAAIELIN		239
CYP153A1	IVGGNDTTRNSMTGGVYALNLFNPFVFLKNNP-----SLIP		368
CYP153AspOC4	IVGGNDTTRNSMTGGVYALNLFNPFVFLKNNP-----SLIP		368
CYP153A13a	IVGGNDTTRNSMSGVLALNQFPEQFEK LKANP-----KLIP		341
CYP153Maq	IVGGNDTTRNSMSGGLVAMNEFPREFEKLKAKP-----ELIP		341
CYP153A16	IVGGNDTTRNSMSGVLALNEFPDQFEK LKANP-----ELIP		332
CYP153M.gamma	IVGGNDTTRNSMTGGVLHLHQNPSEMAK LKANH-----GLIP		296
CYP153A6	IVGGNDTTRNSMTGGVLALNEFPDEYRKL SANP-----ALIS		290
CYP153Psp	IVGGNDTTRNSMTGGVLALNENPDEYRKL CANP-----ALIA		288
CYP153A8	IVGGNDTTRNSISGGVIALNQNPDAYLKL NNDP-----GLIT		292
CYP153A11	IVGGNDTTRNSISGGVIALNQNPDEQY EKLRQHP-----SLIG		297
CYP153A7	IVGGNDTTRNSMTGGVLALHKNPDQFAKL KANP-----ALVE		289
CYP52A10	LLAGRDITAGLLSFAVFELGRNPEVWSKLRQEIGHKFG LDSYSRVEDISFELLKLC EYLYK		372
CYP52A11	LLAGRDITAGLLSFAVFELGRNPEVWSKLRREEIGDKFGLD PDSRIEDISFELLKLC EYLYK		372
CYP52A17	LLAGRDITAGLLSFAVFELARHPEI WAKLREEIEQQFGLGEDSRVEEITFESLKRCEYLYK		370
CYP52A4	LVAGRDITAGLLSFLFELSRNPTVF EKLKEEIHNRFGAKEDARVEEITFESLKLCEYLYK		391
CYP52A3	MVAGRDITAGLLSFAVFELARNPKIWNKLR EEVEVNFGLGDEARVDEISFETLKKCEYLYK		377
CYP124	VVAGNETTRNAITHGVLALSRYPEQRDRWWSDFD-----GLAP		302
P450BM3	LIAGHETTSGLLSFALYFLVKNPHVLQKAAEEAARVLVDPVP-----SYKQVKQLKYVG		316
P450Bsbeta	VLRPIVAISYFLVFSALALHEHPKYKEWLRSGNS-----RERE		277
	:: : : : *		
CYP153A1	NMVSEIIRWQTPLAYMRRIAKQDVELNGQ-----TIKKGDKVVMWVYSGNRDERVI		419
CYP153AspOC4	NMVSEIIRWQTPLAYMRRIAKQDVELNGQ-----TIKKGDKVVMWVYSGNRDERVI		419
CYP153A13a	NMVSEIIRWQTPLAYMRRVAKQDVELNGQ-----TIKKGDRVLMWYASGNQDERKF		391
CYP153Maq	NMVSEIIRWQTPLAYMRRIAKQDVELGGQ-----TIKKGDRVVMWYASGNRDERKF		392
CYP153A16	NMVSEIIRWQTPLAHMRRIAKADTVLNGQ-----FIRKGDVLMWYASGNRDERVF		383
CYP153M.gamma	SMVSEIIRWQTPLPHMRRATRDVELNGT-----VIPKGRVVLWVYSGNRDSNAI		347
CYP153A6	SMVSEIIRWQTPLSHMRRALQDTELGK-----HIRQGDKVVMWVYSGNRDPEAI		341
CYP153Psp	SMVPEIVRWQTPLAHMRRALQDTELGK-----SIRKGDKVIWVYSGNRDPEAI		339
CYP153A8	SMVPEIIRWQTPLTHMRRALQDWEIGGK-----KIRKGDVVMWYLSGNRDETVI		343
CYP153A11	SMVPEIIRWQTPLTHMRRALADSEIGGK-----RIAKGDVVMWYLSGNRDETVI		348
CYP153A7	TMVPEIIRWQTPLAHMRRATAIDSELGGK-----TIRKGDVVMWYLSGNRDEVI		340
CYP52A10	AVLNETLRLYPSVPRNARFAAANTTLP HGGGPDGMSPILVRKQQTVMYSVYALQRDEKYY		432
CYP52A11	AVINETLRLYPSVPRNARFAAANTTLP HGGGPDGMSPILVRKQQTVMYSVYALQRDEKYY		432
CYP52A17	AFLNETLRIYPSVPRNFRIATKNTTLP RGGGSDGTSPILIQKGEAVSYGINSTHLDPVYY		430
CYP52A4	ACVNEALRVYPSVPHNFRVATRNTTLP RGGGKDGMSPIAIKKGQNVMYTISATHRDPYIY		451
CYP52A3	AVLNETLRMYPVSPINFRATRDITLPRGGGKDGNSP IFVPKGSSVVYSVYKTHRLKQFY		437
CYP124	TAVEIIVRWASPVVYMRRTLTQDIELRGT-----KMAAGDKVSLWYCSANRDESKF		353
P450BM3	MVLNEALRLWPTAPAFSLYAKEDTVLGGEY-----PLEKGDLMVLIPQLHRDKTIW		368
P450Bsbeta	MEVQEVRRYYPFGPFLGALVKKDFVWNNC-----EFKKGTSVLLDL YGTNHDPRLW		328
	: : : : *		

Figure 6.2. Section of a multiple alignment of CYP153A, CYP52 and other CYP sequences (ClustalW2, Gonnet matrix, gap open: 10, gap extension: 0.20, gap distances: 5). The alignment explains mutations T302V/M, G307A, L354I/F and M357N in CYP153A *M. aq.* Residue L354 is aligned with A328 in P450 BM3 (Substitutions of A328 with I/L/V/F influence its selectivity on alkanes).

6.3 Supplementary tables

Table 6.3. Macroyclic musk products derived from C₁₆-C₁₈ saturated and unsaturated fatty acids

Fatty acid	Inter-mediate	Macrocyclic product				Price/ Kg (€)*	Producer
		Name	Ring size	Structure			
C _{16:0} (palmitic)	ω-OHFA	Silvanone	17		240	Givaudan, International Flavors and Fragrances Inc., Vigon International	
	α,ω-DCA	Exaltolide	16		450	China Aroma Chemical Co., Ltd., Firmenich, Soda Aromatic, Symrise, Vigon International	
		Exaltone	15		136	Givaudan, Firmenich, Chemos GmbH	
		(<i>R,S</i>)-Muscone	15		1100	Firmenich, Vigon International	
		(<i>R</i>)-Muscone	15		n.r.	None	
C _{17:0} (margaric)	α,ω-DCA	Isomuscone	16		156	Symrise, Vigon International	
C _{18:0} (stearic)	ω-OHFA	18-Octadecanolide	19		n.r.	None	
	α,ω-DCA	17-Heptadecanolide	18		n.r.	None	
		Dihydrozibetone	17		n.r.	None	
9(<i>Z</i>)-C _{18:1} (oleic)	ω-OHFA	Zibetone	17		n.r.	None	

* Referential prices as of July, 2012 (www.vigoninternational.com). n.r., not reported

Table 6.4. Amino acid sequence similarities between the putative natural redox partners of CYP153A16 or CYP153A *P. sp.* and CamA or CamB

Putative natural redox partner 1: Ferredoxin reductase			CamA (422 aa): Ferredoxin reductase from <i>P. putida</i>		
Strain	Gene name	aa	Identity	Similarity	Score
<i>Mycobacterium marinum</i> M.	MMAR_3153	400	50 %	64 %	354
<i>Polaromonas sp.</i> JS666	Bpro_5300	405	47 %	63 %	357
Putative natural redox partner 2: Ferredoxin			CamB (107 aa): Ferredoxin from <i>P. putida</i>		
Strain	Gene name	aa	Identity	Similarity	Score
<i>Mycobacterium marinum</i> M.	MMAR_3155	106	41 %	63 %	87
<i>Polaromonas sp.</i> JS666	Bpro_5299	106	50 %	68 %	103

performed via blastp, <http://blast.ncbi.nlm.nih.gov>

Table 6.5. Retention times of products analyzed by GC

Product \ Chain length	Retention time [min]							
	C ₅	C ₆	C ₇	C ₈	C ₉	C ₁₀	C ₁₁	C ₁₂
2-alcohol	—	—	9.2	11.2	14.8	14.8	10.9	12.5
Aldehyde	—	—	—	11.3	13.1	14.9	11.0	12.6
1-alcohol	5.5	8.5	10.6	12.5	14.2	15.8	12.1	13.5
fatty acid	—	—	—	14.3	15.7	17.2	13.4	14.5
unidentified product 1*	—	—	—	—	17.3	18.6	14.8	16.0
unidentified product 2*	—	—	—	—	17.4	18.7	14.9	16.2
α,ω -diol	—	—	—	17.0	18.4	19.4	15.7	17.1

FS-Supreme-5 column (30 m x 0.25 mm x 0.25 μ m); — not detected

*unidentified products 1 and 2 were obtained only with CYP153A16. Experiments with CYP153A16 and 1-decene or α,ω -decanediol as starting substrate material showed these compounds were neither epoxidation products nor further oxidized α,ω -diols (e.g., dialdehydes or ω -hydroxyaldehydes).

6.4 Supplementary figures

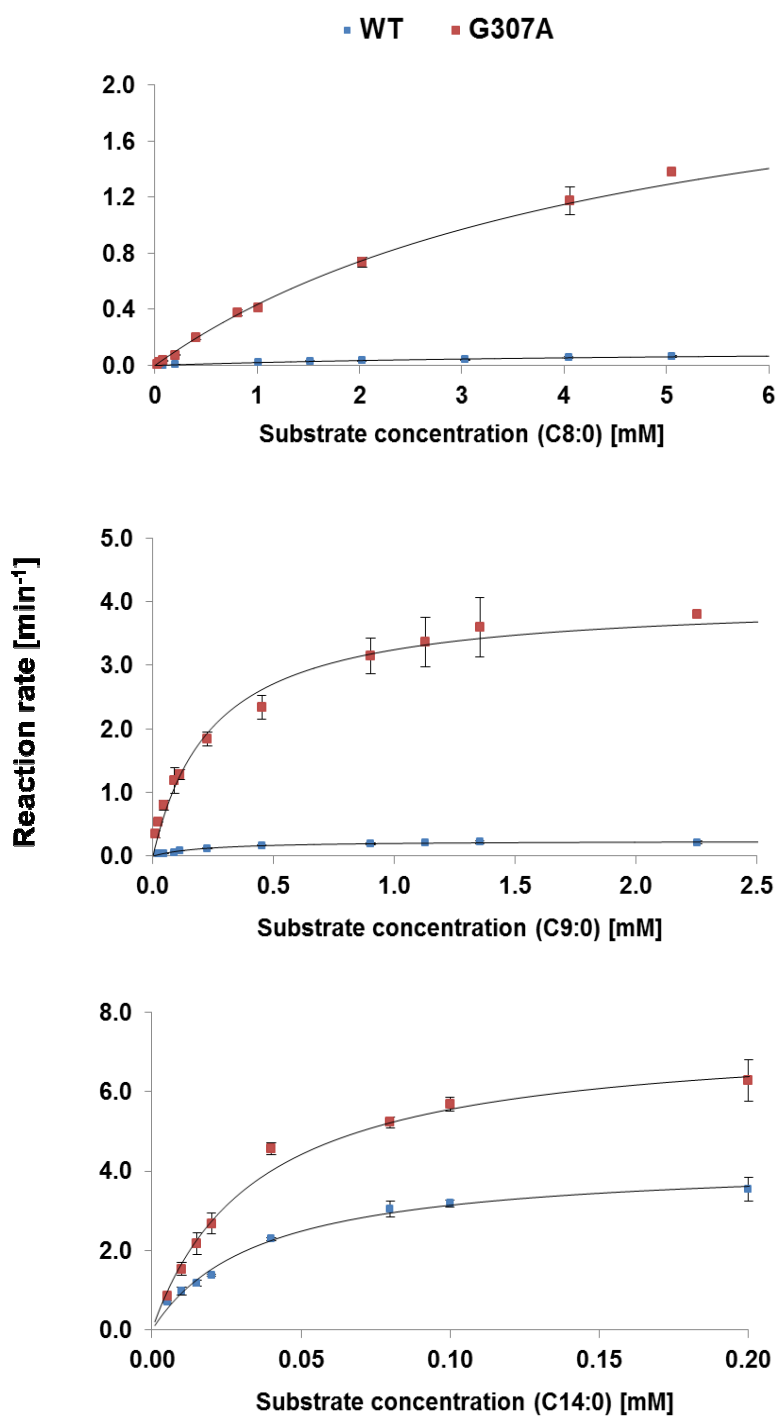


Figure 6.4. Michaelis-Menten plots of octanoic, nonanoic and tetradecanoic acids in reactions catalyzed by CYP153A *M. aq.* Wild type (blue) and variant G307A (red). Measurements were done with concentrations below the substrate solubility limit.

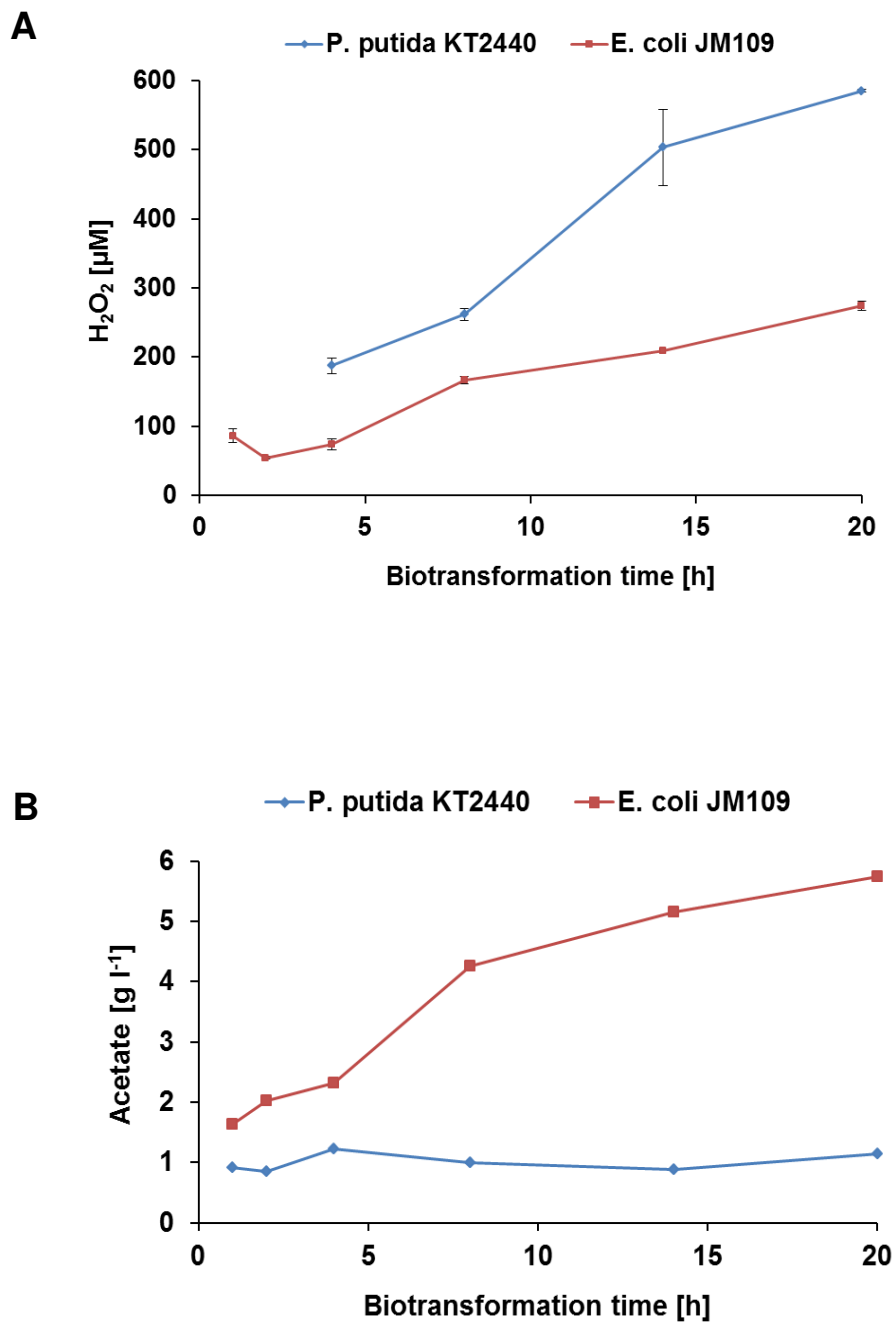


Figure 6.5. Formation of hydrogen peroxide (A) and acetate (B) by *P. putida* KT2440 and *E. coli* JM109 cells harboring pJOE-CYP153A *M. aq.* (G307A)-CPR_{BM3} in bioconversions of dodecanoic acid with glucose/glycerol-feeding only at the start of biotransformation.

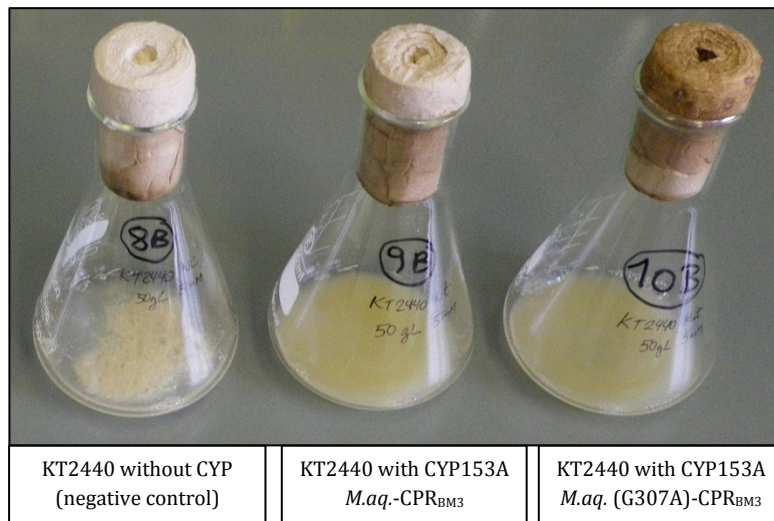
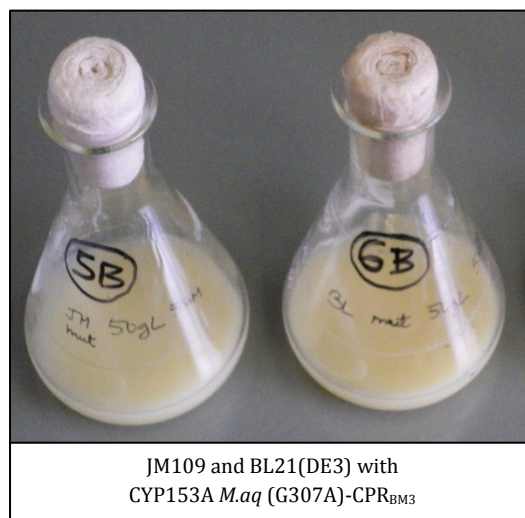
Pseudomonas putida*Escherichia coli*

Figure 6.6. Aggregation in *P. putida* KT2440 cells after 10 h bioconversions of 1 g l⁻¹ dodecanoic acid. Cell aggregation occurred in all *P. putida* variants, but it was more drastic in cells not harboring the CYP construct. *E. coli* cells without CYP (not shown) and with CYP did not aggregate. Biotransformations were run with glucose/glycerol feeding every 4 hours.

Manuscript

Full Paper

Production of 1-octanol from *n*-octane by *P. putida* KT2440 with heterologous P450 monooxygenase

Tobias Vallon^a, Matthias Glemser^a, Sumire Honda Malca^b, Daniel Scheps^b, Joachim Schmid^c, Martin Siemann-Herzberg^a, Bernhard Hauer^b and Ralf Takors^{a,1}

^aInstitute of Biochemical Engineering, Universitaet Stuttgart, Allmandring 31, 70569, Stuttgart, Germany

^bInstitute of Technical Biochemistry, Universitaet Stuttgart, Allmandring 31, 70569 Stuttgart, Germany

^cInsilico Biotechnology AG, Meitnerstrasse 8, 70563, Stuttgart, Germany

¹Corresponding author. E-mail: takors@ibvt.uni-stuttgart.de

This is the pre-peer reviewed version submitted to *Chemie Ingenieur Technik*.

Copyright © Wiley-VCH Verlag GmbH & Co. KGaA. Reproduced with permission.



Production of 1-octanol from n-octane by *Pseudomonas putida* KT2440 with heterologous P450 monooxygenase

Journal:	<i>Chemie Ingenieur Technik</i>
Manuscript ID:	cite.201200178
Wiley - Manuscript type:	Forschungsarbeit
Date Submitted by the Author:	15-Oct-2012
Complete List of Authors:	Vallon, Tobias; University Stuttgart, Institute of Biochemical Engineering Glemser, Matthias; University Stuttgart, Institute of Biochemical Engineering Malca, Sumire; University Stuttgart, Institute of Technical Biochemistry Scheps, Daniel; University Stuttgart, Institute of Technical Biochemistry Schmid, Joachim; Insilico Biotechnology AG, Siemann-Herzberg, Martin; University Stuttgart, Institute of Biochemical Engineering Hauer, Bernhard; University Stuttgart, Institute of Technical Biochemistry Takors, Ralf; University Stuttgart, Institute of Biochemical Engineering
Keywords:	Alkane, Alkohole, Biotransformationen, Sicherheitstechnik

Dedicated to the 70th anniversary of Prof. C. Wandrey

Production of 1-Octanol from *n*-Octane by *Pseudomonas putida* KT2440 with Heterologous P450 Monooxygenase

Tobias Vallon^a, Matthias Glemser^a, Sumire Honda Malca^b, Daniel Scheps^b, Joachim Schmid^c, Martin Siemann-Herzberg^a, Bernhard Hauer^b, Ralf Takors^{a*}

^a Institute of Biochemical Engineering, University of Stuttgart, Allmandring 31, 70569 Stuttgart, Germany

^b Institute of Technical Biochemistry, University of Stuttgart, Allmandring 31, 70569 Stuttgart, Germany

^c Insilico Biotechnology AG, Meitnerstraße 8, 70563 Stuttgart, Germany

*Corresponding author:

Prof. Dr.-Ing. Ralf Takors, IBVT - University Stuttgart, Allmandring 31, D-70569 Stuttgart, Germany

Phone number: +49 (0)711-685 64574

Email address: takors@ibvt.uni-stuttgart.de

Fax number: +49 (0)711-685 65164

Keywords: two-phase biotransformation; alkane; hydroxylation

Abstract

A two-phase biotransformation process for selective hydroxylation of *n*-octane to 1-octanol via *Pseudomonas putida* KT2440 harboring heterologously expressed P450 monooxygenase from *Mycobacterium marinum* is presented. Maximum cell-specific conversion rates of 12.7 mg_{octanol} g_{CDW}h⁻¹ were observed not only in shaking flasks but also in 3.7L bioreactor studies. Notably the latter have been performed obeying strict safety precautions thus lowering volumetric power input, aeration rates and substrate concentrations. Based on a stoichiometric network of *Pseudomonas putida* KT2440 topological studies were carried out. As a conclusion, potential limitations of NAD(P)H and/or ATP supply at production conditions can be excluded. In contrast, the great potential of the host for further improving performance data is outlined.

Introduction

Pseudomonas strains such as *Pseudomonas putida* KT2440 are gaining increasing interest for industrial applications due to their native ability to withstand potential stress conditions properly (1)-(4). For instance, Rühl et al. (5) identified solvent tolerant *Pseudomonas* strains showing n-butanol resistance up to 6% and Blank et al. (2) observed non-deteriorated substrate uptake rates in the presence of organic solvents which is a significantly different behavior compared to uptake reductions that usually occur with e.g. solvent stressed *E. coli*. Because genome sequencing was already finished in 2002 (5) metabolic engineering tools can be well applied for constructing novel recombinant *Pseudomonas putida* KT2440 producers.

Motivated by these basic properties *Pseudomonas putida* KT2440 has been chosen as a promising host for recombinant 1-octanol formation. The basic idea was to selectively oxidize *n*-octane via recombinant *Pseudomonas* activity to produce 1-octanol. It was anticipated that high product titers should be possible due to the strain's capacity to withstand organic solvent stress. Furthermore, heterologous octane oxidation should be achieved via recombinant expression of P450 monooxygenase CYP153A16 originating from *Mycobacterium marinum*. In addition, *Pseudomonas putida* strains have been reported to be suitable hosts for the expression of CYP153A monooxygenases and their natural redox partners. In this sense, pseudomonads have been utilized for the growth-based selection of CYP153A mutants (6) and for the whole cell-mediated biotransformation of alkanes, alkenes and alicyclic compounds ((8)(8)). CYP153A16 from *Mycobacterium marinum* has been reported to be poorly expressed in *E. coli*.

1-Octanol has been chosen as an attractive product because it is used in the chemical industry as starting material for the synthesis of ethoxylates, alkyl sulfates and ether sulfates, in petroleum chemistry as anti-foaming agent, as a solvent in paints, varnishes and surface coatings and in agricultural chemistry, e.g., to inhibit excessive growth of tobacco plants (11). Besides, it serves as additive in the perfume industry (12), totally summing up to ~3.2 million tpa production worldwide (13). The naphta-derived substrate *n*-octane is available at large quantities with reasonable prices compared to the product value of 1-octanol. However, any process approach dealing with *n*-octane needs to take into account its relatively high vapor pressure, its low water solubility and its low flash point which consequently set severe constraints on technically safe 1-octanol production from *n*-octane. Interesting enough, not only these basic properties need to be taken into account but also their interplay with

fermentation conditions. For instance bioreactor power input via stirring and aeration should be carefully installed to prevent critical droplet formation in head space (14)-(14). Besides technical issues, the successful expression of P450 monooxygenase CYP153A16 from *Mycobacterium marinum* in *Pseudomonas putida* KT2440 needed to be shown for the first time as well.

It is therefore the goal of this contribution to present a *Pseudomonas putida*-based 1-octanol production approach using *n*-octane as substrate and applying technically safe production conditions that may serve as a blueprint for scale-up. The latter seems to be worth mentioning with respect to alternative *E. coli* based approaches which are often designed as feasibility studies.

Materials and Methods

Bacterial Strain

In these experiments we used *Pseudomonas putida* KT2440 (DSMZ Braunschweig, Germany) and *P. putida* KT2440 MmarAlk (10).

The genomic DNA from *Mycobacterium marinum* M. ATCC BAA-535 was obtained from the American Type Culture Collection (ATCC). The gene cluster containing the CYP153A16 enzyme and its natural redox partners from *Mycobacterium marinum* M. were cloned into the L-rhamnose-inducible p4782.1 (pJOE,(16)) vector for expression in *Pseudomonas putida* KT2440. Expression vector pJOE was obtained from Josef Altenbuchner, Institute of Industrial Genetics, University of Stuttgart (Stuttgart, Germany).

For protein expression, *Pseudomonas putida* KT2440 cells were transformed with the plasmid by electroporation. Transformants were then cultivated in 200 ml liquid media with 30 $\mu\text{g ml}^{-1}$ kanamycin. Strains containing the pJOE construct were grown in Terrific Broth (TB) (17). To prevent carbon- and energy source depletion, 5 g l^{-1} glucose was added to TB medium 6 h after starting the cultures.

Media

If not mentioned otherwise, chemicals were purchased from Fluka (Buchs, Switzerland). Special chemicals are listed in the analytical section.

M12 Mineral salts media containing 2.2 g l^{-1} $(\text{NH}_4)_2\text{SO}_4$, 0.4 g l^{-1} $\text{MgSO}_4 \times 7 \text{H}_2\text{O}$, 0.04 g l^{-1} $\text{CaCl}_2 \times 2 \text{H}_2\text{O}$, 0.02 g l^{-1} NaCl , 2 g l^{-1} KH_2PO_4 and trace elements (2 mg l^{-1} $\text{ZnSO}_4 \times 7 \text{H}_2\text{O}$, 1 mg l^{-1} $\text{MnCl}_2 \times 4 \text{H}_2\text{O}$, 15 mg l^{-1} $\text{Na}_3\text{-Citrat} \times 2 \text{H}_2\text{O}$, 1 mg l^{-1} $\text{CuSO}_4 \times 5 \text{H}_2\text{O}$, 0.02 mg l^{-1} $\text{NiCl}_2 \times 6 \text{H}_2\text{O}$, 0.03 mg l^{-1} $\text{NaMoO}_4 \times 2 \text{H}_2\text{O}$, 0.3 mg l^{-1} H_3BO_3 (Merck), 10 mg l^{-1} $\text{FeSO}_4 \times 7 \text{H}_2\text{O}$).

Shake flask media: Glucose, 4 g l^{-1} ; M12 mineral salts containing trace elements; phosphate buffer, kanamycin.

Batch media: 10 g l^{-1} glucose; M12 mineral salts containing trace elements; phosphate buffer, kanamycin

Feed media: 150 g l⁻¹ glucose; 150 mM CaCl₂ × 2 H₂O, 150mM; 1 M MgSO₄, 150 g l⁻¹ NaCl; trace elements; phosphate buffer.

Induction solution: L-rhamnose, (0.2% (w/v), 2g l⁻¹; FeSO₄ × 7 H₂O, 0.1 mM

Antibiotics: Kanamycin 30 μg ml⁻¹ filter sterilized

Cultivation

Working cell bank: Strains were stored in 16% (v/v) glycerol stock at -70°C (storage condition: exponential growth at OD_{600nm} = 2).

Pre cultivation: A shake flask culture (130 ml) was inoculated with 13.6 ml cells from a working cell bank (OD_{600nm} = 2) in a 500 ml baffled shake flask. The culture was incubated for 6 hours at 30°C under shaking. For biotransformation in shaking flasks cells were induced after 4.5 h and 2 hours later production was started by adding 10% (v/v) *n*-octane.

Cultivation: Batch fermentation was started by inoculating the pre culture (150 ml) in 1170 ml batch media (10 g l⁻¹ glucose) in a 3.71 KLF Bioreactor (Bioengineering AG, Wald, Switzerland). The cells were cultivated at T = 30°C and pH = 7.0 ±0.05 (controlled by addition of 25% (v/v) NH₄OH solution), stirring speed increased from 500 rpm up to 1200 rpm depending of dissolved oxygen concentration (> 30%) (aeration rate V_G = 2 nl min⁻¹, temperature set to 30°C, pressure set to 1.5 bar). After C-limitation feed pump was started with 75 ml h⁻¹.

Biotransformation: 3 hours prior to production induction solution was added, pH was set to pH = 6 by addition of approximately 15 ml 10% (v/v) phosphoric acid. Also safety operation procedures were adjusted (pressure raised to 2.2 bar, reduction of aeration rate to 1 nl min⁻¹ air and additionally 2 nl min⁻¹ nitrogen in reactor head space, limiting of stirring speed to 1200 rpm). Frothing was suppressed by addition of 500 μl contraspum 210 (Zschimmer and Schwarz, Lahnstein, Germany), Biotransformation was started by adding 10% (v/v) *n*-octane and by replacing the feed media with glucose solution (50% (w/v) glucose, feed rate 25 ml h⁻¹).

Reference experiments with *P. putida* KT2240 were performed under same parameters and conditions excluding induction and production phase.

Sampling and analytical methods

Sampling: Samples were withdrawn with a capillary sampling probe as developed by Theobald (18). The sampling of the extracellular substrate was carried out by filtration with a 0.2 µm pore size ceramic membrane (FIPS sampling probe, Flownamics, Madison, USA).

GC-FID: Quantification of carboxylates and alcohols was performed on a GC Hewlett Packard 5890 series II (Agilent, Waldbronn, Germany) equipped with an Agilent 6890 autosampler and a flame ionization detector. The column (Permabond CW20-M 0.25 µm, 30 m x 0.32 mm ID, Macherey-Nagel, Düren, Germany) was loaded with 0.5 µl aqueous sample or 1.0 µl organic sample. The flow rate of the helium carrier gas was set to 2.0 ml min⁻¹. Injector 220 °C and detector 220 °C; oven program: 50 °C, heating to 90 °C (4 °C min⁻¹); heating to 220 °C (10 °C min⁻¹); 220 °C, 4 min; cooling to 50 °C (30 °C min⁻¹).

HPLC-RI: Agilent Technologies Type 1200 Series isocratic (Agilent, Waldbronn, Germany) was used for the quantification of organic acids. A Rezex ROA-Organic Acid H+ 250 x 4.6 mm column equipped with a SecurityGuard Cartridge Kit with Carbo-H 4 x 3.0 mm ID Cartridges was used (all from Phenomenex, Aschaffenburg, Germany). A Flow rate of 0.2 ml min⁻¹ of 5 mM sulphuric acid (HPLC-grade Sigma-Aldrich, Taufkirchen, Germany) and temperature of 35 °C were used.

Glucose quantification was done with LaboTRACE (TRACE Analytics, Braunschweig, Germany)

Enzymatic assays: For gluconate quantification the D-gluconic acid Kit (Megazyme, Wicklow, Ireland) was used. The glucose concentration was measured using an enzymatic assay (R-Biopharm AG, Darmstadt, Germany).

Cell dry weight: 10 ml of broth from the bioreactor was dried with a MB35 Moisture Analyzer (Ohaus Europe GmbH, Switzerland). Filtrate samples were individually quantified and later subtracted from the corresponding biosuspension.

Optical density: Samples were diluted in 0.9% (w/v) NaCl solution, measured at wavelength 600 nm with Ultraspec 1100 pro (GE Healthcare, formerly Amersham Biosciences, USA). In presence of organic solvents the samples were put on ice for 45 seconds and the organic phase was collected. The remaining phase was remixed, diluted and quantified.

Modeling and Simulation

For estimation of exchange fluxes, the process has been subdivided into 4 process phases. Within each process phase, exponential growth with a constant mean growth rate has been assumed, as well as constant biomass specific rates of substrate uptake and product formation. Rates have been determined simultaneously for all phases and all consumed and produced substances, including biomass, in a nonlinear optimization process.

Using a genome based stoichiometric model, substrate uptake and product formation rates have been reconciled for each process phase, such that supply and demand of all intracellular metabolites is balanced with a minimum of quadratic deviations between estimated and reconciled rates. The stoichiometric model was based on the annotated genome of *Pseudomonas putida* KT2440 (5) and consisted of 1093 reactions for 607 balanced compounds. It exceeded the reactome of *Pseudomonas putida* KT2440 by a set of recombinant biotransformation reactions, including the P450-mediated oxidation of *n*-octane to 1-octanol. For rate reconciliation, overdetermined submodels were identified for each process phase by applying convex analysis, maximizing energetic efficiency within each submodel.

The substrate uptake and product formation rates have been used to determine the formation and utilization fluxes for reduction equivalents (NADH, NADPH) and energy metabolites (ATP) for each process phase. By constraining the stoichiometry in respiration, ATP generation efficiency in the respiratory chain (P/O-ratio) has been chosen to be 1.75 for both the unmodified strain and the strain carrying recombinant P450 monooxygenase. This is the same level as assumed by Nogales et al. (19).

Results and Discussion

The goal of this study was to investigate an aerobic 1-octanol production process using *n*-octane as substrate for the selective hydroxylation via P450 monooxygenase CYP153A16, which was heterologously expressed in the host *P. putida* KT2440. While the basic feasibility of P450 monooxygenase mediated oxidation of C5-C12 alkanes has already been shown by heterologous expression in *E. coli* in shaking flask scale (10), this contribution aims at studying 1-octanol production in a 3.7 L bioreactor. Noteworthy, experimental conditions needed to be installed such that sensitive properties of *n*-octane (flash point: 13°C; vapor pressure 1.47 kPa (20°C), water solubility 0.007 g l⁻¹ (20°C) are carefully considered. Because 1-octanol is hardly miscible in water, the production process consists of two liquid phases: The first, aqueous phase harbored *P. putida* cells that converted slightly resolved *n*-octane into 1-octanol and the second, organic phase consisted of *n*-octane, basically serving as a sink preventing 1-octanol accumulation in the water phase.

Safety Precaution Measures

If a safe, industry-like production process is planned, highest interest should be paid to the critical explosion limits caused by the use of *n*-octane. To be precise, not only the obvious sensitive headspace concentration for *n*-octane and oxygen had to be considered, but also the formation of critical water/solvent droplets need to be prevented. As outlined by Schmid et al. (14) their presence, can significantly increase the risk of non-wanted headspace explosion, presumably by creating local, critical ignition.

As a consequence aeration and stirring (i.e. superficial velocity and volumetric power input) have been limited to non-critical values (see Materials and Methods). Furthermore additional measures were taken such as the increase of operating pressure, tight control of oxygen concentration and electrical grounding of the experimental set-up. For precaution the bioreactor pressure was raised to 2.2 bar when *n*-octane has been used. (Remark: Based on Raoul and Dalton's law the relative gas fraction of explosive octane reduces by increasing the absolute pressure.) Additionally, aeration via sparger was limited to 1 nl min⁻¹, (~0.3-0.5 vvm). Furthermore, nitrogen ventilation (2 nl min⁻¹) of the bioreactor headspace was installed to prevent the creation of an explosive atmosphere. Consequently, only sub-critical oxygen

concentrations in the headspace were allowed (< 8% (v/v)). Finally additional electric grounding of all reactor parts was installed to prevent ignition by static discharges.

Noteworthy, these measures have been taken for the sake of safe experimental conditions. They are motivated by the explosive properties of *n*-octane and they could be alleviated in case of applying less challenging substrates. While these actions are well qualified for risk protection they cause sub-optimal mass transfer conditions inside the liquid phase. Because of reduced stirring and aeration, substrate import and product export to and from the microbial cells may be deteriorated.

Process Approach

During the first process phase biomass is produced using glucose as the main carbon source. Because no *n*-octane is added so far, cultivation conditions can be installed optimally for cell growth (see Material and Methods). When the planned biomass concentration is achieved, glucose supply is reduced significantly to a minimum. At the same time, process conditions were switched to 'safe mode' because octane supply was started. The basics of 1-octanol production are outlined in figure 1. Notably, the selective oxidation of *n*-octane to 1-octanol via P450 monooxygenase does not require for additional carbon supply at first sight. But it is well known, that these enzymes activate so far non-active C-H bonds via hydroxylation not only requiring oxygen but also redox equivalents such as NADH or NADPH. To ensure their supply via basic metabolic activity and to fulfill cellular maintenance demands in the presence of organic solvents, a low glucose feed was yet installed. Hence, 1-octanol production was performed with resting cells complying with their maintenance needs.

Considering the safety restrictions for *n*-octane, experimental studies were performed as indicated in figure 2. *P. putida* grew to cell densities of $\sim 18 \text{ g}_{\text{CDW}} \text{ l}^{-1}$ within 16 h using glucose as main carbon source. While cell growth was exponential at process start, a constant substrate feed was installed after ~ 8 h to ensure biomass formation at limited growth conditions without potential oxygen limitation. About 2 h before the end of the growth phase, the rhamnose induced expression system coding for P450 monooxygenase was induced via rhamnose addition at glucose limited conditions. As a result monooxygenase activity was provided for the subsequent *n*-octane biotransformation to 1-octanol.

Figure 3 deciphers typical courses of substrate and product concentrations during a 3.7 L bioreactor run. Phase I is characterized by exponential growth with *P. putida* consuming the main carbon source glucose. As a basic property of glucose metabolism in *Pseudomonas* strains, gluconate is produced via periplasmatic glucose dehydrogenases from glucose and phosphorylated to gluconate-6-phosphate (19). This is why gluconate accumulates initially and it is converted further in phase II. Cell growth is reduced by the limited supply of glucose in phase III which also lacks gluconate formation. 1-octanol production takes place in phase IV.

Applying safe operations procedures we achieved 1-octanol titer of 330 mg l⁻¹ after 1.75 h (Figure 4). The specific 1-octanol formation rate ($12.4 \pm 2.1 \text{ mg g}_{\text{CDW}}^{-1} \text{ h}^{-1}$) for whole cell biocatalysis by CYP153A16 is in the range of performance values of alternative approaches using resting *E. coli* cells with P450 monooxygenase CYP153s (20)(21) and CYP153A6 (6). Application with *P. putida* GPo12 (formerly known as *P. oleovorans*) have shown higher conversions of octane to 1-octanol (8)(22), but in these studies 1-octanol was used as energy and carbon source at the same time.

It needs to be outlined that 1-octanol production via P450 monooxygenase in *P. putida* was accompanied by low by-product formation. Common by-products such as iso-octanol could not be detected at all, 1,8-octanediol titers accumulated to less than 1% only. The tendency of low by-product formation is remarkable with respect to potential savings in further downstream processing of 1-octanol containing broth. These process simplifications need to be taken into account when the current approach is compared to relatively high 1-octanol formation rates with AlkB monooxygenase in *E. coli* (23). The latter were accompanied by equimolar formation of octane carboxylic acid. Besides, the current approach represents a ‘one-pot’ example, not only considering industry-like safety concepts but also preventing any cell harvesting from a primary culture followed by its transfer to a 2nd reaction vessel. Notably, the approach has been demonstrated in lab-bioreactor scale and not only under milliliter and/or shaking flask conditions which rather give evidence to feasibility than to technical realization.

Figure 5 indicates that the current approach is well scalable comparing preliminary shaking flasks studies and final 3.7 L bioreactor results. *n*-octanol formation rates were always found to be in the range of 9.5 to 12.7 mg g_{CDW}⁻¹ h⁻¹. Biological triplicates in shaking flasks revealed product formation variance of $12.6 \pm 1.2 \text{ mg g}_{\text{CDW}}^{-1} \text{ h}^{-1}$. Hence shaking flask results are very similar to reactor studies. Differences in final 1-octanol titers were mainly due to variations in

initial *n*-octane concentrations and *n*-octane supply which have been changed in the course of experimental design.

Impact on Cellular Redox and Energy Management

As outlined above, the selective oxidation of *n*-octane basically represents a hydroxylation at C-H bond thus requiring for reduction equivalents such as NADH and/or NADPH. The reduced nucleotides need to be supplied by basic central metabolism and may represent a significant drain in overall redox balances. To investigate how much cellular metabolism is affected by 1-octanol formation, the stoichiometric model of *Pseudomonas putida* (see Material and Methods) has been applied for topology studies. Figure 6 gives an overview of the flux balance analysis assuming a realistic P/O ratio of 1.75 [12] and considering fixed substrate uptake and product formation rates during 1-octanol formation. Presuming no biomass production, only 0.4% of the reductions equivalents are needed to cope with the experimentally determined 1-octanol formation rates. In case of maximum cell growth, this fraction increases up to 0.6%. Hence the vast majority of NAD(P)H supply (with or without growth) is still available for oxidative phosphorylation. Together with the catabolic ATP synthesis in central metabolism, a significant ATP supply is enabled that can either be used for cell growth or for other demands, not specified in Figure 6.

To evaluate the capacities of the *P. putida* system further, an extreme scenario of tenfold increase of 1-octanol formation rate was assumed, still fixing glucose uptake rates at the 'old' values. Under this condition, the biotransformation contributes to the total balance of NADH, NADPH and CoQH₂ only by approximately 5%. This demonstrates that the native redox capacity of *P. putida* offers a great potential for further increasing 1-octanol formation rates without hitting the regeneration limits of the system.

Complementary to the question of redox capacity, the cellular maintenance ATP demand is worth studying to judge whether or not maintenance needs are at a challenging level. Based on the stoichiometric *P. putida* model a flux balance approach has been performed, again fixing measured rates for substrate uptake and biomass formation. To estimate the impact of plasmid-encoded gene expression, maintenance ATP requirements were calculated not only for the *P. putida* 1-octanol producer but also for the parental *P. putida* KT2440 wild type. The latter was in the focus of supplemental chemostat studies published elsewhere (25). Data of the parental strain are thus based on steady-state experiments, while maintenance demands of the

1-octanol producer were extracted from the cell growth phase I-III of fedbatch experiments discussed above.

In case of the wild type KT2440, ATP maintenance requirements m_{ATP} [$\text{mmol}_{\text{ATP}} \text{g}_{\text{CDW}}^{-1} \text{h}^{-1}$] were found to be $(23.6 \pm 5.9) + \mu * (78.0 \pm 16.5)$. $(20.0 \pm 9.6) + \mu * (142.2 \pm 37.4)$ were calculated for the currently used 1-octanol producer (see table 1). Obviously, ATP requirements are the same for both strains at resting cell conditions. However, slightly increasing needs are identified for growing 1-octanol producers harbouring the heterologous monooxygenase on plasmid. The slope of the growth (μ) dependent ATP demand is higher for producing cells than for non-producers.

Considering the fact that 1-octanol formation was realized with almost resting cells, i.e. no significant cell growth μ could be detected during phase IV (see figure 3), maintenance requirements of the 1-octanol producer should be similar to wild type demands except for potential increases reflecting raised cellular needs to cope with the production stress conditions. Indeed only somewhat increased ATP requirements were derived from the measurements during 1-octanol production phase. The maintenance ATP flux was determined as $33.2 - 38.0 \text{ mmol}_{\text{ATP}} \text{g}_{\text{CDW}}^{-1} \text{h}^{-1}$. However, these absolute values are yet far from being critical with respect to cellular total ATP formation capacities (2). Summarizing neither redox regeneration nor ATP supply unravel obvious limits for 1-octanol formation. In contrast, the strain offers great potential for further improvement of 1-octanol performance data.

Summary and Conclusion

It has been shown that the heterologous expression of P450 monooxygenase in *P. putida* KT2440 succeeded allowing the selective oxidation of *n*-octane to 1-octanol. Safe, industry-like product formation could be achieved in 3.7 L scale, revealing 1-octanol formation rates of $\sim 12 \text{ mg g}_{\text{CDW}}^{-1} \text{ h}^{-1}$. At these production conditions neither the formation of reduction equivalents nor ATP maintenance demands significantly limit 1-octanol formation. In contrast, the strain's properties offer great promise for further improvement of performance data.

The question arises what is the most prominent factor limiting product formation in the current approach? Table 2 gives an overview of competing studies. *E. coli* has been chosen as the host system in all approaches except for the one presented in this contribution. It is fair to state that performance data of the *P. putida* producer are well keeping up with those of the others – apart from the approach of Grant et al. (23). Noteworthy, safe production conditions have been installed for the *Pseudomonas* approach, while most of the others were realized in significantly smaller scale. However, the approach of Grant et al. (23) is outperforming, roughly by a factor of 10. This seems to be remarkable because the native *Pseudomonas oleovorans* alkane utilizing systems *alkB* was expressed in *E. coli* (26). Recently, Gudiminchi et al. (27) have demonstrated that overexpression of the *alkB* P450 monooxygenase in *E. coli* did not yield at increased performance data. Obviously this host system has reached a (high level) boundary for biotransformation.

Considering the current *P. putida* example one may wonder whether mass transport limits 1-octanol formation. Isken and de Bont (2) already outlined that the uptake of organic solvents in bacteria is usually driven by diffusion. Taking into account the poor substrate solubility of about $7 \text{ mg}_{\text{octane}} \text{ l}^{-1}$ (at 20°C) and considering the volumetric 1-octanol formation rate of $12.7 \text{ mg}_{\text{octanol}} \text{ g}_{\text{CDW}}^{-1} \text{ h}^{-1} * 20 \text{ g}_{\text{CDW}} \text{ l}^{-1} = 254 \text{ mg}_{\text{octanol}} \text{ l}^{-1} \text{ h}^{-1}$, less than 100 s are theoretically enough to totally replenish maximum dissolved *n*-octane levels with the observed biological activity of the cells. Studying the *n*-octane based growth of *P. oleovorans*, Schmid et al. (27) identified maximum octane transfer rates $> 45 \text{ mmol l}^{-1} \text{ h}^{-1}$ which are ~ 20 fold higher than the *n*-octane biotransformation rates observed here. Notably, with 2500 rpm and 1.9 vvm significantly better mixing and aeration conditions were installed by Schmid et al. (27) than applied in this approach. So, it cannot be excluded that safety precautions finally limited diffusion-driven-*n*-octane transport to the cells. Additionally, biotransformation rates may be

hampered by 1-octanol export as well which, again, could be affected by the operating conditions installed.

However, irrespective of potentially limiting mass transport conditions, the host *P. putida* offers a great potential for heterologous hydroxylation processes because of its low maintenance demand and its high reductive power thus offering himself as a platform organism for other approaches as well.

Acknowledgments

This study was supported by the German Ministry of Education and Research and the company BASF SE.

We thank Dr. Michael Breuer (BASF SE, Ludwigshafen, Germany) for supervising and coordinating the project consortium.

References

- (1) J. L. Ramos et al., *Annu Rev Microbiol* **2002**, *56*, 743-68.
- (2) L. M. Blank et al., *FEBS J* **2008**, *275* (20), 5173-90.
- (3) S. Isken, J. A. de Bont, *Extremophiles* **1998**, *2* (3), 229-38.
- (4) S. Isken, A. Derks, P. F. Wolffs, J. A. de Bont, *Appl Environ Microbiol* **1999**, *65* (6), 2631-5.
- (5) J. Ruhl, A. Schmid, L. M. Blank, *Appl Environ Microbiol* **2009**, *75* (13), 4653-6.
- (6) K. E. Nelson et al., *Environmental Microbiology* **2002**, *4* (12), 799-808.
- (7) D. J. Koch, M. M. Chen, J. B. van Beilen, F. H. Arnold, *Appl Environ Microbiol* **2009**, *75* (2), 337-44.
- (8) J. B. van Beilen et al., *Appl Environ Microbiol* **2005**, *71* (4), 1737-44.
- (9) E. G. Funhoff et al., *J Bacteriol* **2006**, *188* (14), 5220-7.
- (10) D. Scheps et al., *Org Biomol Chem* **2011**, *9* (19), 6727-33.
- (11) in *The MAK-Collection for Occupational Health and Safety*, Wiley-VCH Verlag GmbH & Co. KGaA, **2002**.
- (12) J. Falbe, H. Bahrmann, W. Lipps, D. Mayer, in *Ullmann's Encyclopedia of Industrial Chemistry*, Wiley-VCH Verlag GmbH & Co. KGaA, **2000**.
- (13) P. Jianlin, *China Chemical Reporter* **2005**, *Vol. 16* (Issue 23), p19.
- (14) R. G. Mathys, A. Schmid, B. Witholt, *Biotechnol Bioeng* **1999**, *64* (4), 459-77.
- (15) A. Schmid, A. Kollmer, B. Sonnleitner, B. Witholt, *Bioprocess Eng* **1999**, *20* (2), 91-100.
- (16) T. Stumpp, Wilms, B., Altenbuchner, J., *Biospektrum* **2000**, *6*, 33-36.
- (17) J. Sambrook, D. Russell, *Molecular Cloning: A Laboratory Manual*. Cold Spring Harbor Laboratory Press, **2001**.
- (18) U. Theobald, W. Mailinger, M. Reuss, M. Rizzi, *Anal Biochem* **1993**, *214* (1), 31-7.
- (19) J. Nogales, B. O. Palsson, I. Thiele, *BMC Syst Biol* **2008**, *2*, 79.
- (20) T. del Castillo et al., *J Bacteriol* **2007**, *189* (14), 5142-52.
- (21) T. Fujii et al., *Biosci Biotechnol Biochem* **2006**, *70* (6), 1379-85.
- (22) N. Fujita et al., *Biosci Biotechnol Biochem* **2009**, *73* (8), 1825-30.
- (23) J. B. van Beilen et al., *Appl Environ Microbiol* **2006**, *72* (1), 59-65.
- (24) C. Grant, J. M. Woodley, F. Baganz, *Enzyme Microb Technol* **2011**, *48* (6-7), 480-6.
- (25) T. Vallon, Rendgen, B., Siemann-Herzberg, M., Takors, R., *Journal of Biotechnology* **submitted**.

- (26) G. Eggink, R. G. Lageveen, B. Altenburg, B. Witholt, *J Biol Chem* **1987**, 262 (36), 17712-8.
- (27) R. Gudiminchi et al., *Applied Microbiology and Biotechnology* **2012**, 1-10.
- (28) A. Schmid, B. Sonnleitner, B. Witholt, *Biotechnol Bioeng* **1998**, 60 (1), 10-23.

Figure 1: Basic principle of 1-octanol formation from *n*-octane using P450 monooxygenase (CYP153A16) from *Mycobacterium marinum* which was heterologously expressed in *P. putida* KT2440. *n*-Octane is imported via diffusion and converted to 1-octanol in the cytosol. Besides oxygen, reduction equivalents such as NADH are needed for hydrogenation of the substrate which are delivered by concomitant glucose metabolism in (almost) resting cells.

Figure 2: Process Design under Safety operation procedures (parameters to avoid explosive atmosphere in bioreactor headspace): process parameter *in vivo* biotransformation of *n*-octane to 1-octanol by *Pseudomonas putida* MmarAlk (p4782.1 MMAR_3155 MMAR_3154 MMAR_3153) using a 3.7 L bioreactor; solid black line: concentration of biomass c_x [$\text{g}_{\text{CDW}} \text{ l}^{-1}$]; solid grey line: concentration of oxygen air supply [%], dotted line: pressure [bar]; broken line: air supply rate V_G [nl min^{-1}]; induction with 2 g l^{-1} (0,2 % w/v) L-rhamnose und 0.1 mM FeSO_4 min. 2 h before addition of 10% (v/v) *n*-octane. 0-8 h batch phase; 8-16 h fed-batch phase (constant feed rate); 16-18 h biotransformation

Figure 3: Time courses of glucose and gluconate during the initial exponential growth phase (I), the growth-limiting fed-batch phase (II), the induction period (III) and the *n*-octane conversion to 1-octanol with ‘resting’ cells at phase IV. The process was performed at 3.7 L scale.

Figure 4: *In vivo* biotransformation of *n*-octane to 1-octanol by *Pseudomonas putida* MmarAlk using a 3.7 L bioreactor; \times : cell dry weight c_x [$\text{g}_{\text{CDW}} \text{ l}^{-1}$]; \circ : optical density 600 nm; \bullet : concentration of 1-octanol c_{octanol} [mg l^{-1}]; induction with 2 g l^{-1} (0,2 % w/v) L-rhamnose und 0.1 mM FeSO_4 2.5 h before addition of 10 % (v/v) *n*-octane.

Figure 5: *In vivo* biotransformation of *n*-octane to 1-octanol by *Pseudomonas putida* MmarAlk (p4782.1 MMAR_3155 MMAR_3154 MMAR_3153), concentration of 1-octanol c_{octanol} [mg l^{-1}] from shake flask scale up to optimized bioreactor experiments. \blacktriangle : shake flask scale; \circ : 3.7 L bioreactor scale. \square : 3.7 L bioreactor scale with optimized conditions. Solid line: start biotransformation.

Figure 6: Distribution of the sources and sinks for reduction equivalents (NADH, NADPH, and ubiquinol CoQH₂) and energy metabolites (ATP) during the octanol production phase of the fed-batch process, replicate 1. With respect to growth rate, two extreme scenarios are

described: no growth (top numbers) and growth with a maximal growth rate of 0.43 h^{-1} (bottom numbers), assuming no ATP is consumed without obvious use.

Table 1: Growth rate μ dependent rate of ATP hydrolysis without any purpose that is obvious from stoichiometry.

Table 2: Overview of competing approaches for 1-octanol production making use of (heterologous) monooxygenase activity.

** estimated

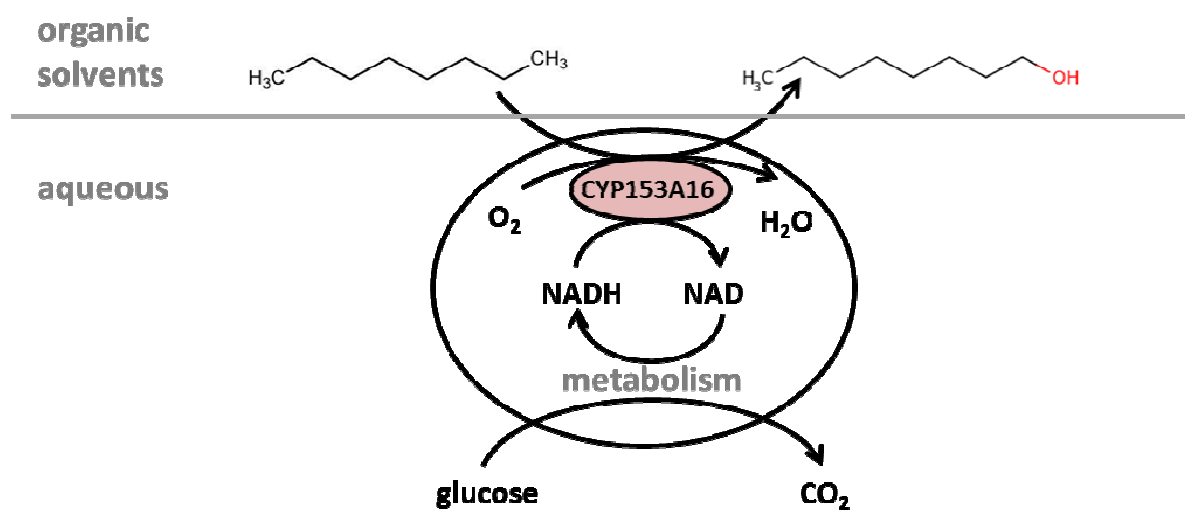


Figure 1: Basic principle of 1-octanol formation from *n*-octane using P450 monooxygenase (CYP153A16) from *Mycobacterium marinum* which was heterologously expressed in *P. putida* KT2440. *n*-Octane is imported via diffusion and converted to 1-octanol in the cytosol. Besides oxygen, reduction equivalents such as NADH are needed for hydroxylation of the substrate which are delivered by concomitant glucose metabolism in (almost) resting cells.
102x41mm (300 x 300 DPI)

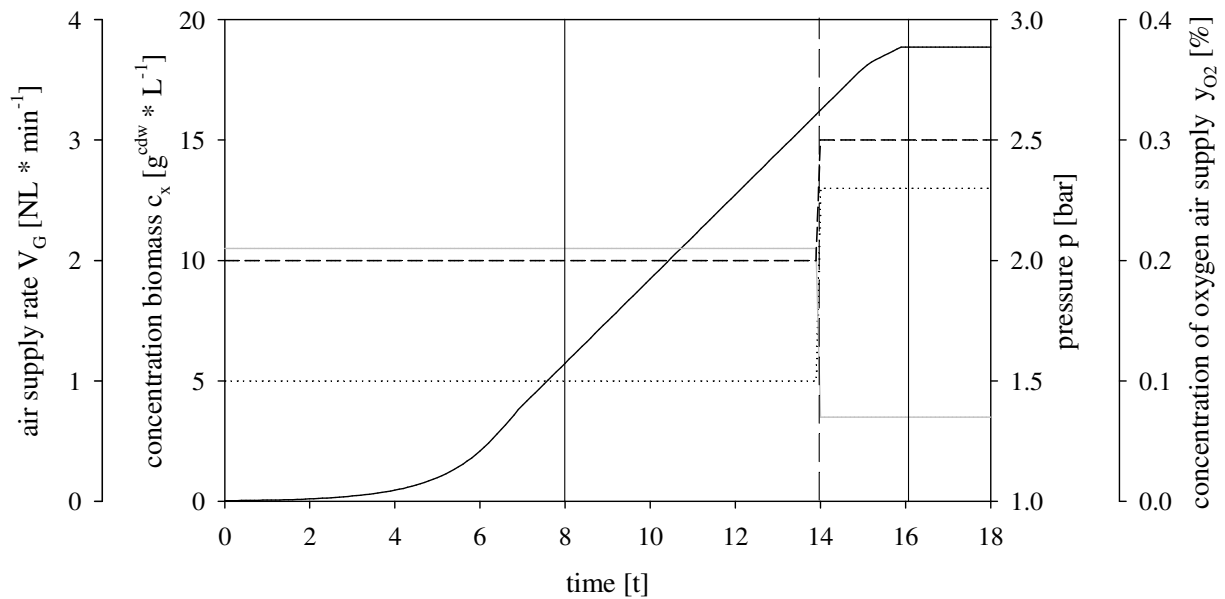


Figure 2: Process Design under Safety operation procedures (parameters to avoid explosive atmosphere in bioreactor headspace): process parameter *in vivo* biotransformation of *n*-octane to 1-octanol by *Pseudomonas putida* MmarAlk (p4782.1 MMAR_3155 MMAR_3154 MMAR_3153) using a 3.7 L bioreactor; solid black line: concentration of biomass c_x [$g_{cdw} l^{-1}$]; solid grey line: concentration of oxygen air supply [%], dotted line: pressure [bar]; broken line: air supply rate V_G [$nl min^{-1}$]; induction with 2 g l^{-1} (0.2 % w/v) L-rhamnose und 0.1mM $FeSO_4$ min. 2 h before addition of 10% (v/v) *n*-octane. 0-8 h batch phase; 8-16 h fedbatch phase (constant feedrate); 16-18 h biotransformation
106x54mm (300 x 300 DPI)

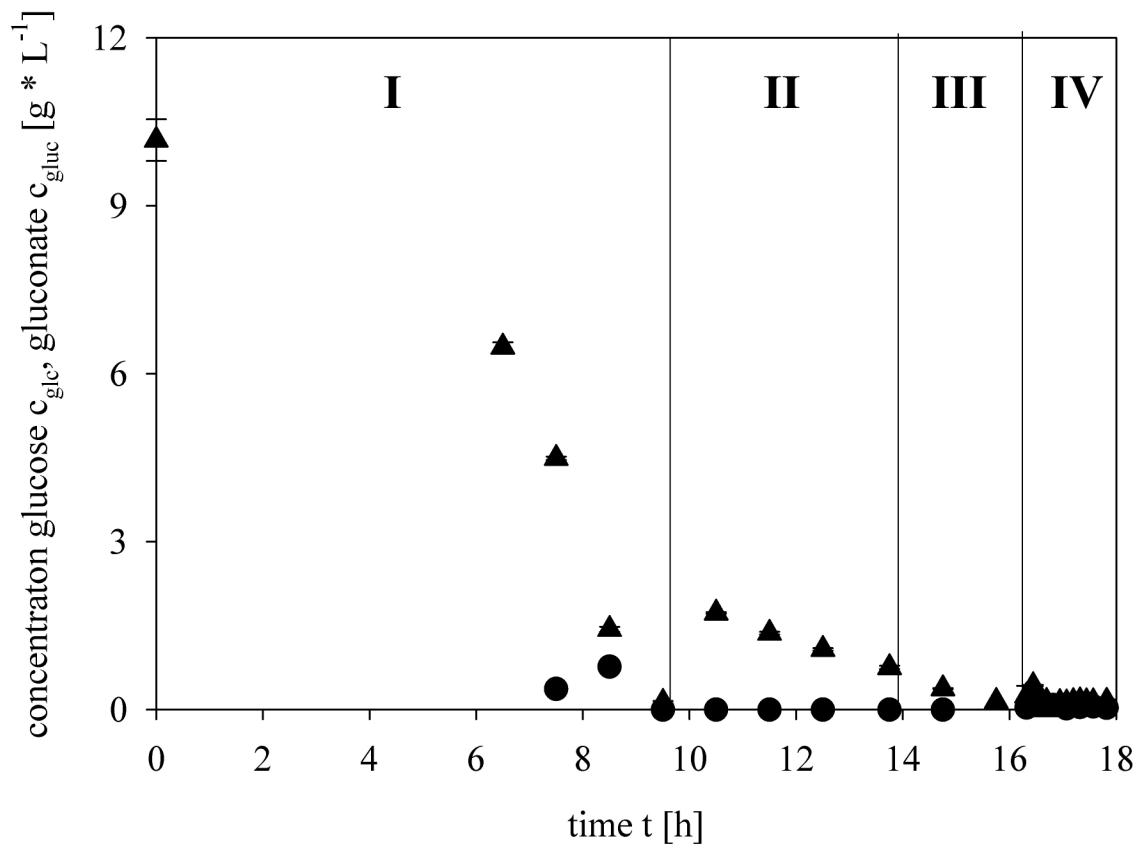


Figure 3: Time courses of glucose and gluconate during the initial exponential growth phase (I), the growth-limiting fed-batch phase (II), the induction period (III) and the *n*-octane conversion to 1-octanol with 'resting' cells at phase IV. The process was performed at 3.7 L scale.
113x78mm (300 x 300 DPI)

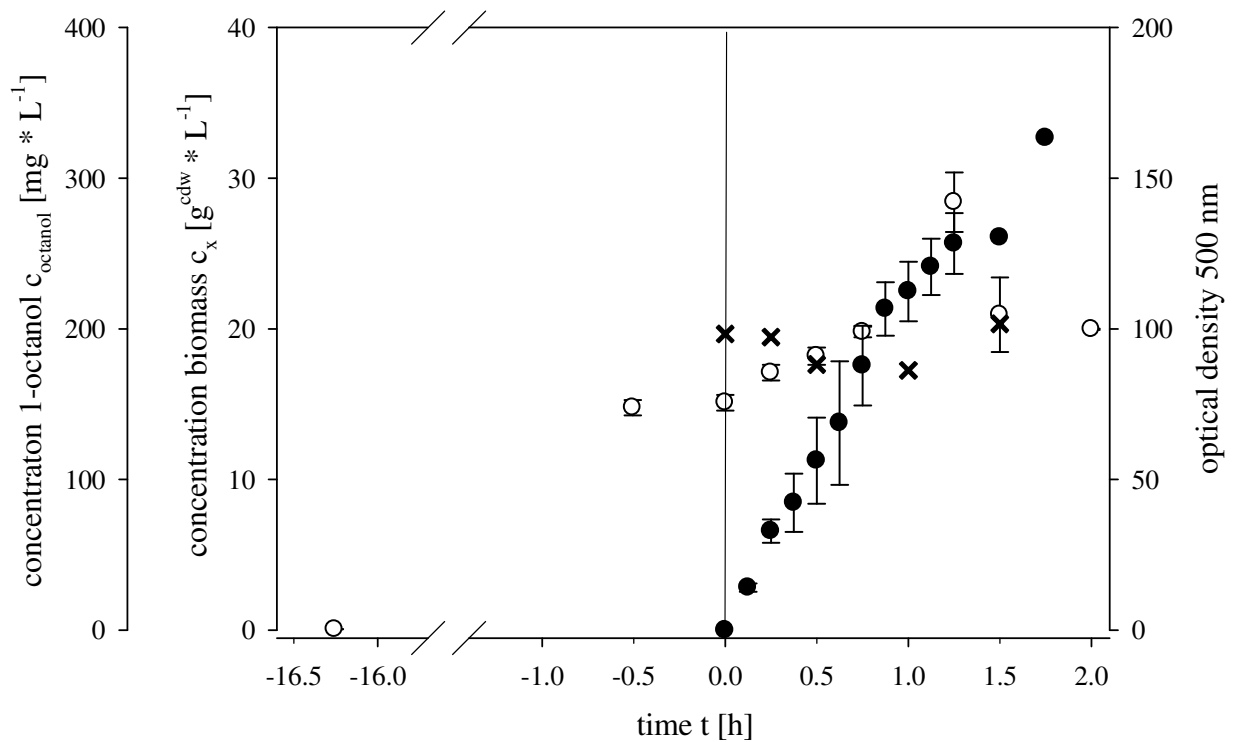


Figure 4: *in vivo* biotransformation of *n*-octane to 1-octanol by *Pseudomonas putida* MmarAlk using a 3.7 L bioreactor; ×: cell dry weight c_x [$\text{g}_{\text{CDW}} \text{L}^{-1}$]; ○: optical density 600 nm; ●: concentration of 1-octanol c_{octanol} [$\text{mg} \text{L}^{-1}$]; induction with 2 g L^{-1} (0.2 % w/v) L-rhamnose und 0.1mM FeSO_4 2.5 h before addition of 10% (v/v) *n*-octane
120x73mm (300 x 300 DPI)

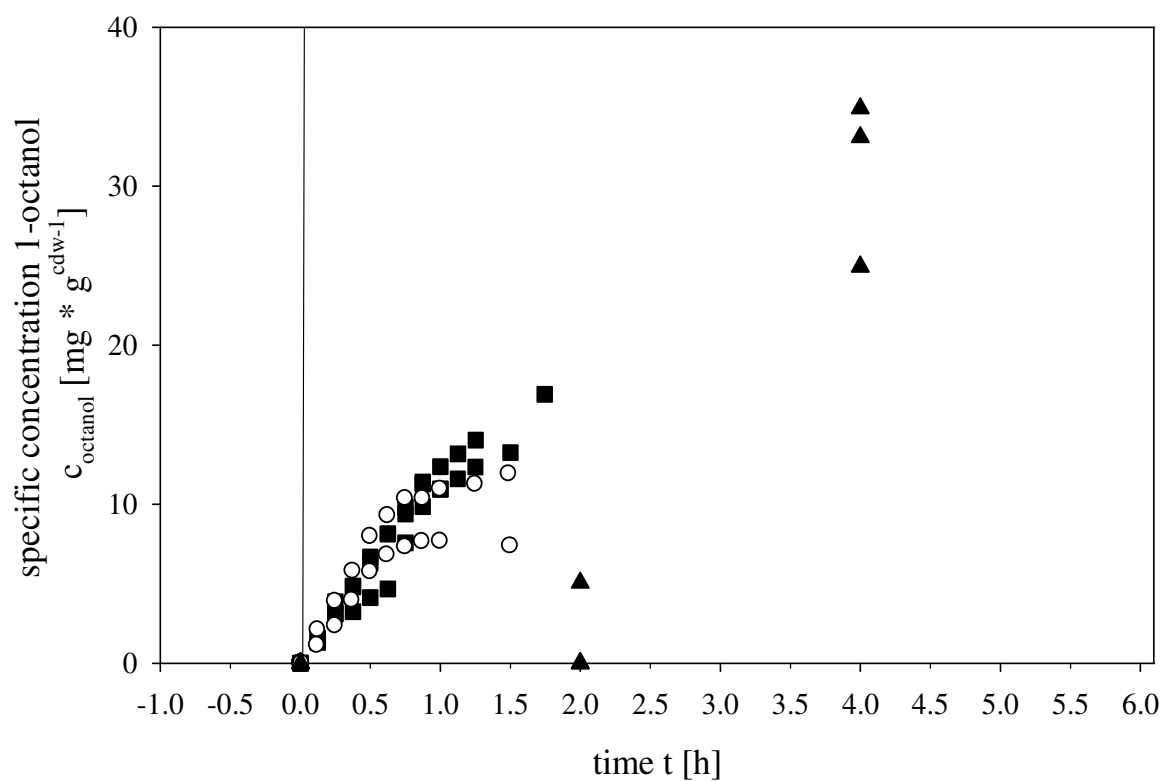


Figure 5: *in vivo* biotransformation of *n*-octane to 1-octanol by *Pseudomonas putida* mmarAlk (p4782.1 MMAR_3155 MMAR_3154 MMAR_3153) specific concentration of 1-octanol C_{octanol} [$\text{mg} \cdot \text{g}_{\text{CDW}}^{-1}$] from shake flask scale up to optimized bioreactor experiments. \blacktriangle : shake flask scale; \circ : 3.7 L bioreactor scale. \square : 3.7 L bioreactor scale with optimized conditions. Solid line: start biotransformation
128x81mm (300 x 300 DPI)

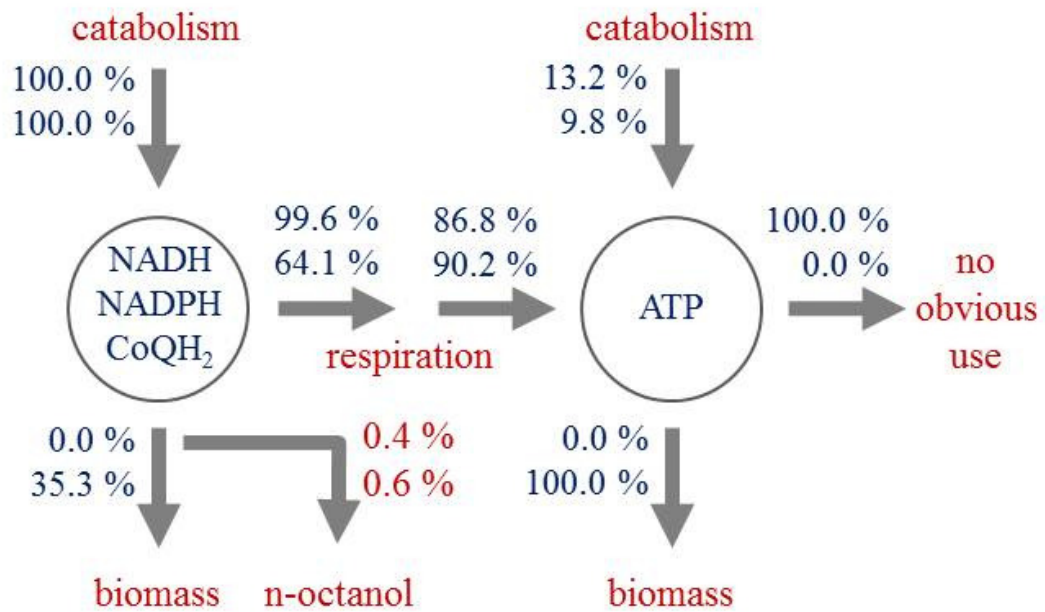


Figure 6: Distribution of the sources and sinks for reduction equivalents (NADH, NADPH, and ubiquinol CoQH₂) and energy metabolites (ATP) during the octanol production phase of the fed-batch process, replicate 1. With respect to growth rate, two extreme scenarios are described: no growth (top numbers) and growth with a maximal growth rate of 0.43 h⁻¹ (bottom numbers), assuming no ATP is consumed without obvious use
123x73mm (300 x 300 DPI)

Table 1

strain	Rate of ATP hydrolysis without obvious purpose (mmol ATP g _{CDW} ⁻¹ h ⁻¹)
KT2440	(14.1 ± 3.5) + μ * (27.6 ± 9.8)
KT2440 + Plasmid	(12.1 ± 5.7) + μ * (67.8 ± 22.2)

Table 2

publication	strain	monooxygenase P450	q_{octanol} [mg*g ^{cdw-1} *h ⁻¹]	max. C_{octanol} [mg*L _{BRM} ⁻¹]	conditions
Hamilton-Kemp et al. 2005	<i>E. coli</i>	strain ATCC 25922	-	53.8	50 mL, 8 h
Fujii et al. 2006	<i>E. coli</i>	CYP153A from <i>Acinetobacter</i> sp. OC4	11	2300	1.5 mL, 24 h
Nodate et al. 2006	<i>E. coli</i> BL21(DE3)	CYP153A13a from <i>Alcanivorax borkumensis</i> SK2	-	800	1.5 mL, 24 h
Fujita et al. 2009	<i>E. coli</i> BL21(DE3)	CYP153A from <i>Acinetobacter</i> sp. OC4	12.2	700	1.5 mL, 24 h
Koch et al. 2009	<i>E. coli</i> BL21(DE3)	CYP153A6 from <i>Mycobacterium</i> sp. HXN-1500	13.3	10	1 mL, 1 h
Bordeaux et al. 2011	<i>E. coli</i> BL21(DE3)	CYP153A13a from <i>Alcanivorax borkumensis</i> SK2	30.5	n/a	5 mL, 24 h
Grant et al. 2011	<i>E. coli</i> BL21(DE3)	AlkB complex from <i>P. putida</i> GPo1	-	680	1000 mL, 30 h
Gudiminchi et al. 2012	<i>E. coli</i> BL21(DE3)	CYP153A6 from <i>Mycobacterium</i> sp. HXN-1500	-	2500	1 mL, 15 h
This work	<i>P. putida</i> KT2440 MmarAlk	CYP153A16 from <i>Mycobacterium marinum</i>	12.7	320 [#]	1500 mL, 1.75 h SOP

Curriculum vitae



Persönliche Daten

Name: Sumire Honda Malca
 Geburtsdatum/-ort: 06.09.1980 in Moquegua, Peru
 Nationalität: Peruanisch
 Email: sumire.honda@itb.uni-stuttgart.de

Hochschulbildung

- 07.2009 - 01.2013 **Promotion bei Prof. Dr. Bernhard Hauer am Institut für Technische Biochemie (ITB) der Universität Stuttgart**
Dissertation: „Substrat-Charakterisierung und Protein Engineering bakterieller Cytochrom-P450-Monooxygenasen für die bio-basierte Synthese omega-hydroxylierter aliphatischer Verbindungen“
- 08.2006 - 08.2008 **Masterstudium Biotechnologie Royal Institute of Technology (KTH), Schweden**
Master-Thesis: „Klonierung, Expression und Charakterisierung von zwei Flavodoxinen und einer NADPH-abhängigen Flavodoxin-Reduktase aus Clostridium acetobutylicum“
- 04.1996 - 12.2001 **Bachelorstudium Pharmazie und Biochemie Universidad Nacional Mayor de San Marcos, Peru**
enthält: allgemeines wissenschaftliches Studium – Abitur-äquivalent (2 Jahre); Bachelorstudium (3 Jahre), Pflichtpraktikum (1 Jahr)

Arbeitserfahrungen und Praktika

- 12.2008 - 06.2009 **Wissenschaftliche Mitarbeiterin am Institut für Technische Biochemie, Universität Stuttgart**
kinetische Charakterisierung der P450-Monooxygenase aus C. acetobutylicum
- 07.2003 - 06.2006 **Zuständig für wissenschaftliche Angelegenheiten Abteilung für Öffentlichkeitsarbeit, Ajinomoto del Peru S.A.**
Unternehmenskommunikation (Medien und Hochschulen) · Produktsicherheit und Verbraucherinformationen · Gestaltung von Trainingsprogrammen zu Produktsicherheit und Produktqualität
- 11.2002 - 06.2003 **Praktikum Abteilung für Öffentlichkeitsarbeit, Ajinomoto del Peru S.A.**
Überwachung internationaler/lokaler Vorschriften und wissenschaftlicher Berichte über Aminosäure und Nukleotide als Lebensmittelzusatzstoffe
01. - 12.2001 **Praktikum Cenprofarma, Zentrum für Qualitätskontrolle Universidad Nacional Mayor de San Marcos, Peru**
physikalisch-chemische und mikrobiologische Untersuchung von Lebensmitteln, Arzneimitteln und Kosmetika

